

1N-34-5R

10 -

P- 98

NAS-8407-FM-9017-482

DEVELOPMENT OF A NONAZEOTROPIC HEAT PUMP FOR CREW HYGIENE WATER HEATING

David H. Walker
Glenn I. Deming
Foster-Miller, Inc.
350 Second Avenue
Waltham, MA 02154

October 1991

(NASA-CR-194189) DEVELOPMENT OF A
NONAZEOTROPIC HEAT PUMP FOR CREW
HYGIENE WATER HEATING Final Report,
Jun. 1989 - Aug. 1991
(Foster-Miller Associates) 98 p

N94-13674

Unclass

G3/54 0183146

Final Report
Contract Number: NAS8-38407

SBIR Contract
Release Date: ~~01-2-93~~ 6-4-93
SBIR-09.04-3200

Prepared for:

National Aeronautics and Space Administration
George C. Marshall Space Flight Center
Marshall Space Flight Center, AL 35812

NAS-8407-FM-9017-482

**DEVELOPMENT OF A NONAZEOTROPIC HEAT PUMP FOR
CREW HYGIENE WATER HEATING**

David H. Walker
Glenn I. Deming
Foster-Miller, Inc.
350 Second Avenue
Waltham, MA 02154

October 1991

Final Report
Contract Number: NAS8-38407

Prepared for:

National Aeronautics and Space Administration
George C. Marshall Space Flight Center
Marshall Space Flight Center, AL 35812

**NASA LICENSE RIGHTS LEGEND
SBIR RIGHTS NOTICE (APRIL 1985)**

This SBIR data is furnished with SBIR rights under NASA Contract No. NAS8-38407 (and subcontract N/A if appropriate). For a period of 2 years after acceptance of all items to be delivered under this contract the Government agrees to use this data for Government purposes only, and it shall not be disclosed outside the Government (including disclosure for procurement purposes) during such period without permission of the contractor, except that, subject to the foregoing use and disclosure prohibitions, such data may be disclosed for use by support Contractors. After the aforesaid 2-year period the Government has a royalty-free license to use, and to authorize others to use on its behalf, this data for Government purposes, but is relieved of all disclosure prohibitions and assumes no liability for unauthorized use of this data by third parties. This Notice shall be affixed to any reproductions of this data, in whole or in part.

TABLE OF CONTENTS

Section	Page
EXECUTIVE SUMMARY	1
1. INTRODUCTION.....	2
2. DESIGN SPECIFICATIONS	5
2.1 Hygiene Water Requirements and Proposed Methods.....	5
2.2 Waste Heat Availability	14
2.3 Material Constraints.....	15
3. SYSTEM CONFIGURATION	17
3.1 Centralized On-Demand	17
3.2 Centralized Delay.....	18
4. WORKING FLUID SELECTION	21
5. SYSTEM MODELING	22
5.1 Storage Tank Model	22
5.2 Cycle COP Model	24
5.3 Heat Exchanger Model	24
5.4 Life Cycle Cost	26
5.5 Trade Studies	27
6. SYSTEM DESIGN	33
6.1 Heat Exchangers	33
6.2 Compressor	37
6.3 Lubrication	40
6.4 Controls	42

TABLE OF CONTENTS (Continued)

Section	Page
7. TESTING	47
7.1 Heat Exchangers	47
7.2 Compressor/Oil Separator.....	54
7.3 Heat Pump Bench Test	56
7.4 Endurance Test	59
8. HEAT PUMP PACKAGING	63
8.1 Prototype Integration	63
8.2 Space Station Integration.....	68
9. CONCLUSIONS AND RECOMMENDATIONS	77
10. REFERENCES	79
APPENDIX A TEST DATA	A-1
REPORT DOCUMENTATION PAGE	90

LIST OF ILLUSTRATIONS

Figure	Page
1. Standard Temperature Profile	3
2. Nonazeotropic Temperature Profile	3
3. U.S. Habitation Module Hygiene Water Distribution	6
4. U.S. Laboratory Module Hygiene Water Distribution	7
5. Crew Activity Profile for a Typical Day	9
6. Water Thermal Conditioning Assumed Timelines	10
7. Water Thermal Conditioning Assumed Timelines	12
8. Power Required Per Use Point For Inline Heating	13
9. Centralized On-Demand Heat Pump Water Heating Concept	18
10. Centralized Delay Heat Pump Water Heating Concept	19
11. Storage Tank Water Level	23
12. Heat Pump Cycle Calculation	25
13. Life Cycle Cost versus Compressor Efficiency	29
14. Life Cycle Cost versus Heat Exchanger Pinch Point	30
15. Life Cycle Cost versus Storage Tank Size	31
16. Condenser Cross Section	34
17. Nonazeotropic Heat Pipe Cycle Calculation	35
18. Sequence of Operation for the Scroll Compressor	38
19. Compressor Scroll Components	39
20. Prototype Heat Pump Compressor	41
21. Cyclone Separator Cross Section	43
22. Flow Pattern in Cyclone Separator	44
23. Cyclone Separator Manufactured Parts	44
24. Nonazeotropic Heat Pump Control Schematic	45

LIST OF ILLUSTRATIONS (Continued)

Figure	Page
25. Heat Exchanger Test Setup	48
26. Schematic of Heat Pump Condenser Layout	49
27. Typical Condenser Return Bend	50
28. Heat Pump Bench Test	51
29. Data Acquisition System	51
30. Typical Condenser Temperature Profile	53
31. Typical Evaporator Temperature Profile	53
32. Heat Rejection versus Speed and Charge	58
33. COP versus Speed and Charge.....	58
34. Heat Rejection versus Speed and Charge	60
35. COP versus Speed and Charge.....	60
36. Heat Pump Package Layout	64
37. Evaporator and Condenser Coils - Uninsulated	65
38. Evaporator and Condenser Coils - Insulated	66
39. Prototype Heat Pump Package	66
40. Heat Pump Storage Tank Package	67
41. Heat Pump Controls and Test Equipment.....	69
42. Assembled Prototype Heat Pump System	70
43. Heat Pump System Schematic.....	71
44. Nonazeotropic Heat Pump Rack Installation	72
45. Nonazeotropic Heat Pump Orbital Replacement Unit	73
46. Nonazeotropic Heat Pump Display Panel	73
47. Nonazeotropic Heat Pump Cutaway View.....	75
48. Cutaway View of Scroll Compressor	76

LIST OF TABLES

Table	Page
1. Expected Hygiene Water Requirements for SSF.....	8
2. Expected Hygiene Water Requirements for SSF (Boeing).....	11
3. Thermal Rejection Loop.....	15
4. Binary Mixture Candidates	21
5. Storage Tank Refill Rates	23
6. Life Cycle Cost Model Inputs	28
7. Life Cycle Cost versus Heat Exchange Tube Size	32
8. Prototype Compressor Run Time	62

EXECUTIVE SUMMARY

The currently planned Space Station Freedom (SSF) intends to utilize point-of-use instantaneous electric cartridge heaters to provide hygiene water heating. The power draw for a typical hot water appliance use would be 2 to 5 kW. With a total production capacity of only 75 kW for the entire space station, the water heating system could pose significant mission constraints. The search for an alternative approach revealed SSF thermal management systems with bus temperatures which make heat pumping a viable option. Furthermore, the potential for a high COP through the use of a nonazeotropic refrigerant mixture is particularly promising due to the large temperature changes required of the heat source (water thermal bus) and heat sink (hygiene water). The purpose of the research carried out in this Phase II SBIR program was to investigate the potential of a nonazeotropic heat pump in reducing the peak power draw in providing hygiene water heating on SSF.

A nonazeotropic heat pump system was conceived which is capable of producing and delivering the required hygiene water according to the anticipated usage schedule of SSF while maintaining the peak power and energy consumption to an absolute minimum. The system required the development of a hermetic compressor/motor package based on a compliant scroll with the ability to operate at a very high overall efficiency while maintaining lubrication in a zero-gravity environment. The design also included compact, lightweight heat exchangers to provide efficient counterflow heat transfer as required by the nonazeotropic working fluid. System performance was demonstrated through the fabrication and testing of a prototype system.

The prototype heat pump system produced the desired amount of hygiene water at the temperatures required by the end use appliances. The measured coefficient of performance ranged from 6.5 to 8.0, nearly double that expected from a single-constituent (i.e., R-12) heat pump. More importantly, the power consumption of the nonazeotropic heat pump was less than 200 W. For the SSF application, this represents a 90 to 95 percent reduction in power draw compared to the currently baselined electric cartridge system. The nonazeotropic heat pump could find many applications in other future manned space exploration such as a lunar base or a mission to Mars.

1. INTRODUCTION

Space Station Freedom (SSF) and other future manned missions will need hot water production for various crew hygiene requirements such as bathing (showers and hand washing), clothes laundering, dish washing, and food preparation. Hot water temperature will range from 110°F for bathing to 140°F for clothes and dish washing. SSF is presently baselined for point-of-use instantaneous electric cartridge heaters. For a fully manned crew of eight, the peak power draw for water heating would typically be 2 to 5 kW but could be as high as 15 kW. With a total production capacity of only 75 kW, the water heating system could pose significant mission constraints.

An alternate approach for water heating is the use of a heat pump that produces hot water by taking heat energy from a waste heat source, such as a thermal bus, raising the temperature of this energy by the application of work, and providing the heat to the hygiene water. The SSF thermal management system will have several thermal buses used in the acquisition, transportation, and rejection of waste heat. Externally, two-phase ammonia loops operating at 62°F and 35°F transport waste heat to a central radiator system for rejection to space. Internally, single-phase water loops connected to the 62°F and 35°F buses collect waste heat from various temperature sources. As a result of this sensible heat transfer, the high temperature water loop will rise to approximately 110°F under high heat load conditions before transferring the waste heat to the external ammonia bus. The relatively high temperature of this water loop makes heat pumping look especially attractive.

A standard vapor compression heat pump utilizing the module waste heat acquisition water loop as a heat source and the hygiene water as a heat sink, would produce heat exchanger temperature profiles similar to those shown in Figure 1. The sensible heating of the hygiene water in the condenser results in a 75°F temperature change as the water is taken from ambient to 145°F. However, the single component working fluid remains isothermal in the phase change process. A similar temperature profile is produced in the evaporator. This inefficient heat transfer process results in a large deviation from the ideal Carnot cycle and an associated decrease in cycle efficiency. If the temperature profiles in the heat exchangers could be more closely aligned, the cycle efficiency could approach that of the ideal cycle.

One means of achieving this is to use a nonazeotropic mixture of refrigerants in the heat pump cycle. Multi-component working fluids offer unique characteristics, which in certain applications, may lead to significant improvements in efficiency. In particular, the phase change process during constant pressure evaporation and condensation does not occur isothermally as with pure refrigerants, but instead occurs over a temperature range known as the "glide". The magnitude of the temperature glide depends on the properties of the mixture constituents. Through proper mixture selection, the heat pump cycle temperature profiles would be similar to those shown in Figure 2. The deviation from the ideal cycle is then reduced and efficiency is increased.

This report describes the work performed under a Phase II Small Business Innovation Research (SBIR) program funded by the NASA Marshall Space Flight Center. The objectives of this program included the following:

- Determine the design specifications for a hygiene water heating heat pump appropriate for the Space Station Freedom
- Conceive a system capable of producing and delivering the required hygiene water according to the anticipated usage pattern while maintaining peak power and energy consumption to an absolute minimum

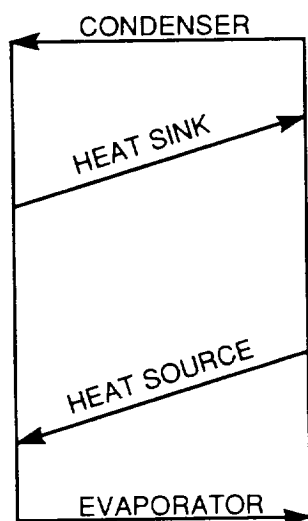
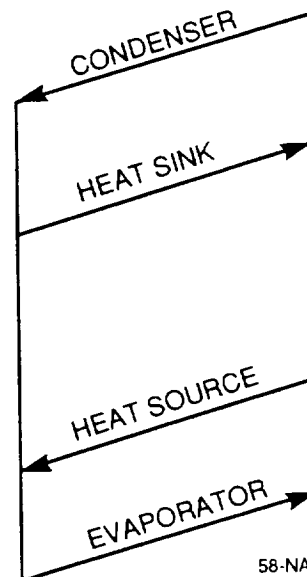


Figure 1. Standard Temperature Profile



58-NAS-9017-1

Figure 2. Nonazeotropic Temperature Profile

- Select the nonazeotropic working fluid constituents and composition to match the temperature glide of the hygiene water and maximize heat pump Coefficient of Performance (COP)
- Develop a hermetic compressor/motor package with the ability to operate at a very high overall efficiency while maintaining lubrication in a microgravity environment
- Design compact, lightweight heat exchangers to provide efficient counterflow heat transfer as required by the nonazeotropic working fluid
- Demonstrate system performance through the fabrication and testing of a bench test system
- Incorporate the heat pump components into a compact prototype package for delivery and evaluation by NASA.

The following sections of this report detail the work that was performed in the program effort. The first section describes the specifications used to design the heat pump system including the hygiene water requirements, the waste heat available, and material constraints. A description of the system configuration is given as well as the working fluid selected and the process used in making that selection. Several models were generated to aid in sizing the various components. A complete description of those models is given along with the results obtained. The system hardware is described in detail followed by a description of the test setup and results. The final prototype package configuration is given along with a conceptualization of the space hardware. Conclusions and recommendations for future work and potential alternate applications are also included.

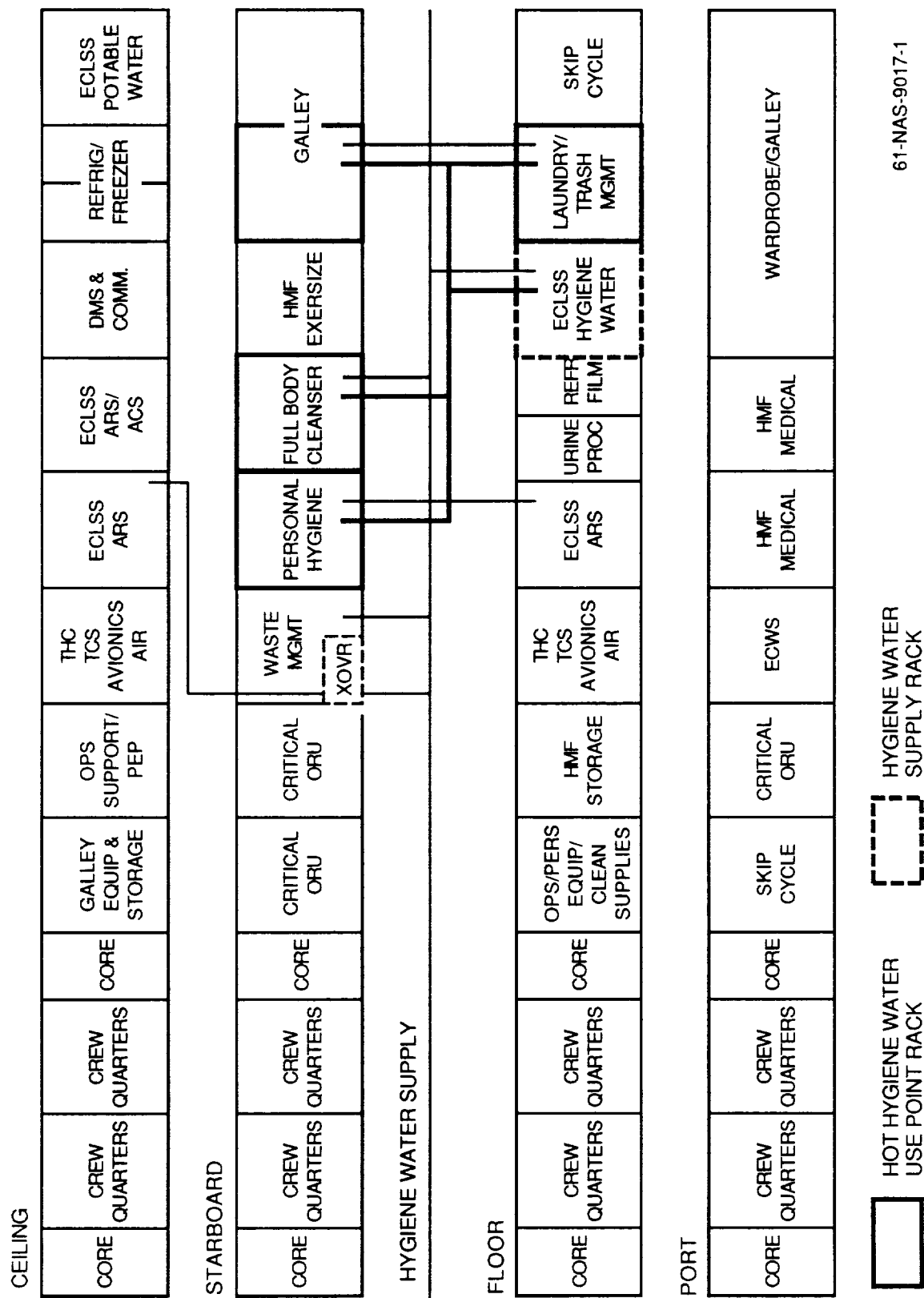
2. DESIGN SPECIFICATIONS

The initial task of the Phase II program was to determine the design specifications for the Hygiene Water Heating Heat Pump. Items to be determined included the number and type of appliances to be serviced, the anticipated usage pattern, and the amount and temperature of the water required by each appliance. Also of interest were the alternative methods considered for meeting the hot water demand. The heat pump system would utilize one or more of the SSF thermal buses as a heat source, therefore, information on thermal management system had to be ascertained. The temperature, variability, and working fluid of the thermal buses had to be determined as well as any interfacing requirements. Finally, materials compatibility issues had to be addressed along with system packaging and safety constraints such as flammability and toxicity. This information was gathered through numerous conversations and meetings with various NASA and Boeing Aerospace personnel. Boeing is the prime contractor responsible for the Environmental Control and Life Support Systems (ECLSS) for the SSF.

The heat pump design and sizing tasks were initiated in June, 1989 and were based on the latest information available. The SSF has been reconfigured since then and the hygiene water requirements have changed slightly.

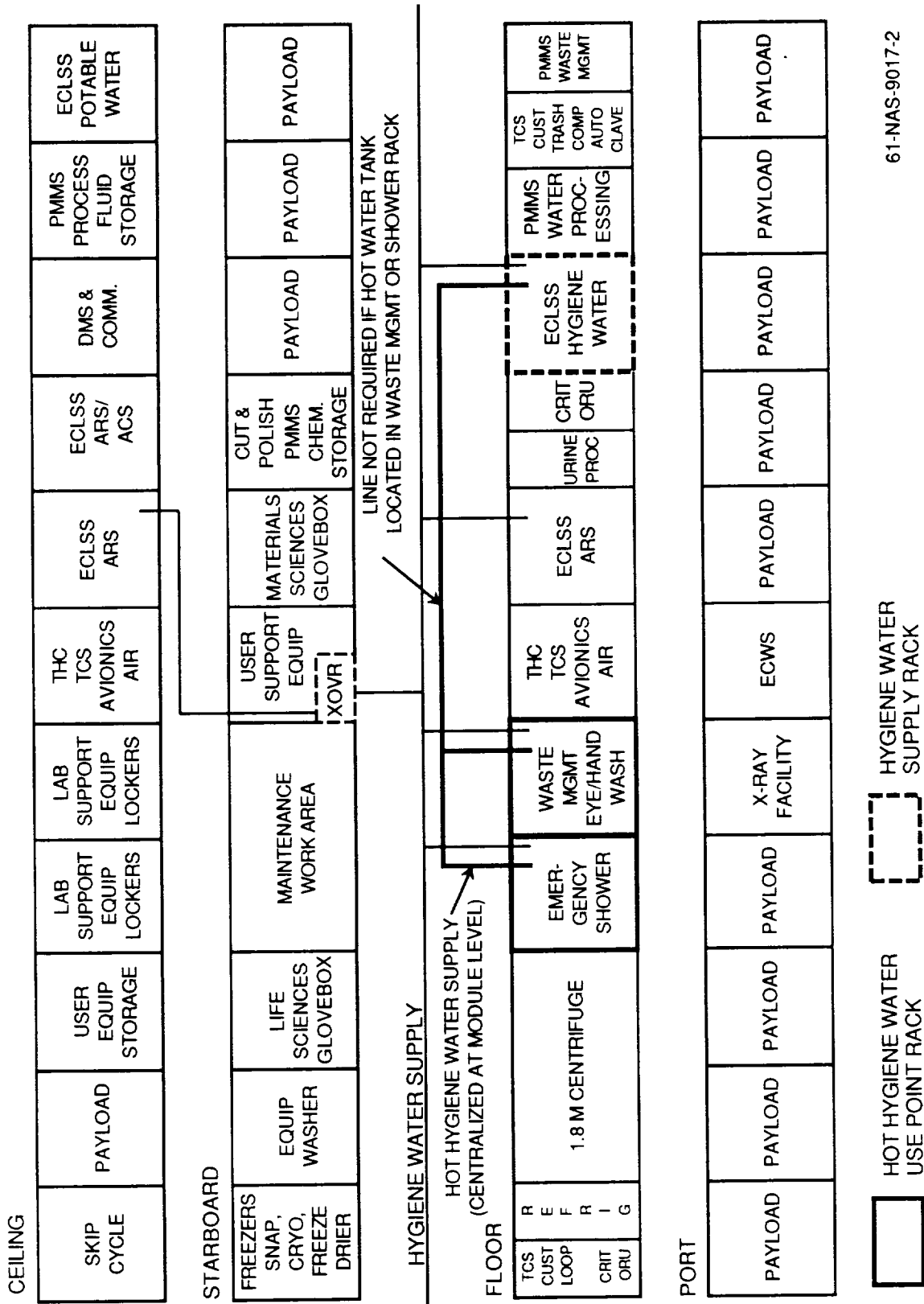
2.1 Hygiene Water Requirements and Proposed Methods

In July, 1989, a study was performed by NASA to examine the expected water thermal conditioning requirements of the SSF (1). Figure 3 is a schematic diagram of the Habitat Module hygiene water distribution system. Figure 4 is a similar diagram for the Laboratory Module. Heated hygiene water is required at six locations: two handwash stations (one in the Habitat Module and one in the Laboratory Module), two showers (one Habitat, one Laboratory), one clothes wash, and one dish wash (both in the Habitat). Table 1 is a summary of the hygiene water requirements as supplied by the Man-Systems Division of JSC. Listed in the table are the delivery temperatures for each appliance, flow rate, water use per appliance operation, and total daily use per appliance. Also listed in Table 1 are the power draws and the total daily energy consumption for each appliance based on the use of electric cartridge heaters. Figure 5 shows an assumed crew activity profile for a typical day. Showers follow the exercise period for each crew member as shown. Handwashes are sequential prior to each meal and sleep period. Clothes washing is done after each group of showers (two/day) and dish washing is done after the joint meal (one/day). Based on this information, an assumed water thermal conditioning timeline was derived as shown



61-NAS-9017-1

Figure 3. U.S. Habitation Module Hygiene Water Distribution



61-NAS-9017-2

Figure 4. U.S. Laboratory Module Hygiene Water Distribution

Table 1. Expected Hygiene Water Requirements for SSF

Water Use	Delivery Temperature °F	Maximum Flow Rate lb/min	Use Rate lb/use	Daily Use lb/day	Cartridge Heater kW	Cartridge Heater kWh
Hand	110	3	1.0	32.0	2.1	0.38
Shower	110	3	8.0	64.0	2.1	0.75
Laundry	140	3	50.0	100.0	3.7	2.05
Dishwash	140	3	48.0	48.0	3.7	0.98
Drink	-	-	-	-	-	-
Totals		12	107.0	244.0	11.6	4.16

in Figure 6. Also shown is an assumed peak profile (worst case scenario) where the simultaneous use of all appliances must be met.

Boeing performed their own study on SSF water thermal conditioning requirements. Table 2 lists the hygiene water requirements as supplied by Boeing. As can be seen, there is some discrepancy between the Boeing and the NASA numbers. Boeing has assumed twice as many handwashes (8/man-day), the same number of showers (1/man-day), one more clothes wash (3/day) and one more dish wash (2/day) than the comparable NASA numbers. In addition, Boeing also assumed the requirement of potable hot water for drinks. The result is a daily use rate of almost twice the value of the NASA study. Figure 7 displays the thermal conditioning timelines for the Boeing study.

The NASA study presented several alternatives for providing the necessary water heating, all of them based on electrical resistance heating. The alternatives were variations of two basic concepts: 1) distributed - each hot water source (either tank or inline "cartridge" heater) provides hot water service to a single use point, or 2) centralized - each hot water source (tank) provides hot water service to multiple use points. A brief description of each alternative follows:

- Centralized at Station Level (Two Tanks) - One (14 gal) tank located in Habitat and one (14 gal) tank in Laboratory. Either tank can service both Habitat and Laboratory through intermodule hot water lines. Storage tank set point temperature range equals 150 to 155°F to deliver 140°F at the furthest use point.

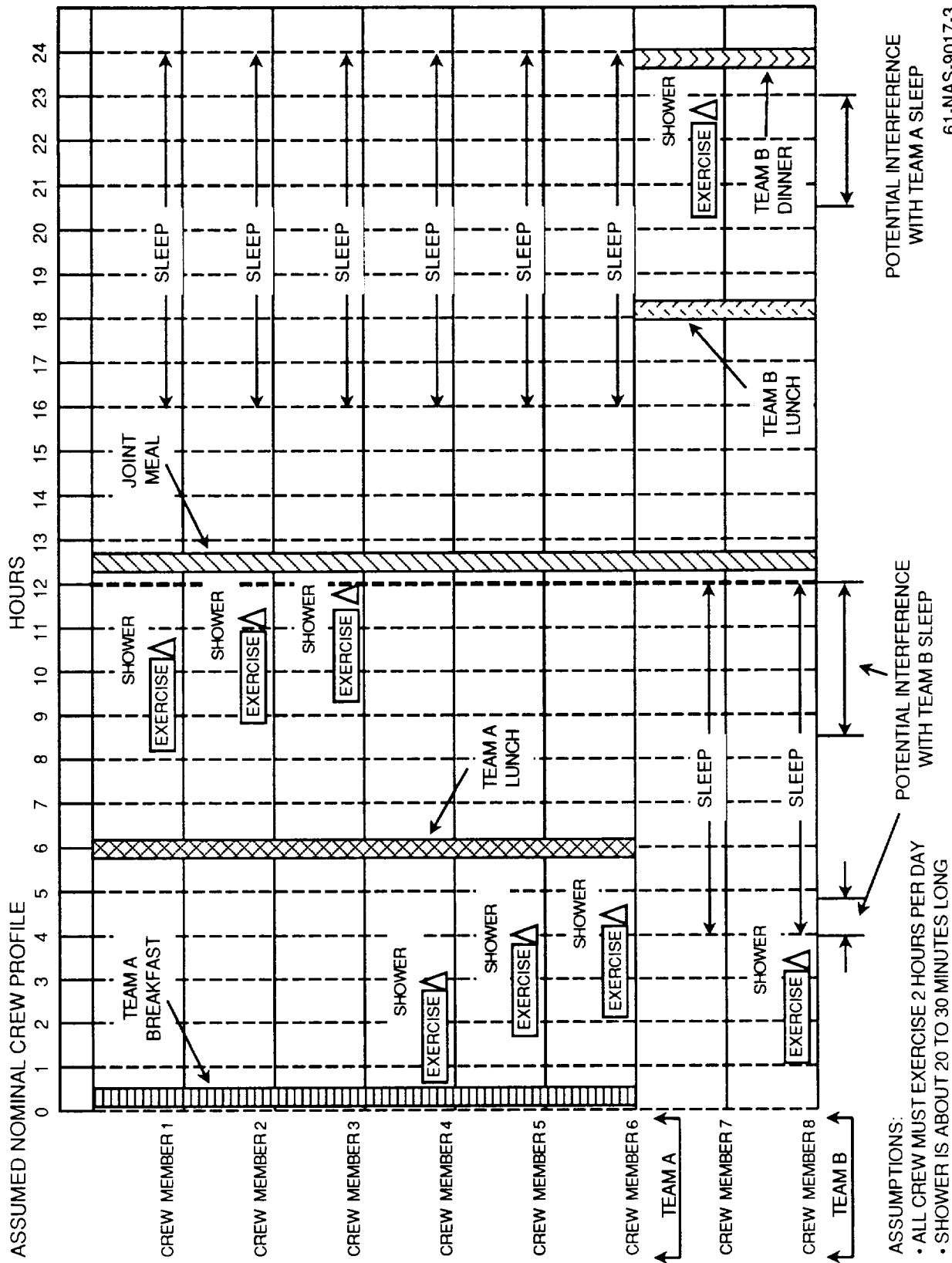


Figure 5. Crew Activity Profile for a Typical Day

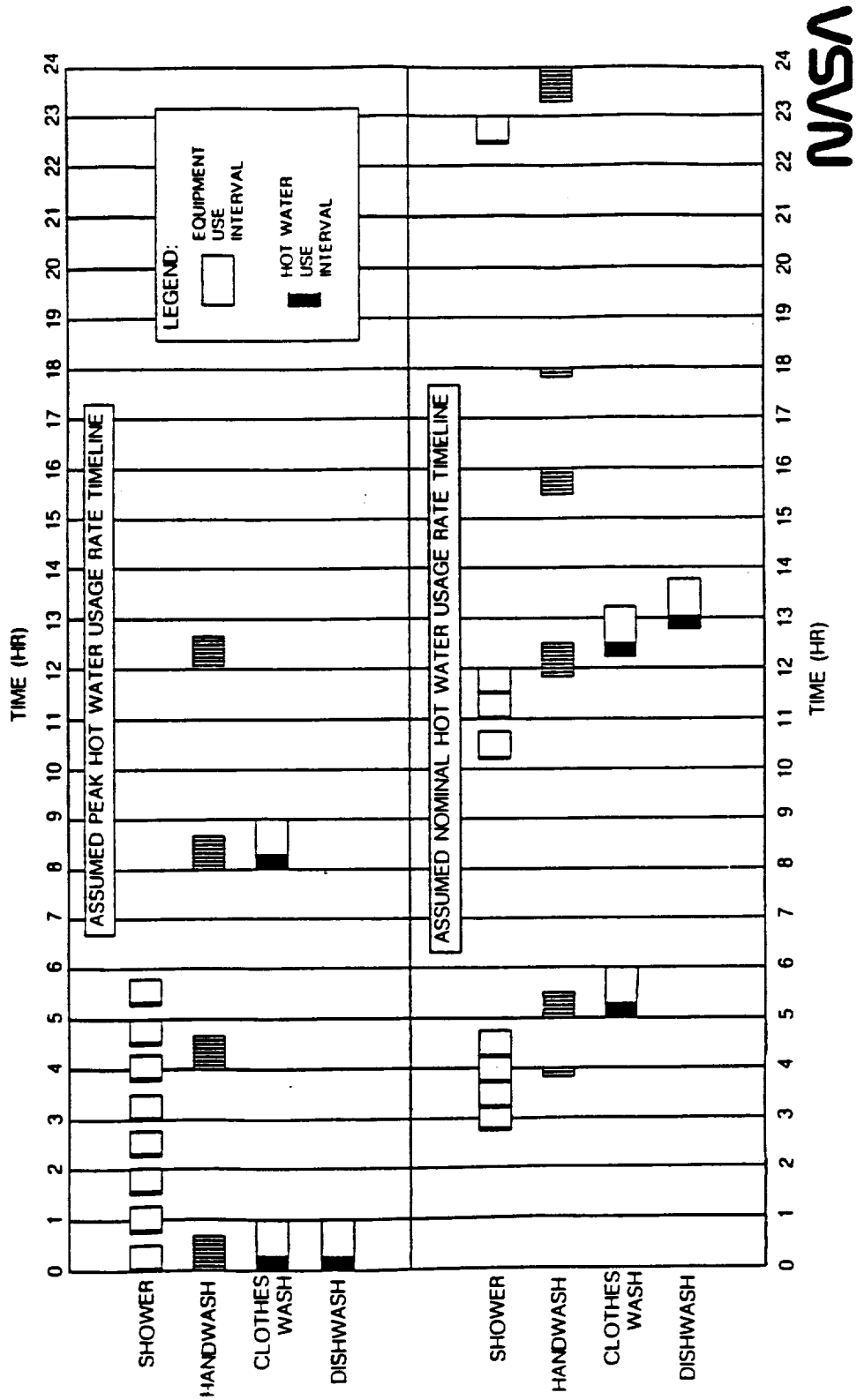
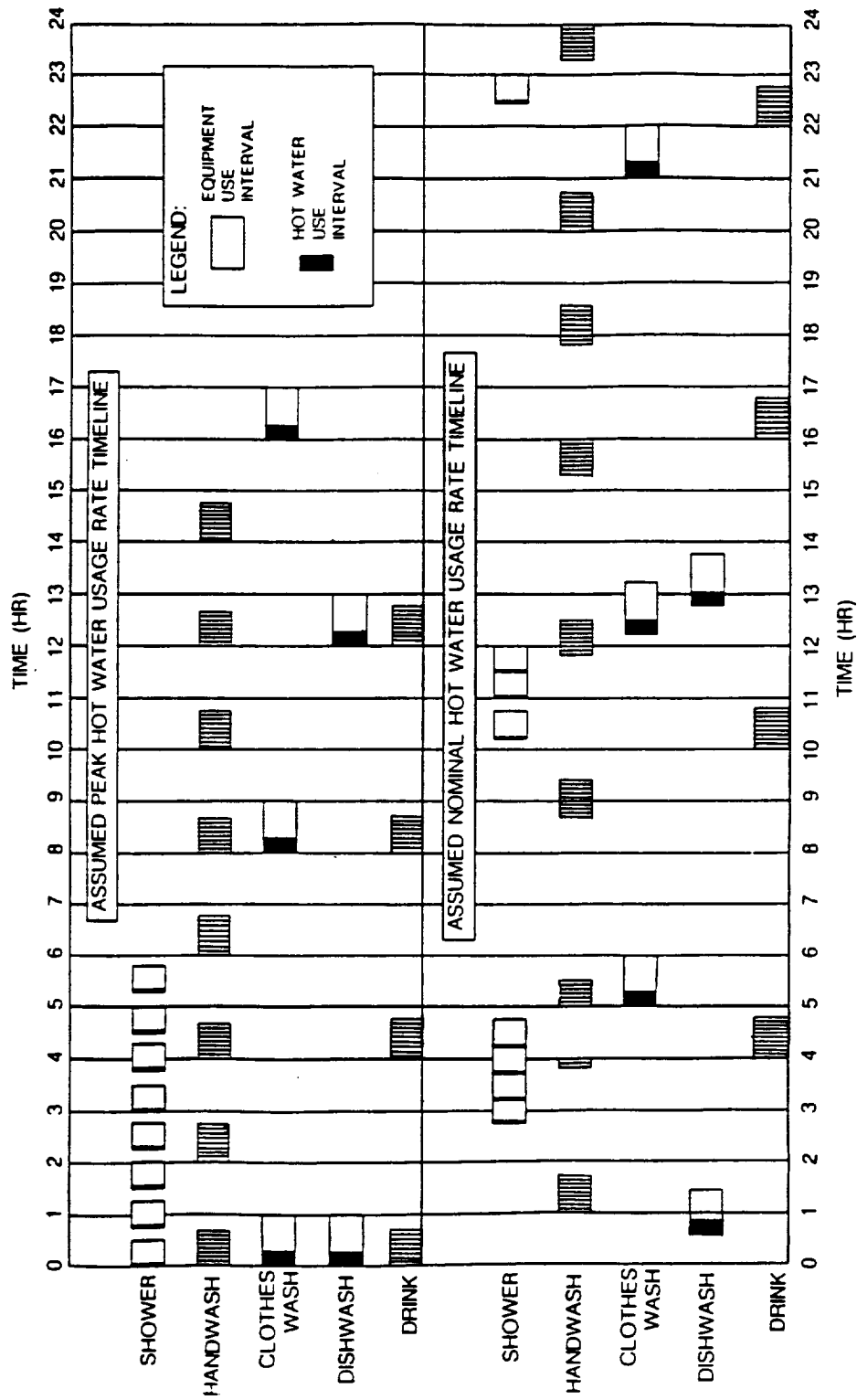


Figure 6. Water Thermal Conditioning Assumed Timelines

Table 2. Expected Hygiene Water Requirements for SSF (Boeing)

Water Use	Delivery Temperature °F	Maximum Flow Rate lb/min	Use Rate lb/use	Daily Use lb/day	Cartridge Heater kW	Cartridge Heater kWh
Hand	110	2.1	1.1	69.8	1.5	0.82
Shower	110	3	8.3	66.4	2.1	0.78
Laundry	120	3	54.8	164.3	2.6	2.41
Dish wash	145	3	47.7	95.5	4.0	2.10
Drink	150	3.8	2.1	66.6	5.3	1.56
Totals		14.9	114.0	462.6	15.5	7.67

- Centralized at Module Level (Two Tanks) - One tank in Habitat and Laboratory of unique sizes (14 gal in Habitat and 2.5 gal in Laboratory). Each tank services hot water use points in that module through interrack hot water lines. Storage tank set point temperature range equals 142 to 147°F (Habitat), 111 to 116°F (Laboratory) to deliver required temperature to furthest use point.
- Centralized at Module Level (Three Tanks) - One dish wash/clothes wash tank (14 gal Habitat), two shower/hand wash tanks (2.5 gal Habitat & Laboratory). Each tank services local (adjacent rack) hot water needs to minimize interrack hot water lines. Storage tank set point temperature range equals 141 to 146°F (dish/clothes), 111 to 116°F (shower/hand).
- Distributed Tank - One tank located in each hot water use rack (6 total): Dish wash and clothes wash (7 gal each), hand wash and shower, Habitat and Laboratory (1.5 gal each). Eliminates need for interrack hot water lines. Storage tank set point temperature range equals 140 to 145°F (dish/clothes), 110 to 115°F (shower/hand).
- Distributed Cartridge - Inline "cartridge" heater heats water to required delivery temperature as it is being delivered (140°F dish/clothes, 110°F shower/hand). Eliminates need for hot water storage tanks or interrack hot water lines.



BOEING

Figure 7. Water Thermal Conditioning Assumed Timelines

Considered in the NASA trade study was the potential for water contained in the hot water line cooling down between uses resulting in water "wasted" down the drain waiting for hot water from a central storage tank. Additional water must then be processed and additional energy must be consumed to produce more hot water. One alternative is to utilize recirculation loops to maintain hot water in lines. However, this alternative is energy intensive and is not feasible unless the SSF is forced to use continuously circulating hot water loops for microbial control. The solution is to minimize line lengths and supply hot water to the use point at slightly higher temperatures resulting in desired mix temperature of cold water in line and hot water from the supply tank. The hygiene supply tanks size may be reduced due to the presence of the hot water storage tanks, thus minimizing the volume penalty associated with the tank options.

The NASA trade study (1) determined the Life Cycle Cost (LCC) of the five systems considered. Included in the LCC were: weight (\$4550/lb), volume (\$900/ft³/month), and energy (\$210/kWh) cost along with development and maintenance cost for a 10-year life. The system with the lowest LCC was the distributed cartridge heaters. This system is currently baselined for the SSF. Figure 8 shows the power required per use point for inline heating as a function of the water flow rate. Initially the dishwasher and laundry were to have flow rates of 30 lb/min of hot

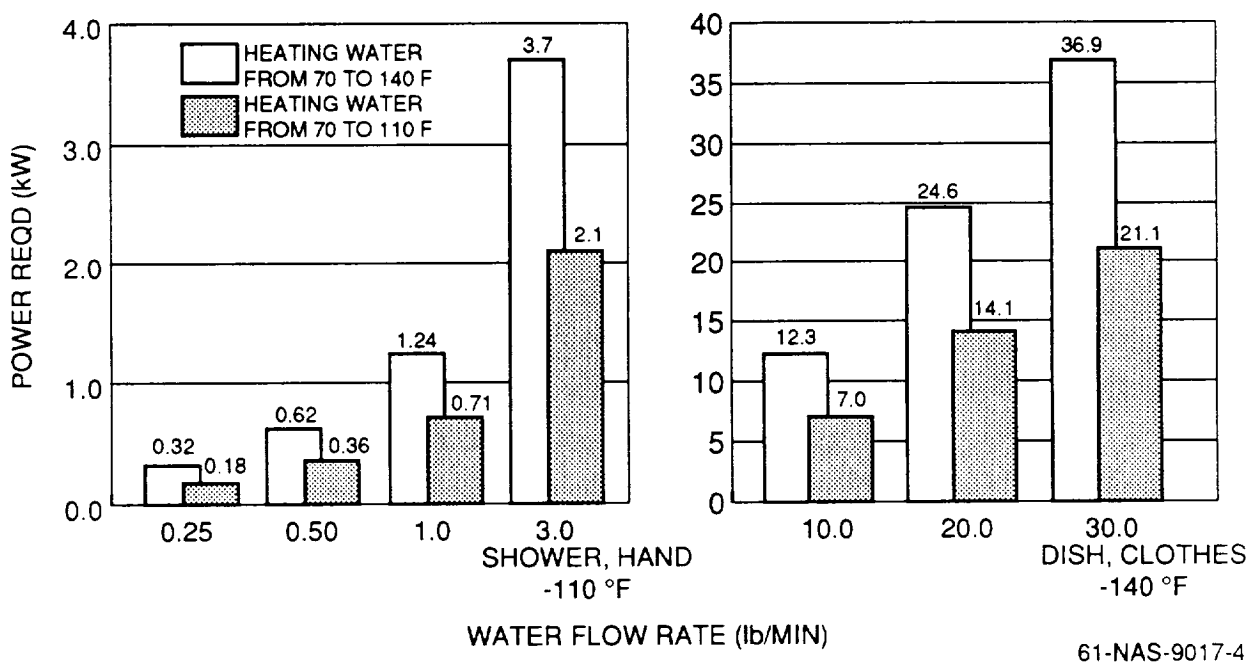


Figure 8. Power Required Per Use Point For Inline Heating

water for the fill cycle. As can be seen, the power required to meet this demand is 36.9 kW, nearly half of the 75 kW available to the entire space station. Once this was determined, the only alternative was to lower the flow rates to those appliances to 3 lb/min, the same as is required for the shower and hand wash. The dishwasher and laundry now draw 3.7 kW each while the shower and hand wash require 2.1 kW (the difference coming from the delivery temperature). Simultaneous use of more than one appliance would bring the power draw up to around 5 kW (7 percent of total station power). A potentially disastrous scenario would be the simultaneous use of all appliances drawing over 15 kW. The potential for the baselined water heating system to cause serious mission constraints is what prompted the search for alternative water heating systems.

2.2 Waste Heat Availability

The proposed SSF will have power levels at 75 kW initially, with growth projected to 300 KW and beyond. Waste heat will be generated not only from the power production process, but also from life support systems, air conditioning, lighting, electronics, experiments, refrigeration and numerous other processes. Each of these processes produce waste heat at different temperatures and different locations within the space station. The currently envisioned thermal management system will employ several thermal buses used in the acquisition, transportation and rejection of waste heat. Externally, two-phase ammonia loops operating isothermally at 62°F and 35°F will transport waste heat to a central radiator system for rejection to space. Internally, a single-phase water loop will collect waste heat from the various temperature sources and transport it to an interface heat exchanger where the waste heat is transferred to the external thermal bus. As a result of the sensible heat transfer from the waste heat sources to the single-phase water loop, the water temperature will rise. Since the water temperature is expected to significantly increase and it is located internally, it was selected as the heat source for the nonazeotropic heat pump water heater.

Initial information provided to Foster-Miller on the Habitat waste water loop is listed in Table 3. The heat rejection load was anticipated to be fairly constant ranging from 13 to 15 kW. To simplify controls, a single loop was anticipated with constant water flow rate and a maximum return temperature of 40°F. The temperature of the waste water loop available for the heat pump system would then be 76 to 82°F. The laboratory module was to have higher heat rejection loads but would vary considerably over time. Shortly after design work began on the Phase II program, a redesign of the waste water loop was done. At that time Body Mounted Radiators (BMR) were being considered. Due to the limited amount of surface area available for radiators, the heat rejection temperatures had to be increased in order to reject the anticipated loads. The water flow

Table 3. Thermal Rejection Loop

- | |
|---|
| <ul style="list-style-type: none">• Heat rejection load - 13 to 15 kW• Water flow rate - 1,230 lb/hr \Rightarrow 731 lb/hr• Heat rejection temperature - 65 to 82°F \Rightarrow 110°F• Maximum return temperature - 40°F |
|---|

rate was, therefore, decreased and the heat rejection temperature increased to 110°F. Recently, another redesign was done, eliminating BMRs and changing to two module water loops, a high and a low temperature loop. As of this writing, the redesign was incomplete, and therefore, not considered in this program.

2.3 Material Constraints

The hygiene water heating heat pump would be interfacing with existing SSF systems, and thus, had to meet the requirements of those systems for integration into the SSF. The primary interfaces are through heat exchangers with the waste water loop and the hygiene water system. Additionally, if the heat pump is to be contained within the crew compartment, it must be designed to meet the safety standards required of all internal equipment.

Initially we had planned on fabricating lightweight tube-in-tube aluminum heat exchangers. However, the potential for corrosion of aluminum in water systems was discussed with Boeing personnel, and it was determined that aluminum is not an allowable material. The allowable alternatives are stainless steel or titanium. Titanium was not considered for the prototype development program due to its high cost but may be considered in the future for space hardware. It was also determined that titanium is incompatible with halogens and cannot be used except for water containment tubing where contact with the heat pump refrigerants is not possible. Further investigation revealed that some composites and plastics may eventually be allowed in SSF. These materials are impractical for refrigerant containment but may provide a lightweight outer tubing for water containment. Further restrictions on the heat exchangers include a limit of 1 psi pressure drop imposed on the waste water loop. No such restrictions were identified for the hygiene water loop.

Conversations with systems safety and reliability personnel at NASA and Boeing revealed that halogenated compounds, such as the heat pump refrigerants, could be life threatening if released into the atmosphere of the crew compartment. The refrigerants are not considered toxic when inhaled in small quantities. However, should any halogenated compounds reach the Trace Contaminant Control System (TCCS), it would destroy the platinum catalytic burner, rendering the system inoperable. Furthermore, when exposed to high temperatures (in the TCCS), the refrigerants would decompose into a toxic hydrofluoric acid. For these refrigerants to be acceptable within the crew compartment, double containment must be designed into the system as well as some form of leak detection. Double containment implies that should a single point failure develop and a leak occur, a second means of containment is present to stop the release of refrigerants. The leak detection system indicates this condition before it results in a hazard to the crew.

3. SYSTEM CONFIGURATION

The main design goal of the nonazeotropic heat pump was to minimize the power draw required for water heating and thus help reduce the demand on the SSF power production system. In order to meet this goal, a central storage tank and delivery system was employed. The heat pump size (and power draw) may be minimized in this concept as production of hot water is independent of the end use requirements. Two types of systems were considered based on the previous NASA study, namely, Centralized On-Demand, and Centralized Delayed. In both concepts, a single tank provides hot water for all appliances in the module. Descriptions of each system considered are contained in the following sections.

3.1 Centralized On-Demand

In the Centralized On-Demand concept the heat pump system maintains a small water flow through the distribution line so that the water available at the appliance is always hot. Figure 9 is a schematic of the Centralized On-Demand heat pump system (the cold water distribution lines to each appliance are not shown). Hygiene water from both the waste treatment storage and the distribution manifold is passed through the condenser of the heat pump system where it is heated to approximately 145°F. The source of this heat is a combination of heat removed from the module thermal rejection loop and the work of compression associated with the heat pump cycle. The heated water then passes to a storage tank that serves to correct differences between hot water demand and the rate at which the water is heated by the heat pump. The circulation pump draws hot water out of the storage tank and delivers it to the distribution line on a continuous basis. As the water flows through the system, it cools slightly due to ambient losses. After the distribution line, a small amount of makeup water from the wastewater treatment storage tank is added to the circulation stream, decreasing the temperature of the water prior to the heat pump. The cool water then enters the condenser for heating to 145°F. The heat pump is sized to run continuously, with a constant water flow rate entering the condenser. The temperature of the water is determined from the ratio of the recirculation stream and the makeup stream from treatment storage. The storage tank size must be selected so that the demand can be met during heavy use periods and the refill rate should be selected so that the heat pump can run continuously for minimum power draw. The advantages of this system include: hot water is available on demand; no water is wasted at the appliances while waiting for hot water; and the water in the loop is maintained at a high temperature continuously, preventing microbial growth. The disadvantages of this design include a large energy consumption to circulate and maintain hot water in the lines.

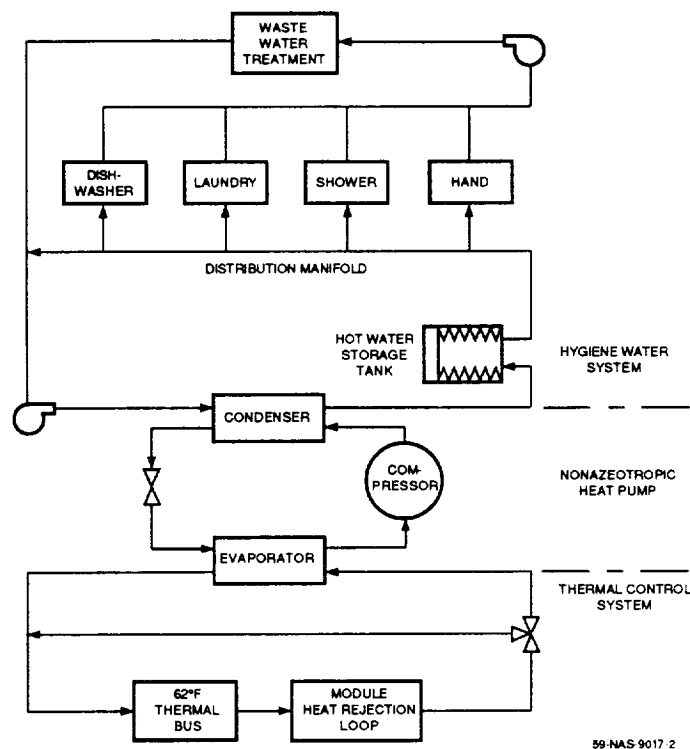


Figure 9. Centralized On-Demand Heat Pump Water Heating Concept

3.2 Centralized Delay

In the Centralized Delay system the heat pump operates only when the hot water storage tank calls for makeup water (after appliance use) or when the tank temperature has dropped below the set point (due to ambient losses). Figure 10 schematically illustrates the operation of the Centralized Delay heat pump system. Water is drawn out of the waste treatment storage tank at approximately 70°F (ambient) and is passed through the condenser of the heat pump system where it is heated to approximately 145°F. The source of this heat is a combination of heat removed from the module thermal rejection loop and the work of compression associated with the heat pump cycle. The heated water is then sent to a storage tank. Hot water is drawn out of the tank as required by the end use appliances.

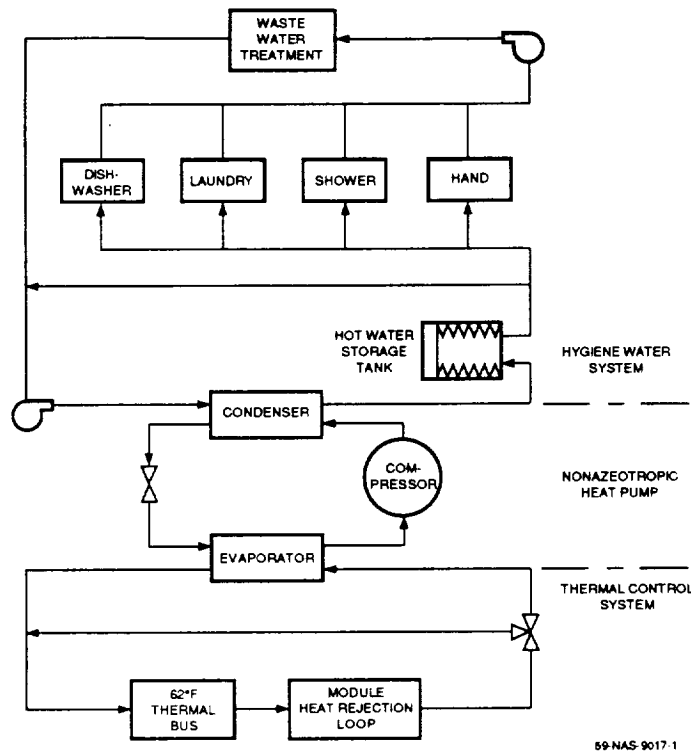


Figure 10. Centralized Delay Heat Pump Water Heating Concept

The storage tank employs a bellows diaphragm with a precharge of air or nitrogen on the back side. The diaphragm expands or contracts with a change in water volume. A pressure sensor may be used to measure the pressure of the water or air in the tank as an indication of water volume. A drop in pressure would signal a decrease in tank water volume which would activate the heat pump compressor and the water pump. Makeup water flows through the heat pump condenser at a constant flow rate until the tank pressure is returned to the full set point. The storage tank size is selected so that the large demands of the dishwasher and laundry can be met while the refill flow rate is selected to minimize the size of the heat pump system and thus the power draw.

A temperature sensor, located in the storage tank, would be used to activate the heat pump system should the water temperature in the tank fall below the set point. In this case, a recirculation pump draws water out of the tank and passes it through the heat pump condenser to reheat it. When the tank temperature increases beyond the set point, the system is deactivated. Due to the higher water temperature entering the condenser in this mode, the discharge pressure will be higher than in normal operating conditions resulting in a lower COP. However, reheat conditions would occur relatively infrequently and for short periods of time.

On the thermal control system side, a small portion of the module water loop at approximately 110°F is routed through the heat pump evaporator providing the heat source. After rejecting heat energy to the evaporator, the cooler water is reunited with the main stream prior to the interface with the external thermal bus. In this configuration, the flow of water through the evaporator may occur at all times (regardless of heat pump status) or it may be turned off when the heat pump is not active.

An initial evaluation of the two heat pump systems described above, revealed that the Centralized On-Demand system would consume more energy providing hot water on a continuous basis than the Centralized Delay system. Since current NASA constraints do not require continuous heating for microbial growth control, the Centralized Delay system was selected for further development.

4. WORKING FLUID SELECTION

A preliminary investigation into the working fluid for the nonazeotropic heat pump was done once the heat sink and source temperatures were defined. To obtain the highest possible cycle efficiency, the phase change temperature glide of the working fluid should match the temperature change of the heat sink and source. In this application, the heat sink (hygiene water) undergoes a 75°F change in temperature as it is heated from ambient to 145°F. The heat source (module heat rejection water loop) is available at 110°F and may be cooled to 40°F for a 70°F change. The first step in the mixture selection process was to identify all potential candidates which produce a 70 to 75°F glide during the phase change.

Computer routines were utilized to generate the thermodynamic properties of various refrigerant pairs and compositions in order to predict the phase change temperature glide. The routines were developed at the National Institute of Standards and Technology (NIST), formerly National Bureau of Standards (NBS) (2). The list of candidate mixtures considered was narrowed down to six mixtures in Table 4 which meet the 70°F glide requirement. A simple model was written to perform heat pump cycle calculations to determine system state points and COP. This model is described in more detail in subsection 5.2. The model was run with the six different working fluids at various compositions. The mixture with the highest COP potential was identified as R-11/R-22. The exact composition of the mixture would be optimized in the more detailed modeling to follow.

Table 4. Binary Mixture Candidates

Mixture	Composition	Evaporator Pressure (psia)
R-13/R-113	0.012	10.7
R-13/R-11	0.035	24.7
R-13/R-11	0.866	244.1
R-22/R-113	0.055	11.8
R-22/R-113	0.710	59.4
R-22/R-11	0.240	32.0

5. SYSTEM MODELING

Several models were developed to assist in sizing and designing system components. The first items to be determined in the design process were the hot water storage tank size and refill rate. Once these two parameters were known the heat pump size could be determined as the tank refill rate is actually the flow rate through the condenser. Cycle calculations were then done to determine compressor size and heat transfer rates. Heat exchanger models were then utilized to select tube diameters and lengths. A Life Cycle Cost (LCC) model was formulated incorporating many of the other models to perform trade studies and arrive at the final system design.

5.1 Storage Tank Model

In order to size the water storage tank and determine the refill rate, a simple model was written to calculate the amount of hot water in the tank as a function of the time of day. The anticipated SSF hygiene water requirements listed in Tables 1 and 2 and the equipment use schedule of Figures 6 and 7 were used as input to the model. In all, four different hot water usage profiles were examined: Boeing Peak, Boeing Nominal, NASA Peak, and NASA Nominal profiles. For a given tank size, the refill rate (hygiene water flow rate through the condenser and into the tank) could be determined. The flow rate was selected so that a fair amount of reserve capacity would be maintained in the tank so that unexpected operation could be handled. At the same time, the flow rate was minimized so that the heat pump size and power draw would be minimized. Table 5 lists the refill rates determined for tank sizes ranging from 6 to 14 gal for each of the hot water usage profiles examined.

Figure 11 shows the storage tank water level versus the time of day for a 14 gal tank with a refill rate of 41 lb/hr subjected to the Boeing Nominal usage schedule. (Tank size and refill flow rate were selected by MSFC as explained in subsection 5.5.) When the curve has a negative slope, an appliance is in use and water is drawn from the tank. Any time the tank level is below 14 gal, the heat pump is activated and the tank is gradually refilled. Under these conditions, the heat pump has a duty cycle of approximately 50 percent. Decreasing the refill rate would result in a higher duty cycle and lower power draw while decreasing the tank size would result in a smaller reserve capacity.

Table 5. Storage Tank Refill Rates (lb/hr)

Water Usage Profile	Tank Size (gal)				
	6	8	10	12	14
Boeing Peak	263	199	143	91	40
Boeing Nominal	112	83	63	41	21
NASA Peak	229	165	106	46	15
NASA Nominal	103	77	56	34	15

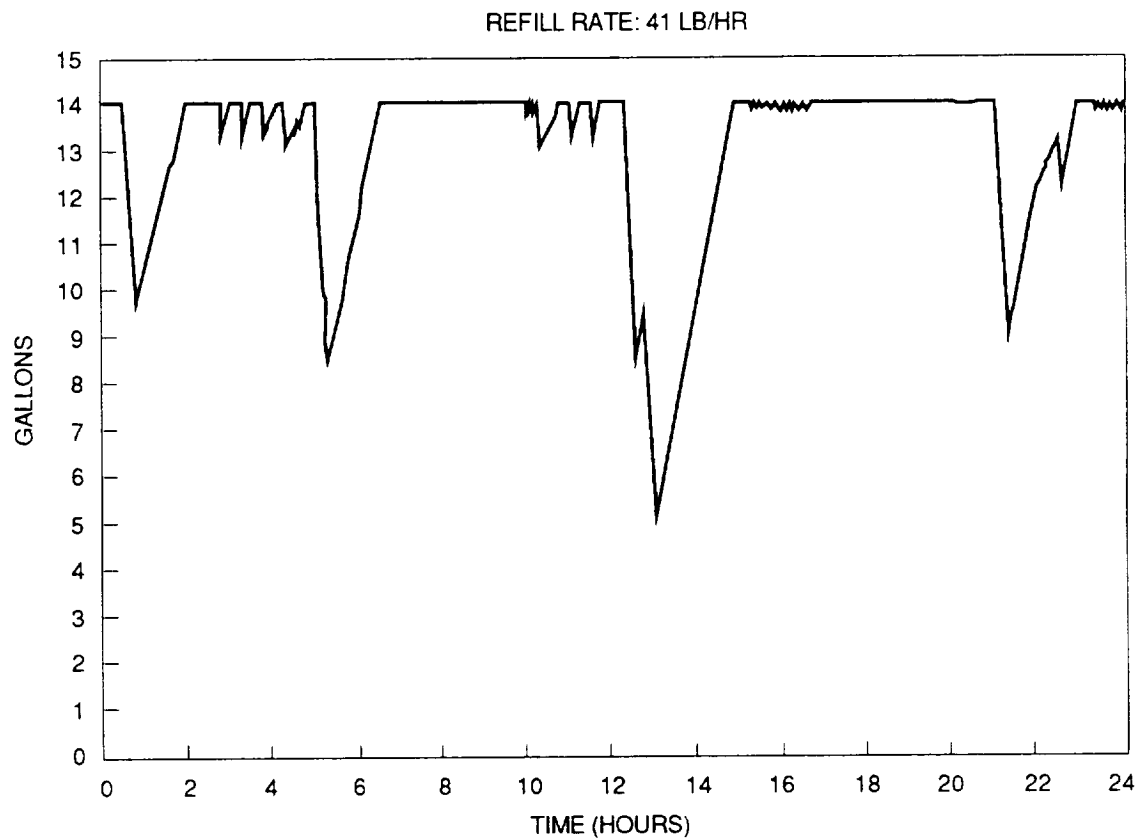


Figure 11. Storage Tank Water Level

5.2 Cycle COP Model

A simple model was developed to calculate heat pump cycle state points, heat transfer, compressor power, and COP. The model is based on the nonazeotropic thermodynamic properties routines (2). The required inputs include the water temperature entering and exiting the heat exchangers, the water flow rate through the condenser, assumed refrigerant pressure drops, compressor efficiency, and refrigerant mixture. The model was used to determine the refrigerant mixture which produced the maximum COP.

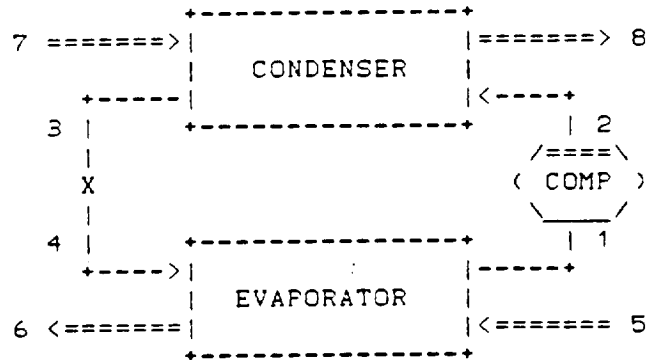
A water temperature of 145°F was selected for the condenser outlet (storage tank inlet) and 70°F was assumed at the condenser inlet. The water temperature entering the evaporator was set at 110°F. A compressor efficiency of 75 percent and heat exchanger pressure drops of 3 psi were assumed. The model was then run for a range of evaporator outlet temperatures and refrigerant mixtures. The mixtures varied both in composition and constituents.

Figure 12 shows the results of this exercise for the maximum COP obtained. These results were generated with a 50°F evaporator outlet temperature. The total temperature change through the evaporator, 60°F is less than the 75°F change through the condenser. This is due to two factors: firstly, the pressure drop in the heat exchangers tends to increase the glide in the condenser and decrease the glide through the evaporator; and secondly, the refrigerant enters the evaporator as a two-phase mixture due to flashing across the expansion device, so that the full phase change temperature glide is not available.

5.3 Heat Exchanger Model

In order to determine the required lengths of the heat exchangers, models for heat transfer and pressure drop were developed for the condenser and evaporator. The routines are similar in that they each model a coaxial counterflow heat exchanger starting at the refrigerant inlet (water outlet) end. The heat exchangers are broken down into sections corresponding to quality changes of 10 percent. The heat transfer coefficient and pressure drop are calculated for each section so that the outlet conditions (refrigerant temperature, pressure, and water temperature) may be determined. The length of heat exchanger required for that section is then calculated. The calculations are repeated for the next 10 percent quality change section and so on until the heat exchanger outlet is reached. The total length required for the heat exchanger is then determined by summing the lengths for each section.

REFRIGERANT MIXTURE ANALYZED: 24. % R22 / 76. % R11
 ASSUMED COMPRESSOR EFFICIENCY: 75. PERCENT



POINT	DEG F	PSIA	H	S	LB/HR
1	104.	37.1	108.3	.20854	25.0
2A	157.	75.5	114.7	.20854	25.0
2	170.	75.5	116.8		25.0
3	74.	71.5	26.7		25.0
4	45.	39.4	26.7		25.0
5	110.				34.0
6	50.				34.0
7	70.				30.0
8	145.				30.0

CONDENSER HEAT REJECTION : 2250. BTU/HR
 EVAPORATOR HEAT ABSORPTION : 2038. BTU/HR
 COMPRESSOR WORK : 212. BTU/HR
 COMPRESSOR POWER CONSUMPTION : 62. WATTS
 COEFFICIENT OF PERFORMANCE : 10.59

Figure 12. Heat Pump Cycle Calculation

The heat transfer coefficient correlation used in the condenser model is one recommended by DeGrush and Stoecker (3). In (3), DeGrush and Stoecker measured condensing heat transfer coefficients for refrigerant mixtures and compared them to the results of several correlations developed for single component refrigerants. A few showed relatively good agreement over limited ranges. For lack of a general condensing coefficient correlation, the best fitting correlation from (3) was used here. The pressure drop correlation was taken from work done at Foster-Miller (4).

Even less has been published for boiling heat transfer coefficients than for condensing of binary mixtures. As a result, a correlation which shows good agreement for single component evaporation was taken from Eastman (5). This correlation was modified with a factor to account for the decreased heat transfer coefficient characteristically found with nonazeotropic mixtures. A 30 percent reduction in the coefficient was assumed. The pressure drop correlation for the evaporator is the same as used in the condenser model.

The required inputs to the condenser and evaporator models are the inlet refrigerant temperature and pressure, the water temperature entering and exiting, the refrigerant mixture, and the tube-in-tube geometry (i.e., OD, ID, number of fins, etc.). The output from the routines are the refrigerant temperature and pressure at the outlet and the total length of coaxial tube required.

5.4 Life Cycle Cost

A model was developed which combines the heat pump cycle COP model with the heat exchanger model for the evaporator and condenser together with a Life Cycle Cost (LCC) routine. The model was used for integrating and sizing heat pump components and for performing trade studies to determine the effects of various parameters on the LCC.

The LCC model first calculates heat pump cycle state points based on assumed heat exchanger performance. The compressor discharge temperature and pressure are then used as input to the condenser routine. The condenser model calculates refrigerant and water conditions throughout the heat exchanger, the refrigerant pressure drop, and the condenser length required. The refrigerant enthalpy at the condenser outlet is then used as input to the evaporator routine (constant enthalpy through the expansion valve). The evaporator model calculates refrigerant and water conditions throughout the heat exchanger, the refrigerant pressure drop, and the evaporator length required.

The temperature and pressure of the refrigerant exiting the evaporator are then input to the cycle model. An iterative method is used until the cycle state points have converged. The heat exchanger heat transfer rates, the compressor power, and the system COP are then calculated.

Once convergence on the cycle state points is obtained, the LCC section calculates the heat exchanger weights and volumes as well as the storage tank weight and volume based on its storage capacity. The weight of the components does not include the working fluid or the water as these are common to all configurations. Compressor run time is multiplied by the power consumption to obtain the energy consumption per day. This value is then multiplied by the number of days in a 10-year life to obtain the total energy. The total weight of the heat exchangers and storage tank is multiplied by \$4,550/lb. The total volume is multiplied by \$900/ft³/month and 120 months in the 10-year life. The total energy is multiplied by \$210/kWhr. The weight and volume of the compressor and expansion device are not included in the analysis at this point because they would essentially be the same for each of the systems investigated and thus cancel out in the comparison.

The LCC model was used to determine the effects of changes in hardware and operational strategies on the total system cost. Table 5 lists the input to the LCC model. The first four inputs define the refrigerant mixture followed by the assumed compressor efficiency. Next, water temperatures in and out of the heat exchangers are specified along with the desired flow rate through the condenser. The minimum temperature differences between the refrigerant and water temperatures in the heat exchangers (also known as the pinch point) are specified as well as the hot water storage tank size. The rest of the inputs define the heat exchanger geometries for a tube-in-tube arrangement.

5.5 Trade Studies

The LCC model was exercised over a range of most of the variables found in Table 6 (water temperatures in and out of the heat exchangers were held constant). Figure 13 show the results of a range of compressor efficiencies from 35 to 75 percent on the LCC. As expected, the energy consumption increases as the compressor efficiency decreases. However, there is a positive side to the efficiency decrease; namely, a decrease in heat exchanger weight and volume. The condenser size is decreased due to the increased refrigerant temperature discharged from the less efficient compressor. The high refrigerant temperature creates a higher temperature difference between the refrigerant and water, resulting in less area required to transfer the same amount of energy. This example illustrates the importance of the trade studies. It is the overall effect on LCC

Table 6. Life Cycle Cost Model Inputs

IR1	Refrigerant A
IR2	Refrigerant B
X	Mass Percent of A
F	Interaction Parameter
EFF	Compressor Efficiency
T5	Water Temperature into Evaporator (F)
T6	Water Temperature out of Evaporator (F)
T7	Water Temperature into Condenser (F)
T8	Water Temperature out of Condenser (F)
H2OM	Water Flow Rate Through Condenser (lbm/hr)
DTE	Delta T Minimum for Evaporator
DTC	Delta T Minimum for Condenser
TANKG	Storage Tank Size (gal)
DOOC	Condenser Outer Tube OD (ft)
DOIC	Condenser Outer Tube ID (ft)
DIOC	Condenser Inner Tube OD (ft)
DIIC	Condenser Inner Tube ID (ft)
NFNC	Number of Fins in Condenser
FINHC	Fin Height (ft)
FINTC	Fin Thickness (ft)
DOOE	Evaporator Outer Tube OD (ft)
DOIE	Evaporator Outer Tube ID (ft)
DIOE	Evaporator Inner Tube OD (ft)
DIIE	Evaporator Inner Tube ID (ft)
NFINE	Number of Fins in Evaporator
FINHE	Fin Height (ft)
FINTE	Fin Thickness (ft)

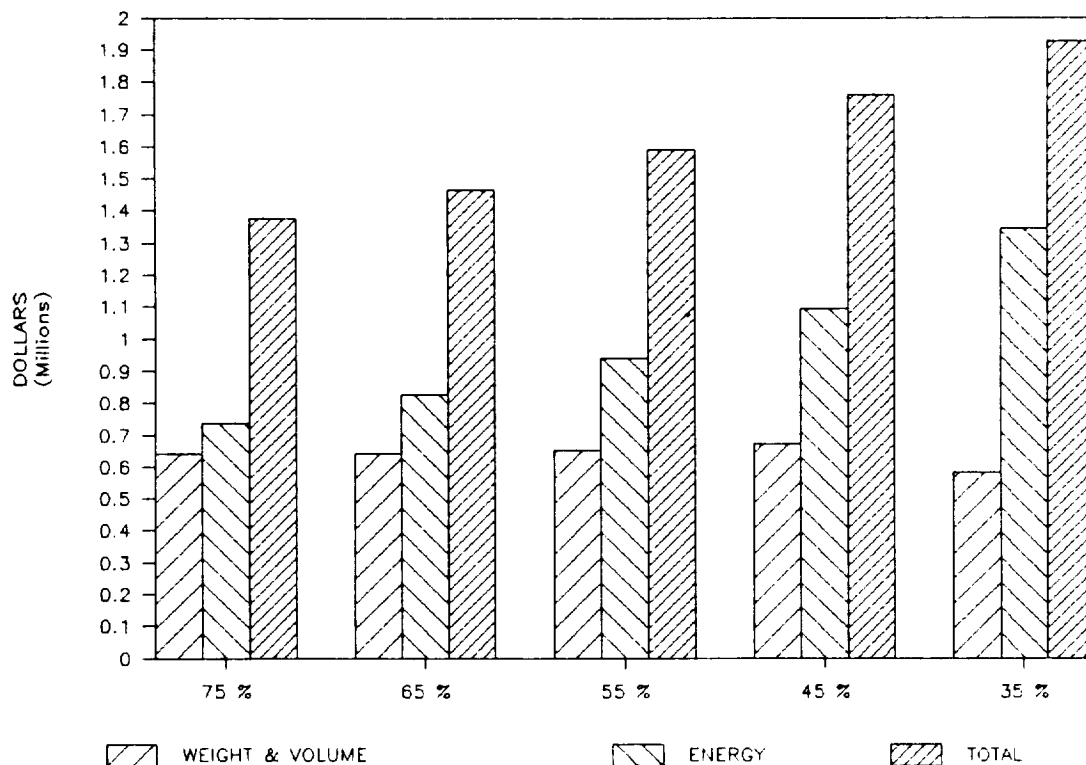


Figure 13. Life Cycle Cost versus Compressor Efficiency

that is important. In this case, the savings from the decrease in system weight and volume are not enough to offset the penalty of increased energy consumption: the highest compressor efficiency possible results in lowest LCC.

Another variable of interest is the heat exchanger pinch point. A small pinch point results in a high COP because the pressure ratio (condenser pressure to evaporator pressure) is minimized. However, the log mean temperature difference for the heat exchangers is at a minimum, thus increasing the heat exchanger area required. Figure 14 shows the results of varying the heat exchanger pinch point on the heat pump LCC. As can be seen, the energy consumption increases and the weight and volume cost decreases with increasing pinch point. The overall result is the same as decreasing the compressor efficiency: the weight and volume savings from increased pinch point are not enough to offset the penalty of increased energy consumption.

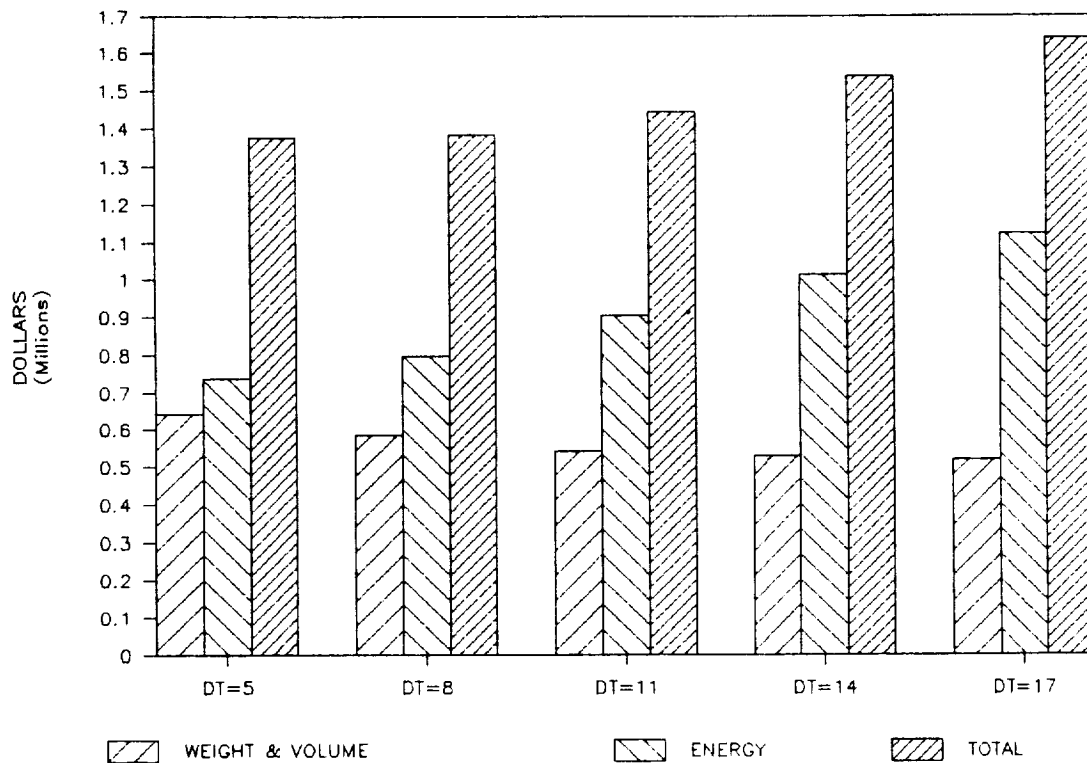


Figure 14. Life Cycle Cost versus Heat Exchanger Pinch Point

The optimum storage tank size was also investigated using the LCC model. Figure 15 shows the LCC as function of tank size for a range covering from 6 to 14 gal. As the tank size decreases, the refill flow rate (and heat pump size) increases as shown in Table 4. The heat exchanger tube geometry was not altered with the flow rate; thus, the pressure drop through the condenser and evaporator increases with flow rate. The pressure drop increase results in a COP decrease (energy increase). As explained above, the COP decrease results in heat exchanger area reduction (due to increased refrigerant temperature) and an associated weight and volume decrease. These complicated relationships can be summarized as shown in Figure 15. As can be seen, the energy consumption increases as the tank size decreases. This is offset somewhat by a weight and volume decrease. The interesting result is a slight dip in LCC at the 12 gal tank size before a gradual increase in LCC with further tank size reductions. After a review meeting at MSFC, a 14 gal tank was selected with the refill rate for the 12 gal tank. This configuration results in a slightly larger heat pump system than is necessary, however, it also provides a larger amount of reserve capacity.

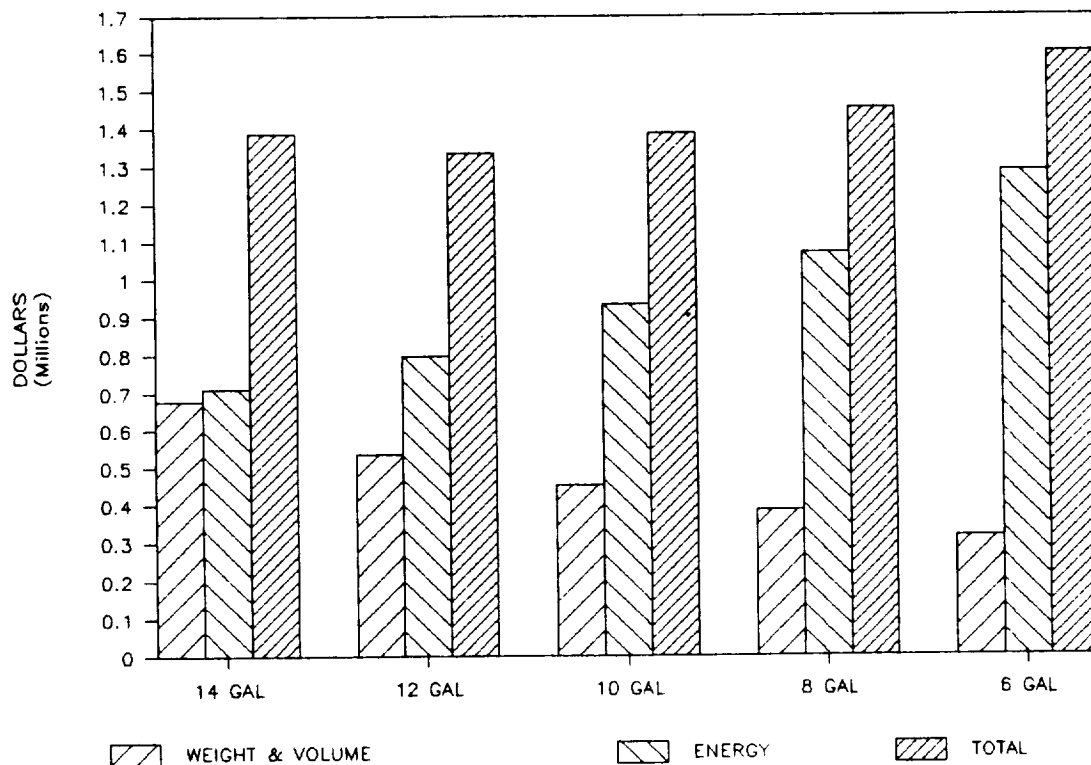


Figure 15. Life Cycle Cost versus Storage Tank Size

The LCC model was also used to determine the optimum tube sizes and lengths for the heat exchangers. It had been determined early on that a tube-in-tube configuration would be best for this application. Nonazeotropic mixtures require a counterflow heat exchange arrangement and coaxial tubes are the simplest means for achieving this. The tubing also lends itself to compact packaging by coiling the tubes into a tight diameter. The inner and outer tube diameters and wall thicknesses were varied in the study. Various numbers and configurations of fins were investigated on the outside of the inner tube and water and refrigerant were varied from the inner tube to the annulus between tubes. In all, 128 different configurations were investigated in the initial study. The top ten candidates are listed in Table 7. Included in the table are the heat exchanger lengths and weight, the heat pump COP, and the LCC. As can be seen, a low COP is desirable but it does not always produce the lowest LCC. The configuration with the lowest LCC used bare tubes, however, the next four all have fins on the outside of the inner tube extending to the inner wall of the outer tube. Also note that the change in LCC for these various configurations is relatively small.

Table 7. Life Cycle Cost versus Heat Exchange Tube Size

Run No.	Tube Sizes	No. Fins	Cond L (ft)	Evap L (ft)	Weight (lb)	COP	LCC (M\$)
34	1/2 x 5/16	0	68.9	74.7	29.2	9.43	1.414
117	5/8 x 5/16	16	31.1	38.8	36.8	9.71	1.418
114	11/16 x 3/8	18	29.4	41.2	42.0	9.83	1.437
120	9/16 x 1/4	14	33.4	25.9	27.2	8.58	1.472
111	3/4 x 7/16	20	27.9	45.5	48.7	9.86	1.473
18	9/16 x 5/16	0	72.5	77.4	52.4	9.40	1.533
8	11/16 x 7/16	0	58.5	68.7	57.2	9.81	1.533
83	7/16 x 1/4	0	113.5	98.5	36.0	8.55	1.536
78	1/2 x 5/16	0	116.9	104.7	45.0	9.06	1.538
3	3/4 x 1/2	0	53.8	73.2	63.4	9.92	1.563

6. SYSTEM DESIGN

System specifications and design criteria were established allowing a heat pump system configuration to be defined. Several models were then formulated to aid in the sizing, selection, and detailed design of the various system components. This section contains descriptions of the individual components designed for the nonazeotropic heat pump system.

6.1 Heat Exchangers

Tube-in-tube heat exchangers were selected for use in the heat pump system for several reasons. In order to match the temperature glides of a nonazeotropic working fluid to the heat sink and source, a counterflow heat transfer arrangement is required. The coaxial tube heat exchanger also has advantages when it comes to packaging as the tubes may easily be coiled in a diameter suitable to surround the other heat pump components. Two types of tube-in-tube heat exchangers were considered: bare tubes, and tubes with extended heat transfer surfaces. The latter was in the form of fins attached to the outside diameter of the inner tube and extending to the inside diameter of the outer tube. In the LCC trade studies, a bare tube heat exchanger had the lowest LCC, however, several finned tube arrangements were not far off. Interfacing with existing systems imposed constraints on the heat exchanger materials of construction. Stainless steel was found to be the only practical consideration for this program. In the search for fabricators of heat exchangers and heat exchange tubing, only one supplier was found that could provide stainless steel finned tube. This manufacturer was in Germany, had long lead times, and was quite expensive. There was also some uncertainty in the ability to coil the finned tubes in a tight diameter. Finned tubes were abandoned at this point and the design effort concentrated on bare tubes.

A review meeting at MSFC following the preliminary design task and LCC trade study revealed the necessity for a redesign of the condenser heat exchanger. The initial design featured coaxial construction with bare tubes and refrigerant flowing in the inner tube with water flowing in the opposite direction in the annulus between tubes. A leak in the inner tubing would allow refrigerant to flow into the hygiene water where it would be transported into the habitated spaces of SSF and released to the atmosphere when hot water is used. A double containment approach to the condenser was required to prevent a single point failure from endangering crew safety.

Several different design options were investigated to provide the double containment including heat pipes and adding a secondary loop. However, the approach which would least increase the LCC was found to be adding a third tube to the coaxial heat exchanger. The third tube would be inserted between the inner and the outer tubes of the previous design. The working fluid would still flow within the inner tube and the hygiene water would flow in the annulus between the middle and outer tubes. The gap between the inner most tube and the double containment middle tube was made as small as possible and filled with static water to promote heat transfer. The pressure of the static water would be monitored for leak detection. Figure 16 shows a cross section of the condenser tubing arrangement.

The LCC model was modified to account for the presence of a third tube in the condenser. The optimization for tube sizes was repeated with the results shown in Figure 17. The condenser consists of a 5/16 in. inner tube, a 3/8 in. middle tube, and a 1/2 in. outer tube. The evaporator does not require a double containment tube; double containment is provided by the hermetic enclosure of the heat pump and the containment of the thermal rejection loop water. The evaporator consists of a 5/16 in. inner tube and a 1/2 in. outer tube.

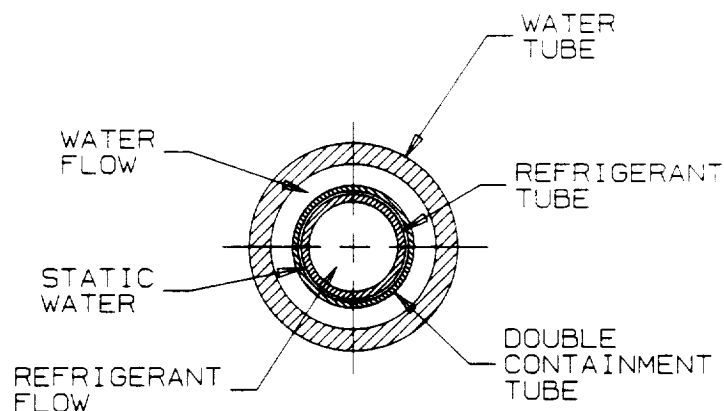
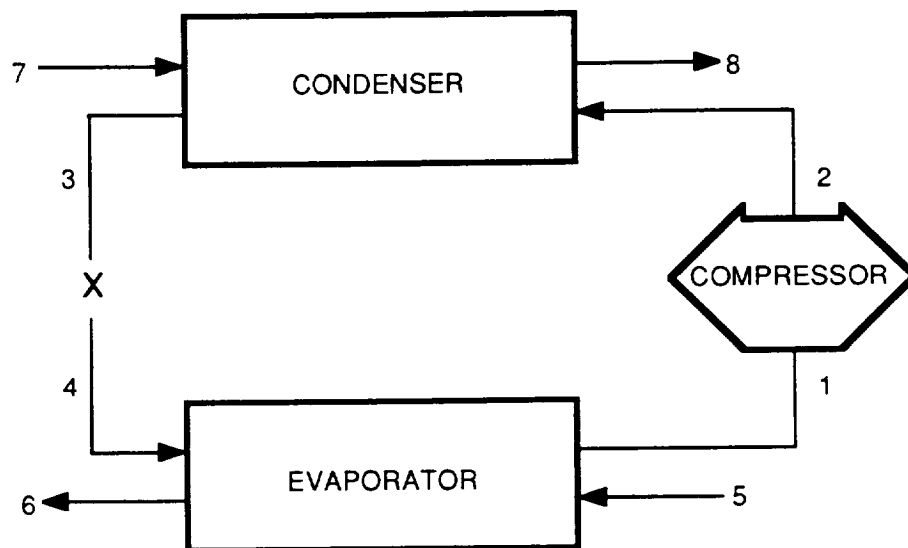


Figure 16. Condenser Cross Section

REFRIGERANT MIXTURE ANALYZED: 24.0% R-22/76.0% R-11
 ASSUMED COMPRESSOR EFFICIENCY: 70.0%



Point	°F	Psia	H	S	lb/hr
1	102.0	35.4	108.1	0.20889	33.4
2A	163.0	79.5	115.4	0.20889	33.4
2	182.0	79.5	118.5		33.4
3	73.0	77.7	26.5		33.4
4	45.0	39.5	26.5		33.4
5	110.0				45.4
6	50.0				45.4
7	70.0				41.0
8	145.0				41.0

CONDENSER HEAT REJECTION: 3075 Btu/hr
 EVAPORATOR HEAT ABSORPTION: 2727 Btu/hr
 COMPRESSOR WORK: 348 Btu/hr
 COMPRESSOR POWER CONSUMPTION: 102W
 COEFFICIENT OF PERFORMANCE: 8.83

Figure 17. Nonazeotropic Heat Pipe Cycle Calculation

CONDENSER CONFIGURATION:

REFRIGERANT IN INNER TUBE

D1 = 0.041667
 D2 = 0.037000
 D3 = 0.031250
 D4 = 0.027917
 D5 = 0.026042
 D6 = 0.021375
 NFINS = 0
 FINH = 0.000000
 FINT = 0.000000

CONDENSER LENGTH: 56.605 ft
 CONDENSER WEIGHT: 17.323 lb
 CONDENSER VOLUME: 0.123 ft³
 CONDENSER REF DP: 1.783 psi
 CONDENSER H₂O DP: 2.880 psi

EVAPORATOR CONFIGURATION:

REFRIGERANT IN INNER TUBE

D1 = 0.041667
 D2 = 0.037000
 D3 = 0.000000
 D4 = 0.000000
 D5 = 0.026042
 D6 = 0.021375
 NFINS = 0
 FINH = 0.000000
 FINT = 0.000000

EVAPORATOR LENGTH: 71.133 ft
 EVAPORATOR WEIGHT: 16.043 lb
 EVAPORATOR VOLUME: 0.154 ft³
 EVAPORATOR REF DP: 4.125 psi
 EVAPORATOR H₂O DP: 0.899 psi

STORAGE TANK WEIGHT: 59.700 lb
 STORAGE TANK VOLUME: 1.944 ft³

COMPRESSOR RUN TIME: 11.283 hr/day
 COMPRESSOR POWER: 102.007W
 COND WATER PUMP POWER: 0.207W
 EVAP WATER PUMP POWER: 0.071W

TOTAL WEIGHT: 93.066 lb
 TOTAL VOLUME: 2.222 ft³
 TOTAL ENERGY: 4203.847 kWh

WEIGHT COST: 423,450
 VOLUME COST: 239,939
 ENERGY COST: 882,808

TOTAL LIFE CYCLE COST: \$1,546,197

Figure 17. Nonazeotropic Heat Pipe Cycle Calculation (Continued)

6.2 Compressor

Operation of a compressor in a zero-gravity environment presents certain unique requirements including:

- Lubrication
- High overall efficiency
- Maintenance free operation
- No refrigerant leakage
- Low vibration and noise.

Several compressor types were evaluated as possible candidates for the heat pump application including piston, rotary, and scroll. Piston type compressors have a high number of parts which must be lubricated and are prone to unbalanced load and, therefore, potential high vibration levels. Rotary compressors are simpler to lubricate, have a high volumetric efficiency, but low mechanical efficiency due to friction between the elements. The scroll compressor is also simple to lubricate, has very low vibration and noise, while both the volumetric and mechanical efficiencies are very high. For this reason, the scroll compressor was chosen for the nonazeotropic heat pump.

The compliant scroll compressor consists of a pair of involute spirals bounded on one side by a flat plate or base (Figure 18). One of the scrolls is fixed while the other moves in a controlled orbit around a fixed point. The meshing of the involutes forms crescent shaped pockets, which, starting from the outside, reduce in volume as the orbiting scroll translates to increase the pressure of the trapped gas. The closed pockets move radially inward until a discharge pocket is uncovered, resulting in the discharge of high pressure gas. Valves are not needed at the inlet or outlet. Because the scrolls are compliant, they can tolerate liquid and oil slugs without damaging the compressor.

The sizing of the compressor was performed following the completion of the LCC trade studies using a 14 gal storage tank. The significant parameters which influence the compressor sizing are:

- Refrigerant mass flow rate: 33.4 lb/hr
- Inlet pressure: 20.7 psi
- Inlet temperature: 103°F
- Discharge pressure : 64.8 psi.

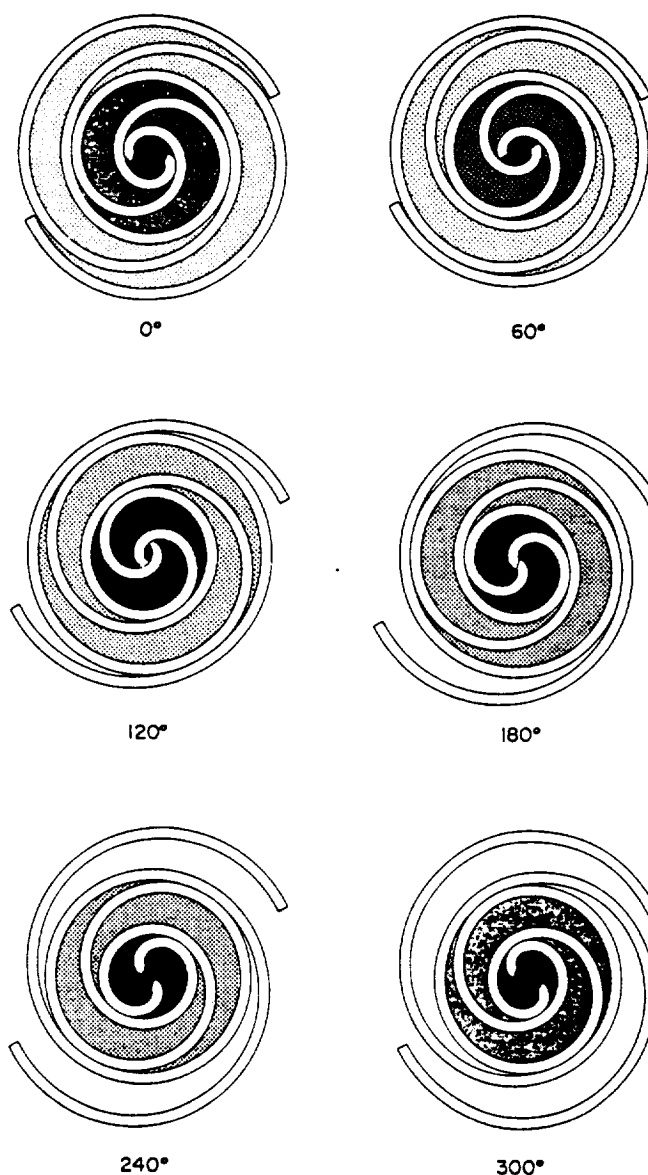


Figure 18. Sequence of Operation for the Scroll Compressor

The required compressor displacement was determined from the mass flow rate and the refrigerant gas density at the compressor inlet which was 0.76 lb/ft^3 . The resulting flow rate was then 1.55 cfm with an assumed volumetric efficiency at 0.5 . Over the speed range of 900 to $3,600 \text{ rpm}$, the required displacement was found to be 3.00 to $0.75 \text{ in.}^3/\text{rev}$.

The scroll components of the compressor are manufactured to very tight tolerances requiring special tooling and machining that would be cost prohibitive under this development program. However, in order to satisfy the requirements listed above for a zero-gravity compressor, it was

decided to design a new unit incorporating the scroll components from an existing commercial unit. A search of available commercial compressors identified a Copeland compliant scroll compressor with a displacement of 1.5 in.³/rev. and a fixed speed of 3,600 rpm as the smallest commercial unit available.

Figure 19 shows the scroll components of the commercial compressor. These components as well as the shaft of the commercial unit were used in the fabrication of the prototype heat pump compressor. A high efficiency brushless dc motor was placed on the shaft replacing the ac motor supplied with the unit. This change not only improves efficiency but also allows the compressor to run at the slower speed of 1800 rpm (which should result in longer life). The commercial unit uses an oil sump located at the base of the hermetic enclosure. The shaft connecting the compressor to the motor is hollow and extends beyond the motor into the oil sump. Oil is pumped up the hollow rotating shaft through centrifugal force and delivered to the points requiring lubrication. The oil then returns to the sump through gravitational forces. For the nonazeotropic heat pump application, which requires operation in low and zero gravity environments, special design measures had to be made to assure proper oil flow.

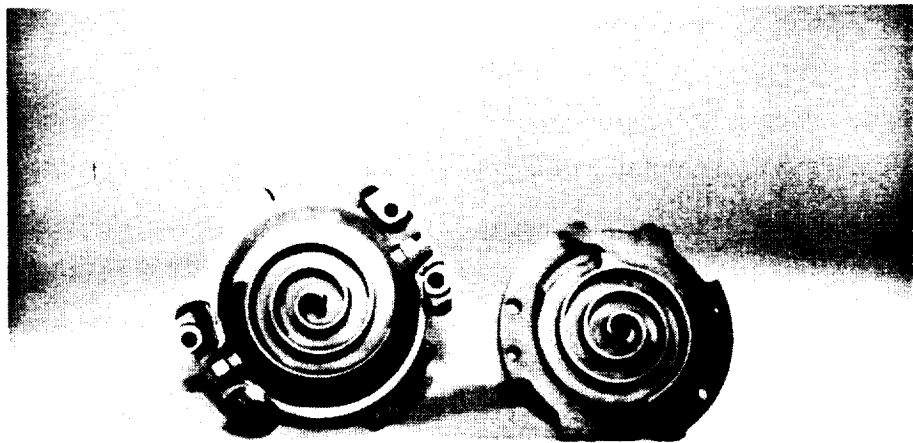


Figure 19. Compressor Scroll Components

Figure 20 shows the prototype version of the high efficiency heat pump scroll compressor. The top portion of the unit consisting of the scrolls and other components as well as the shaft have been retained from the commercial unit. The hermetic "can" of the commercial unit has been cut at 4.5 in. below the discharge port and welded to a steel flange so that the compressor section could be bolted to the middle and lower sections of the semi-hermetic enclosure. The bolted semi-hermetic arrangement was selected as opposed to a welded hermetic can so that the unit could be broken down easily for inspection. The suction inlet has been relocated from the side of the can to the bottom. The refrigerant gas is drawn into the scrolls through a foam wick material which runs circumferentially around the inside of the can to collect oil suspended in the cavity during zero-g operation. Counterweights attached to the shaft to balance the compressor help to sling the oil to the perimeter of the can where it is absorbed by the wick. The suction gas is drawn through the wick at a high enough velocity to entrain oil droplets and carry them into the scroll components. Oil removed from the compressor by the discharge gas is passed through a liquid/vapor separator and returned to the compressor. The returning oil is routed into the end of the hollow shaft where it is pumped to the lubrication points. The oil overflow from the lubrication points ends up in the motor cavity where it is absorbed by the wick material.

Certain other modifications were made to the compressor for this application. A feedthrough for control and power wires was used to maintain a hermetic seal. Motor cooling is normally accomplished in terrestrial applications through convection. In a zero-g environment, alternative methods must be employed. Cooling coils were epoxied to the surface of the hermetic enclosure. Hygiene water is pumped through the motor cooling circuit after exiting the condenser. In this manner, all energy entering the heat pump (waste heat through the evaporator and electricity through the compressor motor) is used in heating hygiene water. Mounting brackets provide for both vertical and horizontal mounting of the compressor to demonstrate its gravity independent operation.

6.3 Lubrication

One of the most important issues to be addressed in the heat pump compressor design is how to maintain lubrication of compressor bearings, mating surfaces, etc., in a weightless environment. As shown in Figure 20, an oil separator and recirculation scheme was selected for this application. The discharge gas stream is routed through the separator where the oil is isolated from the refrigerant gas. The gas is sent on to the condenser while the oil is returned to the compressor. The mechanism selected to accomplish this feat is known as a cyclone separator.

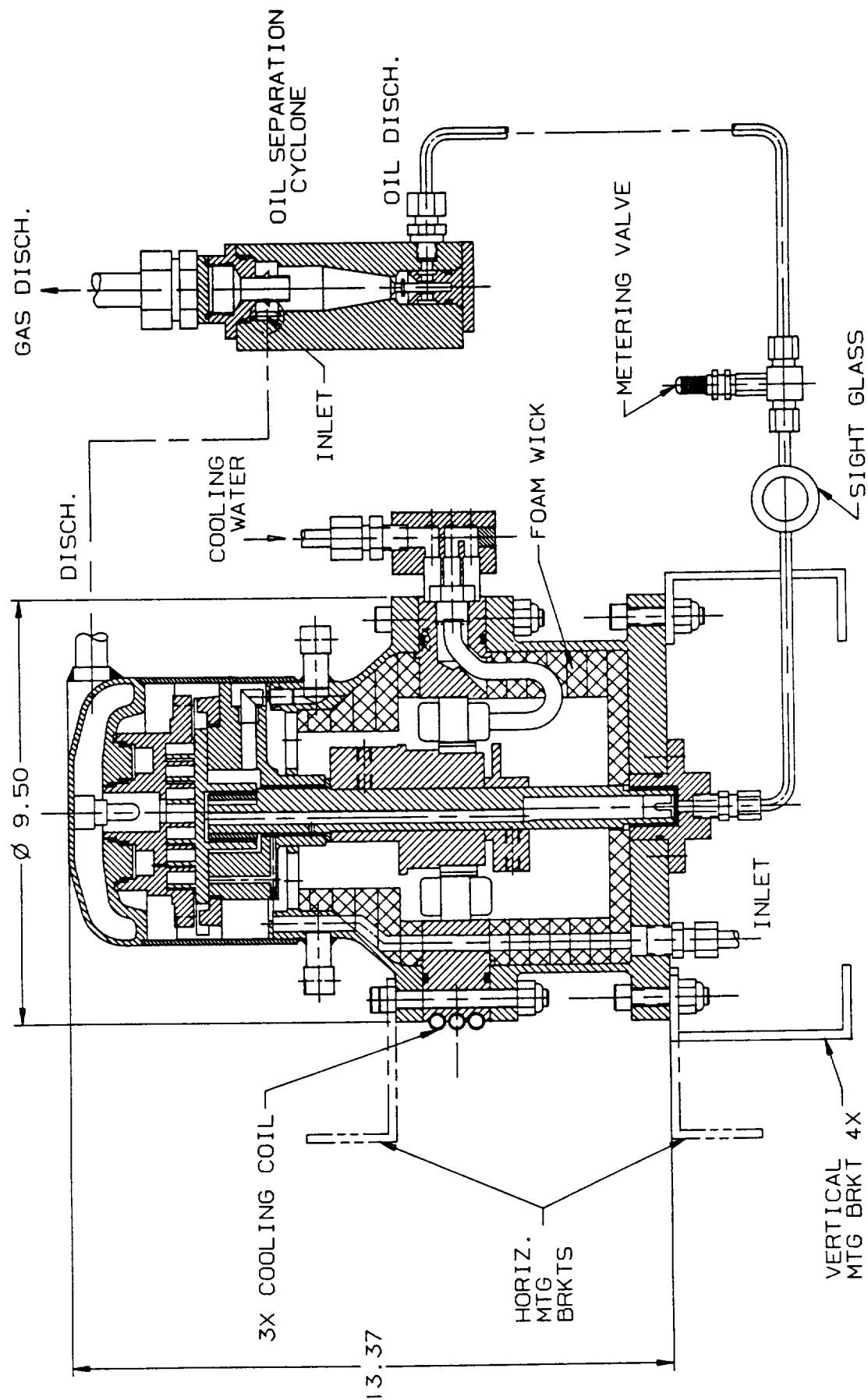


Figure 20. Prototype Heat Pump Compressor

A cyclone is a well known and proven system where particles are removed from spinning gases by centrifugal forces. The advantages of the cyclone over other alternatives are that it is extremely simple to construct, and it has no moving parts. The centrifugal force on particles in a spinning gas stream are much greater than gravity, allowing cyclones to be effective in the removal of very small particles, down to 10 microns or less.

Figure 21 is a full size cross section of the cyclone separator as designed for use in the nonazeotropic heat pump. The high pressure oil-gas mixture enters the cyclone through the inlet port on the left (not shown). The gases are admitted tangentially to the cylindrical upper section which contains a centrally placed exhaust pipe penetrating below the tangential inlet. A conical lower section leads to the oil outlet. The gases entering tangentially as shown in Figure 22, spiral down towards the apex of the cone creating an outer vortex. The oil is slung to the wall and is forced down the conical section to the exit. The gases are then reversed up creating an inner vortex which then proceeds through the exhaust outlet at the top of the cyclone.

The oil which is separated from the refrigerant gas is at the discharge pressure as it leaves the cyclone. A metering valve was used in the bench test to control the oil flow and to reduce the oil pressure to the suction level. The metering valve was replaced with a capillary tube in the final prototype configuration. Figure 23 shows the cyclone separator components before installation into the bench test.

6.4 Controls

The design of the hygiene water heating heat pump was based on the centralized delay concept of operation. In this configuration, the delivery of hot water to the appliances is done independently from the production of hot water by the heat pump. A hot water storage tank allows for a large flow of hot water in a short period of time while permitting the heat pump size and power draw requirements to be kept to a minimum. A control system was designed to activate the heat pump compressor and water pump in response to the storage tank conditions. Figure 24 schematically illustrates the nonazeotropic heat pump control system. The hot water storage tank temperature and pressure are continuously monitored by the heat pump controller. The storage tank contains a flexible diaphragm with a precharge of air or nitrogen on the back side. As the volume of water in the tank increases, the water pressure increases. The tank pressure is maintained high enough to deliver water to the appliances at the flow rates required without an additional pump. As water is drawn out of the storage tank by an appliance in use, the pressure decreases. The controller responds by activating the heat pump compressor and water pump.

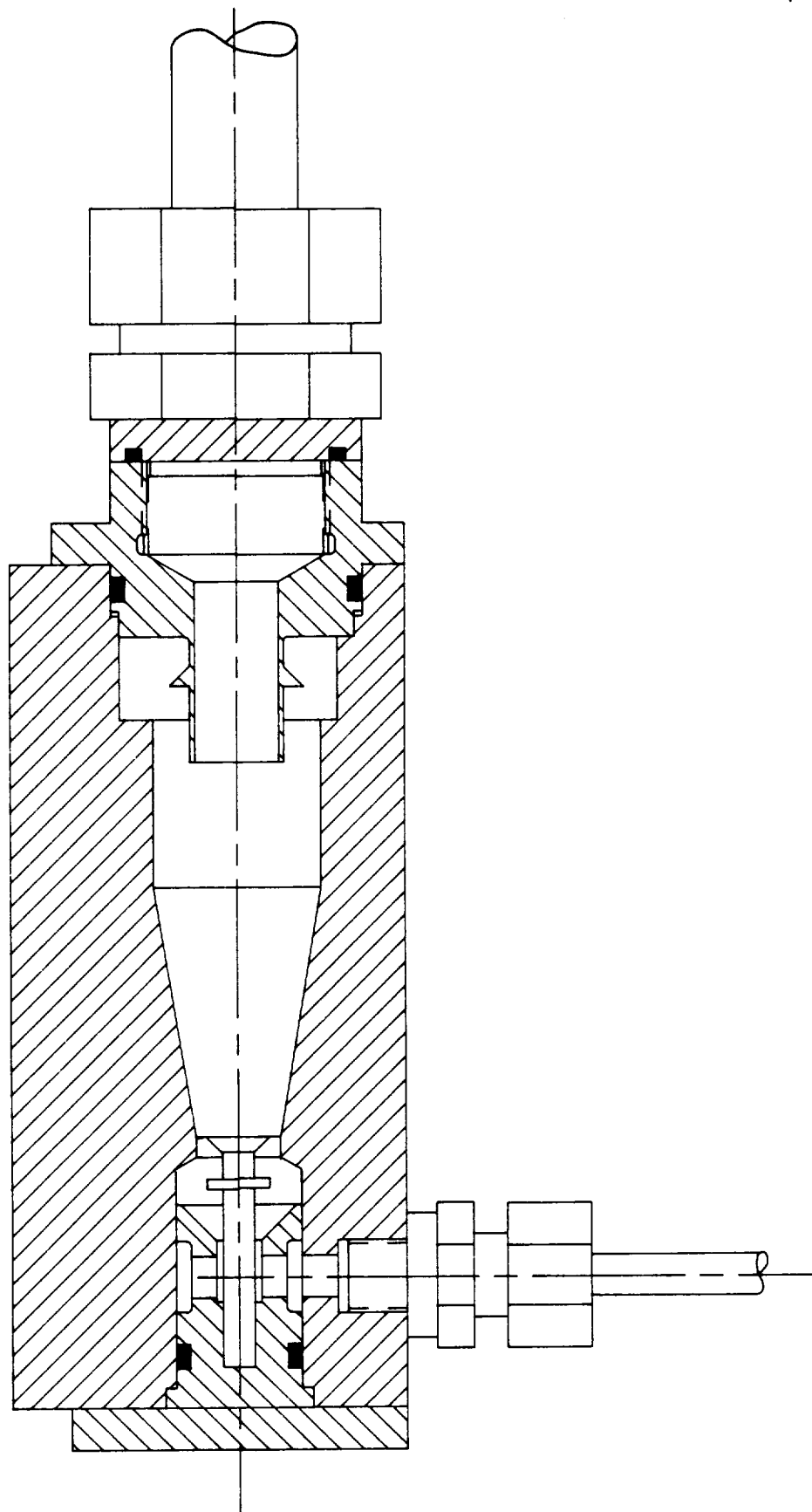


Figure 21. Cyclone Separator Cross Section

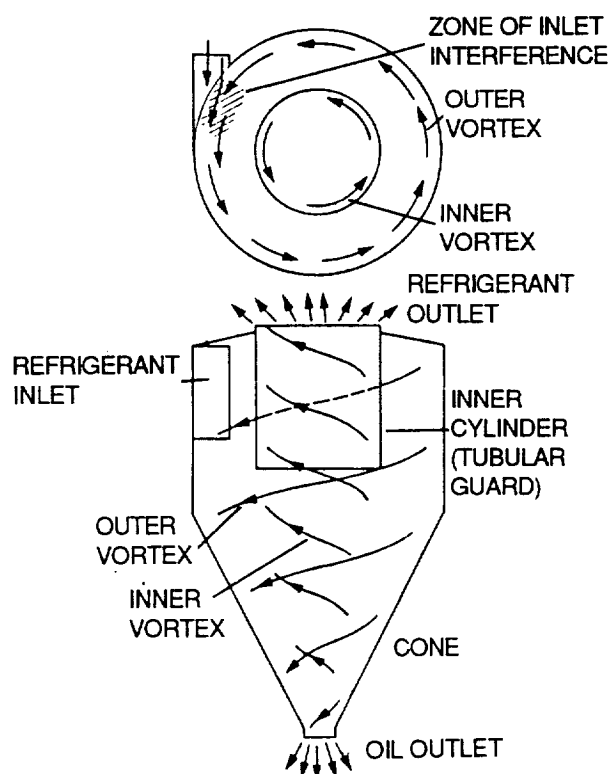


Figure 22. Flow Pattern in Cyclone Separator

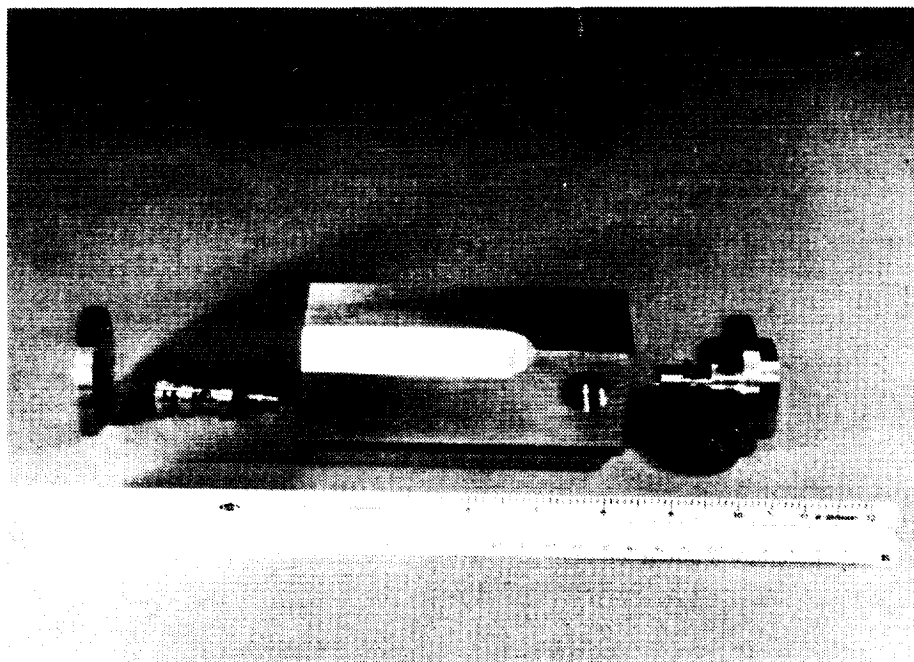


Figure 23. Cyclone Separator Manufactured Parts

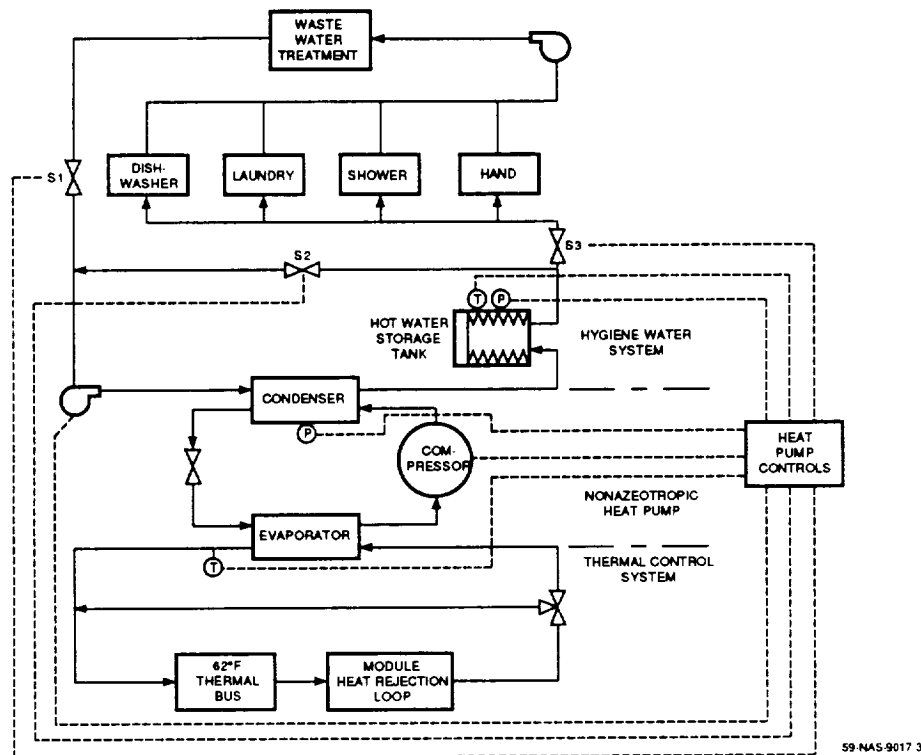


Figure 24. Nonazeotropic Heat Pump Control Schematic

When the appliance is no longer in use, the pressure in the tank slowly increases toward the set point. Figure 11, of Section 5, shows the tank volume of water (which is directly proportional to pressure) as a function of the time of day. Notice the rapid drop in water level (pressure) when an appliance is in use and the extended refill process (as long as two hours). When the tank water pressure reaches the value corresponding to 14 gal (full tank), the controller shuts off the compressor and pump.

If the storage tank temperature should fall below the set point, the controller would activate the compressor and positive displacement circulation pump. The solenoid valve on the makeup water line (S1) will be closed and the valve on the recirculation line (S2) will be opened. This process occurs only if the tank pressure is indicating a full tank. Warm water is then drawn out of the tank and recirculated through the heat pump condenser for the small amount of reheating required. This water is returned to the tank and mixed with the volume of water in the tank until the temperature is above the set point. The pump and compressor are then turned off.

Two other parameters are also monitored by the heat pump controller as a safety measure. If either one of these measurements should be outside of a predefined band, the entire system is shut down and a warning light is activated. The first of these parameters is the evaporator water outlet temperature which is monitored for freeze protection. Normal operation results in a water temperature of approximately 50°F at the evaporator outlet. However, under certain circumstances, this water temperature could decrease. Should the water temperature fall below 35°F, the system will shut down. The second parameter to be monitored for safety is the pressure of the static water loop in the condenser. A leak in the condenser tubing which contains the refrigerant would cause the static water pressure to rise. The static water loop and double containment tube prevent refrigerant from leaking directly into the hygiene water.

An Allen-Bradley SLC 500 Programmable Controller was selected for use in the prototype heat pump system developed under this program. For actual space hardware, a small printed circuit board will be custom designed and fabricated to perform system control. However, to remain within the limited budget of this program, a commercially available programmable controller was purchased. The A-B controller is capable of 4 analog inputs, 12 digital inputs, and 8 digital outputs. Simple ladder logic software was utilized in programming the unit to respond to the analog inputs in the manner described above. A timer circuit was used to activate a solenoid valve on the tank outlet according to the appliance usage schedule. Figure 24 shows this solenoid (S3) which is used for prototype testing to simulate the appliance usage.

7. TESTING

The heat pump development program included several major components designed specifically for operation with refrigerant mixtures in a zero-gravity environment. A system configuration was conceived which would produce hot water at the appropriate temperature while consuming a minimum amount of power. The system also had to deliver hot water to the end use appliances according to a specific usage schedule. Included in the heat pump design are tube-in-tube heat exchangers, a high-efficiency scroll compressor, and a gravity insensitive lubrication system. A test program was planned to verify component performance individually rather than attempting the entire system test initially. The heat exchangers were fabricated first and placed into a bench test system so the performance could be determined without the added complexity of a newly developed compressor. The compressor/oil separator design and fabrication was done simultaneously to the heat exchanger testing. Upon completion of the compressor assembly, it was integrated into the bench test system for heat pump testing. The controls, storage tank, and delivery system were then incorporated into the hygiene water heating system for complete prototype system testing.

7.1 Heat Exchangers

General analytical models for predicting heat transfer coefficients of nonazeotropic refrigerants were not available to aid in the design of the heat pump heat exchangers. Therefore, simplified models based on correlations for single component refrigerants were utilized in the design. The correlations were modified based on limited nonazeotropic data. As a result of the uncertainty in this design process, a bench test system was designed and fabricated to measure the performance of the heat pump heat exchangers. The bench test system and the heat exchangers were fabricated in a manner that allows for easy modification.

A schematic of the heat exchanger bench test setup is shown in Figure 25. An off-the-shelf piston compressor was installed into the bench test system. In order to accommodate the efficiency and flow rate differences between the off-the-shelf unit and the prototype scroll compressor under development, some simple steps were taken. A bypass line allowed for the variation of the refrigerant flow rate through the heat exchangers. A desuperheater at the condenser inlet was used to decrease the refrigerant temperature, thus eliminating some of the inefficiencies of the off-the-shelf compressor. With this arrangement, the state points (temperature, pressure and flow rate) at the heat exchanger inlet were adjusted so that the conditions produced by the off-the-shelf

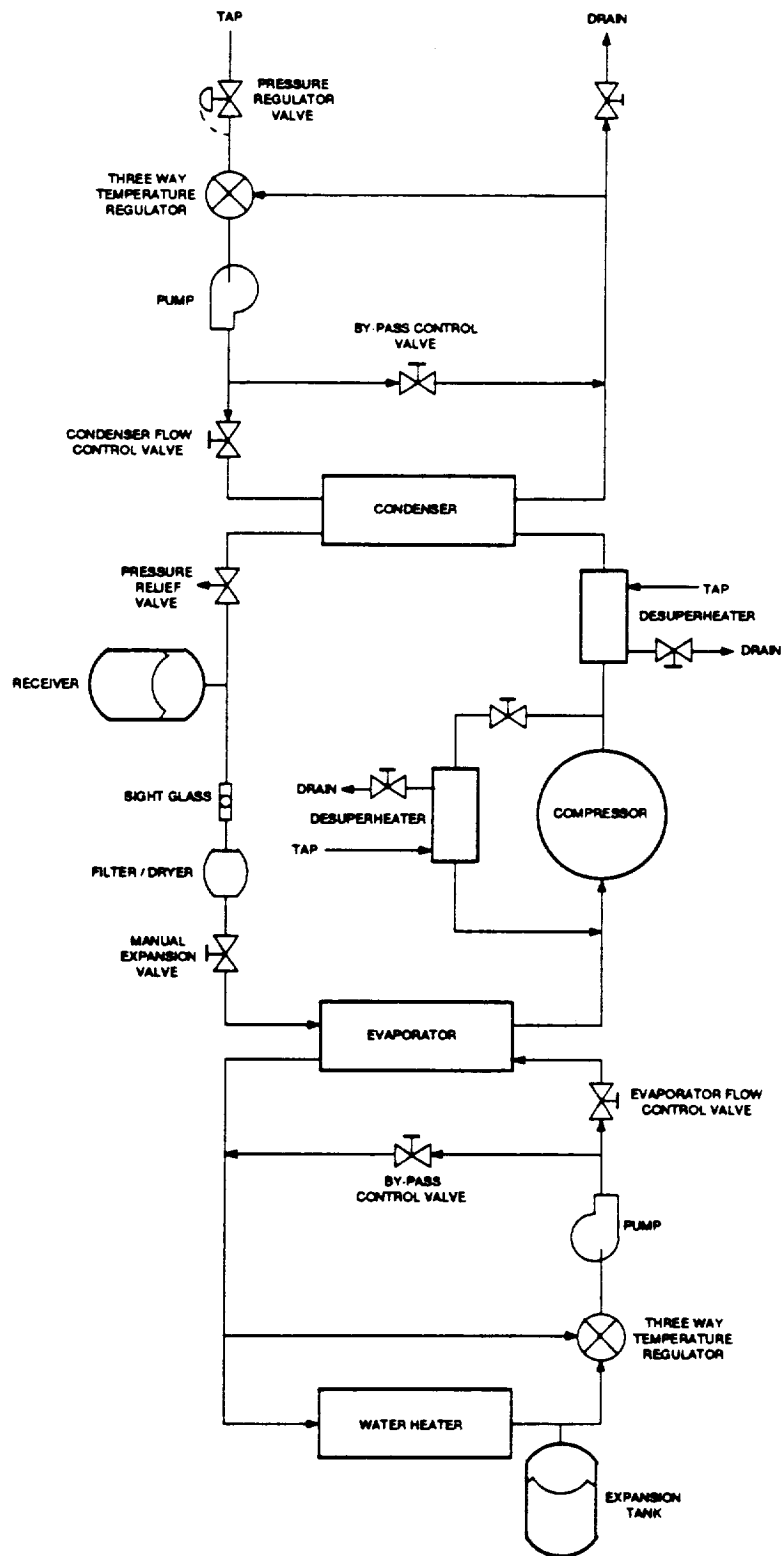


Figure 25. Heat Exchanger Test Setup

compressor would match the design points for the high-efficiency scroll unit. A manual expansion valve was used in the test system so that the evaporator pressure could adjusted and maintained at a fixed level.

The original heat pump heat exchangers were made of stainless steel tubing in a coaxial tube-in-tube arrangement. For the condenser, three concentric tubes were used to satisfy the double containment requirement. The design models predicted optimum performance utilizing 5/16, 3/8, and 1/2 inch tubing. The total length of the triple tube condenser was 56.6 feet. Temperature and pressure measurements were made at several intermediate locations in the bench test heat exchangers. The measurements were to verify the pressure drops and temperature changes of both the refrigerant mixture and the water as they pass through the heat exchangers. Figure 26 schematically illustrates the heat pump condenser layout including the instrumentation points. For ease of disassembly and modification, the condenser and evaporator were laid out in a serpentine arrangement with six sections. Temperature and pressure of both the refrigerant and the water were measured at the inlet and outlet of the heat exchangers. As Figure 26 illustrates, the temperature of the refrigerant and water were also measured at each return bend while the pressure of the refrigerant was measured at every other bend. In order to accommodate the instrumentation and facilitate the return bend, the tube-in-tube arrangement was interrupted at each bend. The

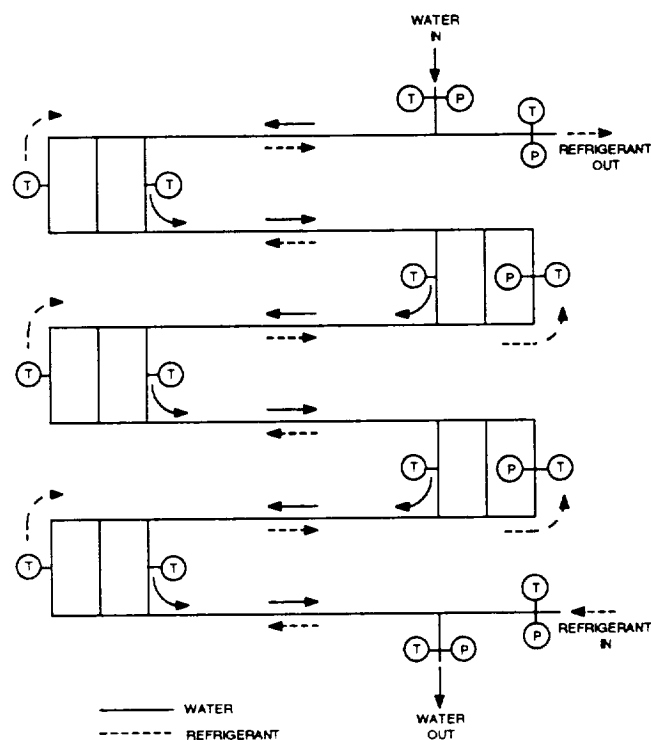


Figure 26. Schematic of Heat Pump Condenser Layout

water was first removed from the outer annulus and directed across to the next segment. The refrigerant, which flows in the innermost tube, makes the widest bend. The static water which resides in the annulus between the 5/16 inch and 3/8 inch tubes was allowed to communicate with the static water in the other segments via the middle connecting tube as shown in Figure 26. The photograph of Figure 27 should help clarify this arrangement.

The evaporator was plumbed in the same manner as the condenser with the exception of the static water tube. The total length of the evaporator was 71 ft. The entire heat pump bench test is shown in the photograph of Figure 28. A rack made of 3/4 inch aluminum tube was constructed to support the lengthy serpentine heat exchangers over the compressor and other components on the bench top. The condenser occupied the upper portion of the rack, with the evaporator directly beneath it.

All of the instrumentation installed in the refrigerant and water lines to measure temperature, pressure and flow rate were connected to the data acquisition system shown in Figure 29. Data from the data logger was directed to either the floppy disk storage unit for later analysis or to the printer for an immediate check on system status. Data was dumped to either of these devices through the use of a print button on the front of the data logger or by programming the data logger

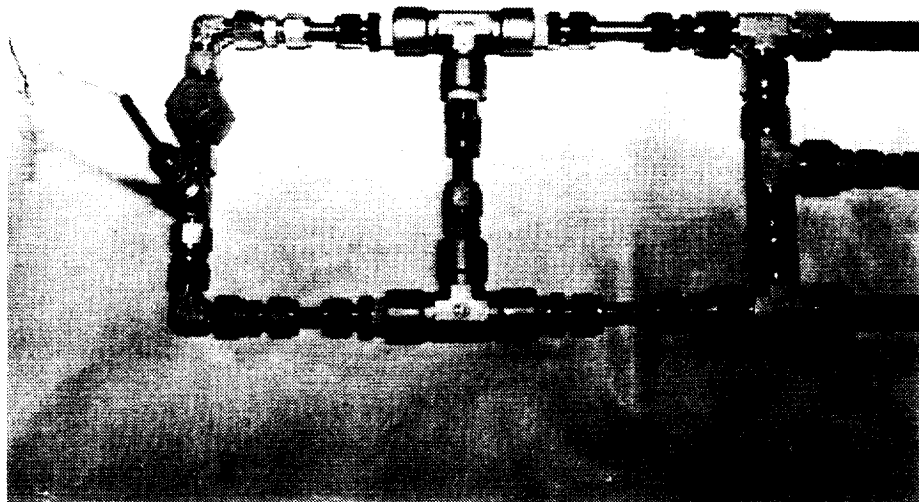


Figure 27. Typical Condenser Return Bend

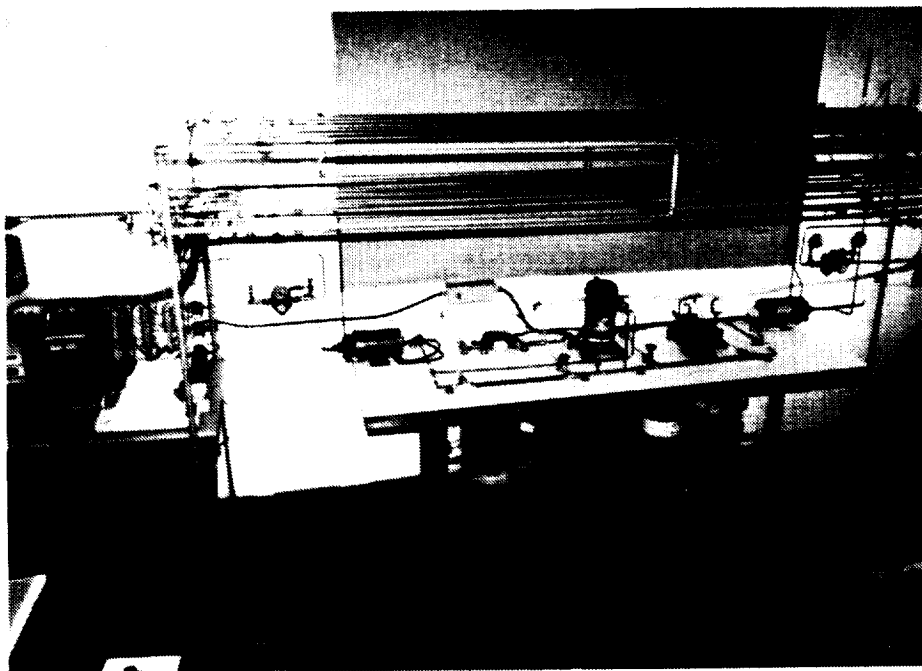


Figure 28. Heat Pump Bench Test

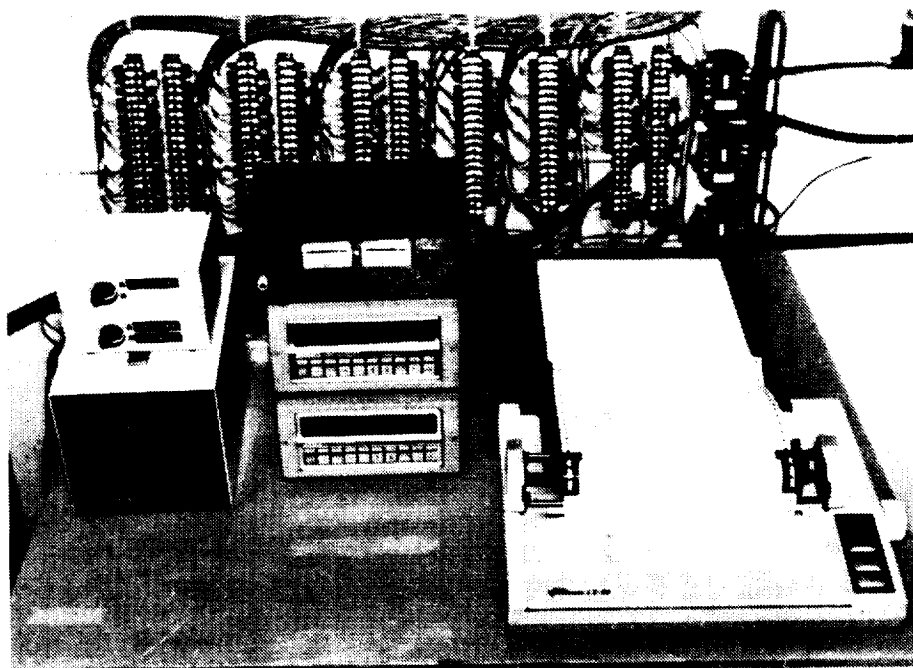


Figure 29. Data Acquisition System

to dump at a specified time interval. The data stored on disk was processed later by a data reduction routine. Appendix A contains a sample summary sheet generated by the routine.

Testing began with various refrigerant charges in order to vary the discharge pressure and the amount of subcooling in the condenser. It was shortly determined that the amount of heat transfer in the evaporator was insufficient so the length was increased by 17 percent. This improved the heat transfer slightly, however, the refrigerant pressure drop was much higher than anticipated. The pressure drop created saturated vapor conditions at a much lower temperature than design. As a result, the temperature glide available through phase change in the evaporator was greatly reduced and the amount of superheat was increased. This reduced the heat transfer capabilities of the heat exchanger.

The test data also indicated a high condensing pressure. In an effort to determine the cause of this, the amount of inventory was reduced until the subcooling at the condenser outlet was reduced to zero. The condensing pressure was still too high indicating a shortage of heat transfer area. The condenser length was then increased by approximately 30 percent. As with the evaporator, the pressure drop through the condenser was higher than anticipated.

An example of the test data is shown in Figures 30 and 31 for the condenser and evaporator temperatures, respectively. As can be seen, the overall temperature glides are very close to the anticipated values. The condenser plot in Figure 30 shows a higher temperature difference between the refrigerant and water at a given point than predicted. This is due to insufficient heat transfer area which also leads to a higher condensing pressure. The evaporator plot in Figure 31 shows a premature dryout of refrigerant as indicated by the step slopes of the temperature curves in the upper right portion of the plot. This is due to the large pressure drop of the refrigerant as discussed above.

Following the initial test runs, the heat exchanger model correlations were updated based on the data collected. The models were then rerun with several larger tubes sizes for both the evaporator and the condenser. The model results were used to rebuild the heat exchangers. For the evaporator, the inner stainless steel tube was increased from 5/16 in. to 3/8 in. while the outer 1/2 in. stainless steel tube was replaced with a 1/2 in. ID nylon tube. The outer tube was changed from stainless steel to nylon for several reasons. Recent developments in space station design indicate serious weight problems. As a result, the material limitations are being reconsidered with the possibility of allowing some composites and other nonmetal material being used in the water

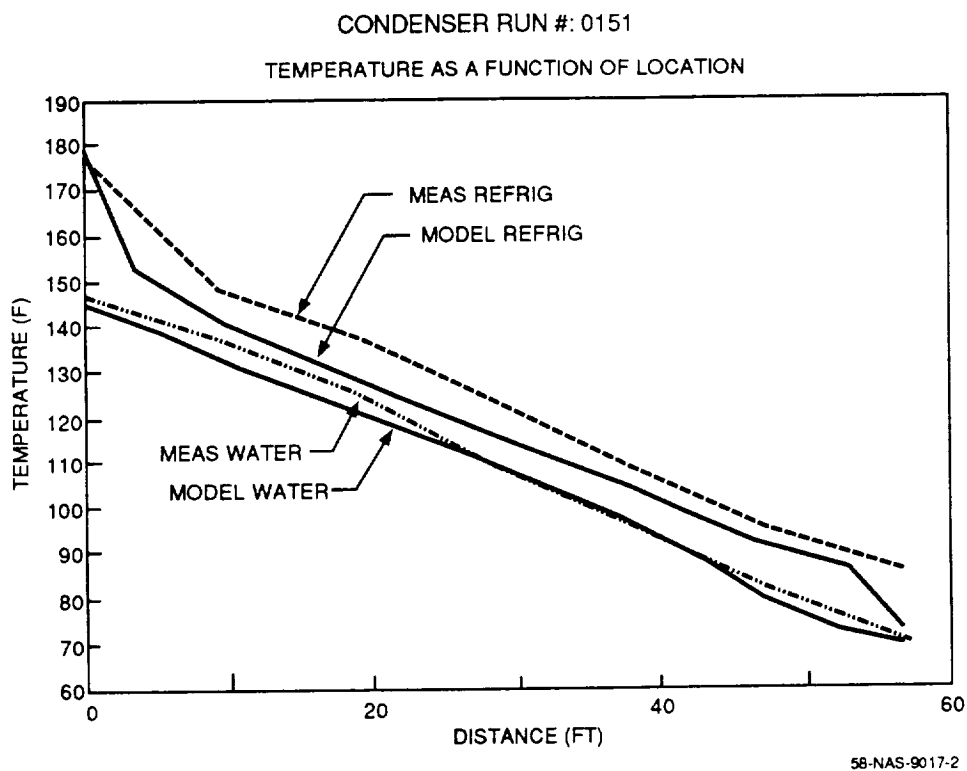


Figure 30. Typical Condenser Temperature Profile

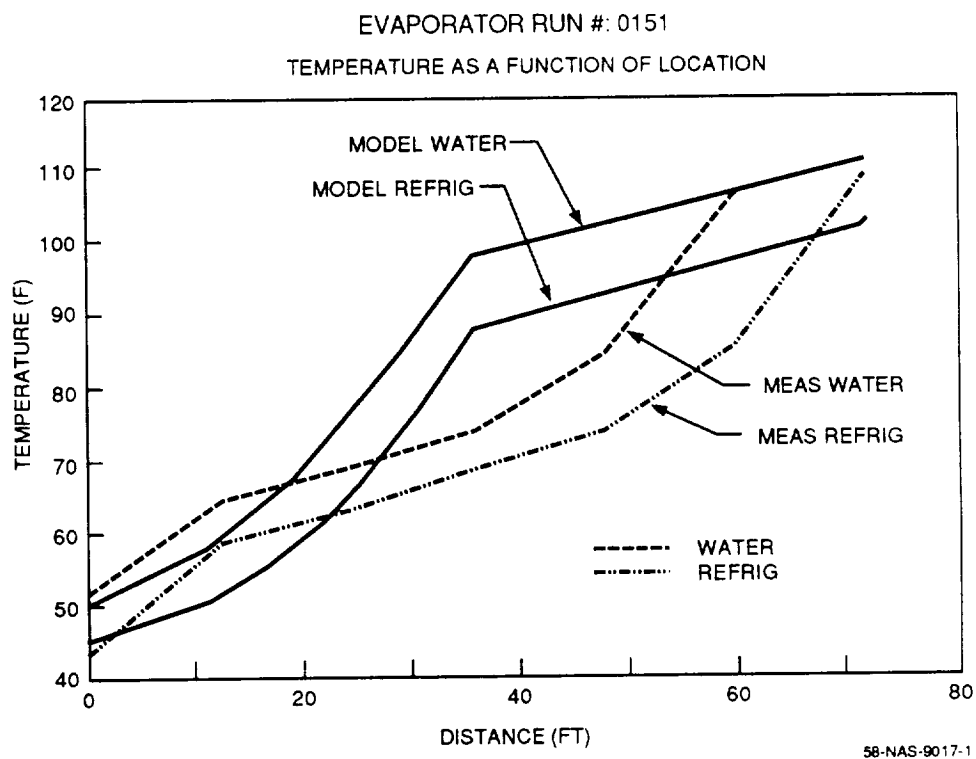


Figure 31. Typical Evaporator Temperature Profile

systems. Regardless of the outcome, the outer tube does not effect the heat transfer or the heat pump performance, so as a cost conserving measure nylon was selected. If it turns out that a nonmetal material is not acceptable for actual space hardware, the weight difference between nylon and the appropriate metal would need to be addressed but the change would not affect the performance of the heat pump. The condenser stainless steel tube sizes were changed from 5/16 in. to 3/8 in. for the inner tube, and 3/8 in. to 7/16 in. for the double containment middle tube. The outer 1/2 in. stainless steel tube was replaced with a 5/8 in. ID nylon tube. The heat exchangers were rebuilt and testing continued.

The test data showed the performance of the evaporator to be greatly influenced by the operation of the condenser. The active length of the evaporator was found to be dependent on the amount of subcooling occurring in the condenser. The length of evaporator over which two-phase evaporation occurred increased as the amount of subcooling of the refrigerant increased. If inadequate subcooling is present, the evaporation process is completed at roughly the midpoint of the evaporator. The remainder of the exchanger sees only superheating of the refrigerant which does little in capturing heat from the heat source. The subcooling of the liquid refrigerant can be increased too much. In this case, evaporation cannot be completed in the evaporator, and a two-phase mixture of refrigerant is returned to the compressor which decreases efficiency. Testing determined that a 100 ft length was suitable for the evaporator since it allowed all refrigerant to be evaporated over a fairly wide range of subcooling conditions.

The length of the condenser was increased to 100 ft in an effort to decrease the condensing temperature and pressure while maintaining the desired water heating capability. Testing showed, however, that any decrease in condensing pressure resulted in a final water temperature less than desired. The added length did little except provide more subcooling of the refrigerant. It was decided that the length of the condenser would be decreased until full condensing could not be achieved or the water heating load could not be met. The final length chosen that met these criteria was 50 ft.

7.2 Compressor/Oil Separator

Once the prototype scroll compressor and oil separator were assembled as shown in Figure 20 they were plumbed into the bench test system for initial performance testing. The goals of these tests were to determine if the oil separation and control system functioned properly, find if the heat pumping capability of the compressor was adequate for the expected heating load and refrigerant mixture, and measure the power required by the compressor. Sight glasses were installed in the

copper plumbing lines at every conceivable location to observe the flow of refrigerant and oil in order to verify the performance of the cyclone separator and lubrication system. Compressor power consumption was measured through a three-phase watt transducer installed in the power feed between the motor controller and the compressor motor. In reality, the power measurement should include the inefficiencies of the motor controller, however, due to the limited funding of this development program, an inexpensive and very inefficient controller was used (less than 50 percent). Power was also measured into the controller, however, the power measured between the controller and the motor was used in all COP calculations.

Demonstration of complete gravity insensitivity is required to show the compressors ability to operate in a zero-gravity environment. The best way to do this is to operate the compressor in various orientations and observe the performance. Therefore, testing was done with the compressor operating both horizontally and vertically orientated. Initial tests were performed with the compressor in a horizontal position. The compressor was run at various speeds and with several different refrigerant charges. An oil mist was observed in the compressor refrigerant discharge line as expected. An oil flow and build up at the metering valve was also observed as expected. Under most operating conditions, a dry vapor was observed exiting the cyclone separator. However, occasionally there was a small amount of oil carried over into the vapor line to the condenser. This was found to be dependent on the amount of oil in the system and the setting of the metering valve on the oil return line. If the system was overcharged with oil and the metering valve was shut down too far, oil would fill the line from the metering valve back to the separator and eventually some would carry over into the vapor line. This problem was remedied through careful oil charging and valve setting.

After initial test runs, the compressor was disassembled. The wick material was found to be totally saturated with oil, indicating that the wick was collecting oil within the compressor housing, as designed. Inspection of the main shaft and bearing surfaces showed no noticeable wear or scoring, indicating that proper lubrication was being maintained. This procedure was repeated throughout the testing to insure proper operation of the lubrication system.

The compressor was then reassembled and placed back into the system in the vertical orientation. The performance of the oil control system degraded dramatically at this point. Little or no oil return was seen from the separating cyclone, suggesting that oil was remaining in the compressor, probably at the bottom. The compressor was then disassembled and inspected. No noticeable wear was seen on the shaft or bushings. Examination of the gas flow path showed that the wick material may have partially blocked this passage. It was also determined that a

considerable portion of the gas flow may bypass the return passage through the wick, which would account for the lack of oil flow into the scroll and out to the separator. The upper portion of the compressor was then sealed to force all gas flow through the wick passage and a tube was installed between the compressor inlet and the top of the wick to help maintain the gas velocity.

The compressor was reassembled and placed in the vertical orientation. Testing again showed very little oil flow. Upon disassembly, a large amount of oil was found on the bottom of the compressor. The problem appeared to be getting the oil to move up the suction passage and into the scroll. In an effort to resolve this, the wicking material in the bottom portion of the compressor was removed and replaced with a tube which ran from the motor section down to the bottom of the compressor. Testing in this configuration caused large amounts of oil to slug into the scroll resulting in noisy, inefficient operation.

The ultimate solution was obtained by removing the tube in the lower part of the compressor and reinstalling the wick. A circular path was cut into the section of wick which lines the bottom of the compressor so that the suction gas travels around the bottom of the compressor before going up the side and into the scroll. Operation in this manner allows oil accumulating in the bottom of the compressor to pass slowly through the wick and be entrained in the suction vapor in a slow steady flow instead of slugs. Throughout many hours of operation an adequate oil flow was observed and smooth compressor operation was obtained. The compressor was disassembled several times to inspect the shaft and bushings for improper wear or scoring. None was observed.

7.3 Heat Pump Bench Test

A large number of tests were run with the heat pump system in a bench test configuration containing the prototype scroll compressor as shown in Figure 28. (Test data may be found in Appendix A.) This configuration allows for easy component inspection and modification. Initial testing determined insufficient heat exchanger performance. The evaporator and condenser were then rebuilt with larger tube sizes and lengths of 100 ft each. A series of tests were then run to determine the required heat exchanger lengths and examine the effect on performance of varying:

- Compressor speed - 1500 to 2400 rpm
- System refrigerant charge - 900 to 1200 grams.

The primary quantities determined from the system measurements were:

- The heat transferred to the refrigerant in the evaporator
- The heat delivered to the hygiene water in the condenser
- The power consumed by the compressor
- The COP of the heat pump.

The measured data allowed an energy balance to be performed by comparing the energy absorbed by the evaporator plus the work input by the compressor to the heat rejection of the condenser. Initial testing showed that a significant heat loss was occurring from the system. It was determined that a large portion of the heat loss was due to the uninsulated surface of the compressor. When the compressor was insulated to reduce this loss, an overheating problem of the compressor developed. The final solution to this problem was found to be wrapping tubing around the compressor and passing the water from the condenser through, collecting the compressor heat in the hygiene water to be heated. The energy balance was improved, although, the discrepancy was still on the order of 300 - 400 Btu/hr (10 - 15 percent). A recalibration of all instruments failed resolve this issue. It was theorized that the remaining heat loss could be attributable to the heat exchangers and connecting tubing. The heat exchangers were insulated, however, they were also laid out in serpentine fashion as shown in Figures 26 and 28, resulting in a large amount of surface area for the heat loss to occur. It was also theorized that the final configuration would have the heat exchangers coiled tightly together, insulated with three inches of foam insulation, and enclosed in a hermetic package, thus reducing the heat loss to insignificant levels. Therefore, the tests proceeded with the COP calculations based on the measured heat input to the evaporator and compressor power consumption ($COP = Q_e + W_c / W_c$).

The test results showing the relation between the heat rejected into the hygiene water in the condenser and the compressor speed and charge is shown in Figure 32. The minimum heating capability to meet the requirements is shown as a dashed line (corrected for heat loss as discussed above). The results showed that the load could be met at any speed for charges of 1100g or greater. For the 1000g charge, a speed of 1600 rpm or greater is required, while for a charge of 900g, compressor speed must exceed 1900 rpm.

The change in COP with speed and charge is shown in Figure 33. The results show that COP tends to decrease as the compressor speed is increased. The highest COP is achieved at a speed of 1500 rpm with a charge of 1000g. The data also shows that at all speeds tested the maximum COP was achieved at a charge of 1000g. The general results suggest that the COP of the heat pump is maximized at the lowest possible operating speed and smallest refrigerant charge. The heat delivered by the heat pump to the hygiene water also decreases as these two quantities are lowered.

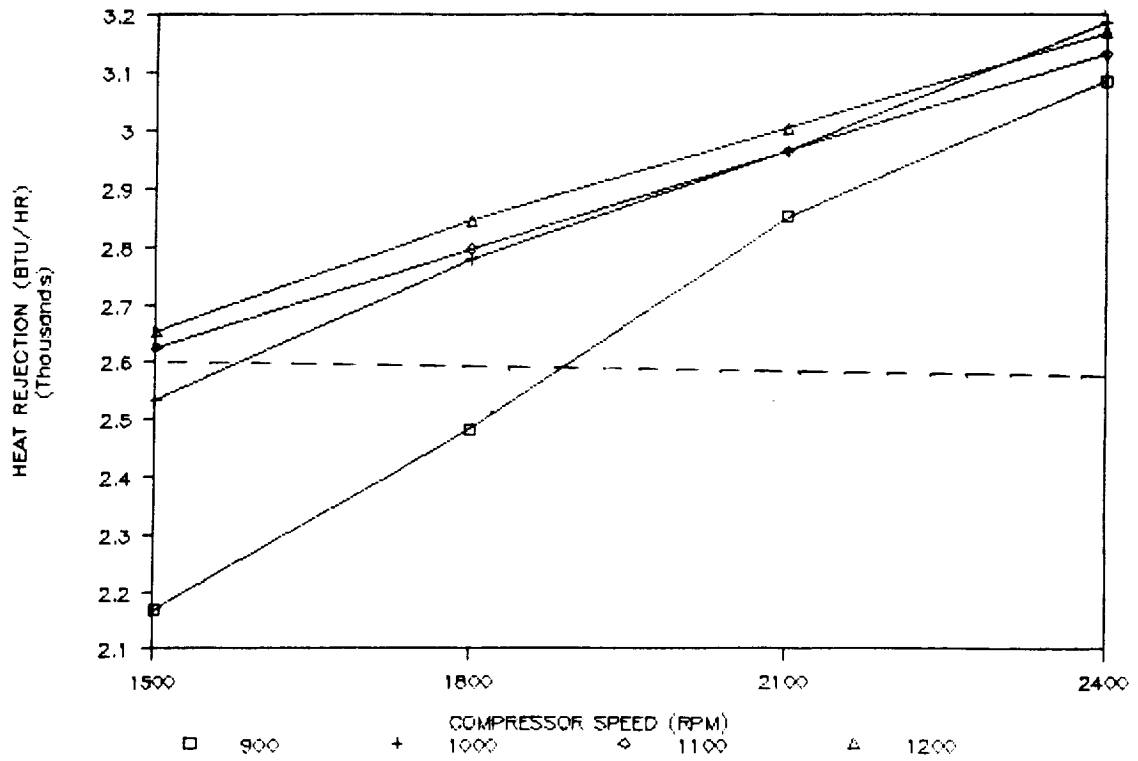


Figure 32. Heat Rejection versus Speed and Charge (100 ft Cond.)

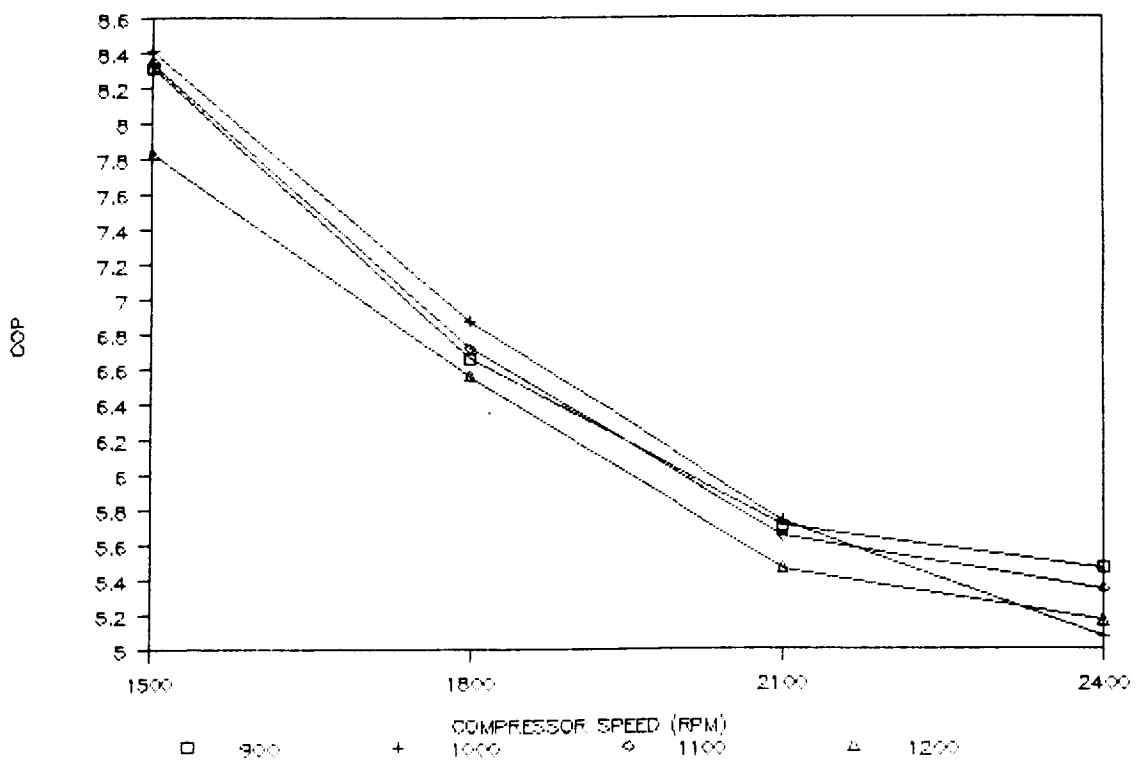


Figure 33. COP versus Speed and Charge (100 ft Cond.)

The net result is that there is some combination of speed and charge that provides adequate heating to the hygiene water in the most efficient manner possible.

The results of the first series of tests were utilized in determining the final heat exchanger lengths. The test data showed the performance of the evaporator to be greatly influenced by the amount of subcooling occurring in the condenser. Testing determined that a 100 ft length was suitable for the evaporator since it allowed all refrigerant to be evaporated over a fairly wide range of subcooling conditions. The length of the condenser was increased to 100 ft in an effort to decrease the condensing temperature and pressure while maintaining the required water heating capability. Testing showed, however, that any decrease in condensing pressure resulted in a final water temperature less than desired. The added length did little except provide more subcooling of the refrigerant. It was decided that the length of the condenser would be decreased until full condensing could not be achieved or the water heating load could not be met. The final length chosen that met these criteria was 50 ft.

Testing was repeated to determine the optimum speed and charge for the new configuration with the adjusted heat exchanger lengths. The amount of charge in the system was decreased due to the reduction in system volume. Figure 34 is a graph of the measured heat rejection values (water heating) versus compressor speed and charge. The speed range investigated was 1500 to 2000 rpm due to the previous findings of increased power consumption at increased speeds. The refrigerant charge range was from 700 to 900 grams. As can be seen, the results are very similar to the previous configuration with the exception of a larger number of data points. The trend is again, increased heat rejection with increased speed and charge. This is to be expected as the increased compressor speed results in increased refrigerant flow rate, while the increase in system charge results in increased discharge pressure and condensing temperature. Both of which, tend to increase the heat rejection.

COP measurements as a function of compressor speed and charge are shown in Figure 35. A single regression line is shown for all the data since no distinguishable relationship as a function of charge is evident for this group of data. The trend is for increased COP with lower speeds (the inverse of the heat rejection relationship). The desired amount of water heating may be obtained at a speed of approximately 1600 rpm where the measured COP varies from approximately 8.0 to 8.7.

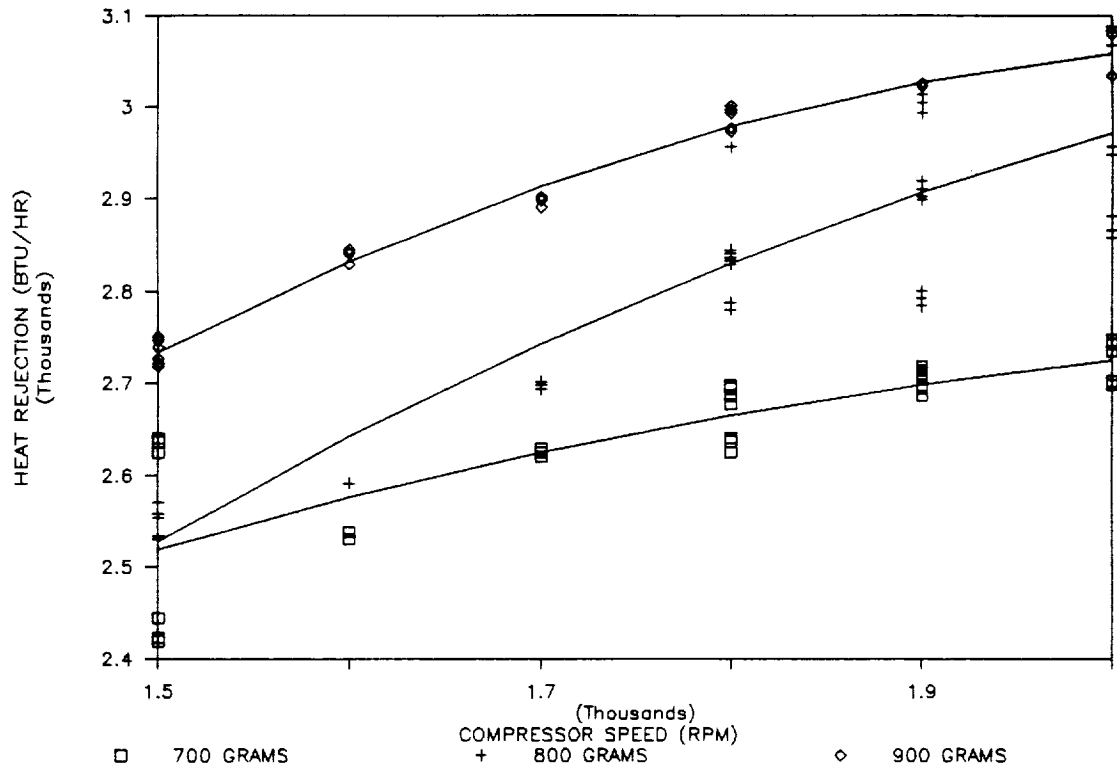


Figure 34. Heat Rejection versus Speed and Charge (50 ft Cond.)

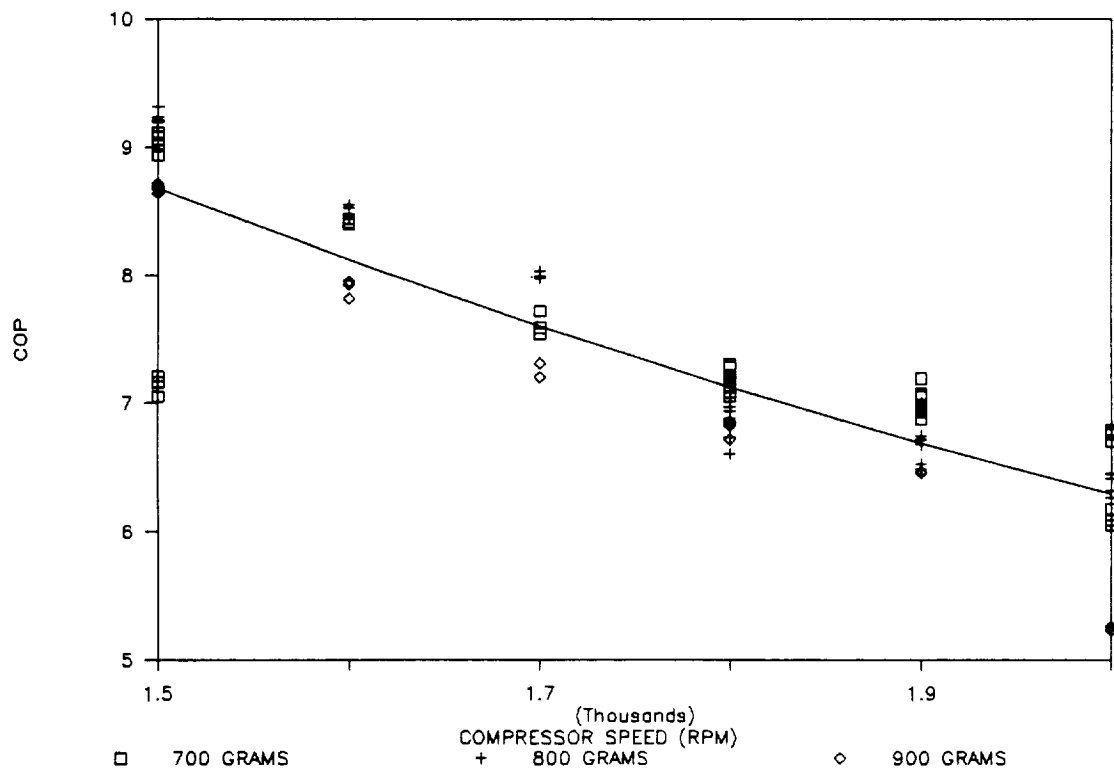


Figure 35. COP versus Speed and Charge (50 ft Cond.)

7.4 Endurance Test

Endurance testing of the heat pump compressor was done concurrent to the performance and evaluation testing of the heat pump system. The endurance test mainly consisted of logging a large number of hours on the compressor/motor package. The prototype unit was disassembled at various time intervals so that the main lubrication points could be inspected for wear. Inspections were done after brief run times following any major changes to the lubrication system and after longer periods of operation when no unusual operating conditions prevailed. At the time of inspection, observations were made of the bushings, shaft, and motor stator and rotor. The lubricating oil was also examined for any indication of metal wear. The scroll components of the compressor also require lubrication for sealing and smooth, nonwearing operation. Unfortunately, these components were not accessible for examination without destroying the unit, and were therefore, not inspected.

Table 8 lists the compressor run time log. This table was generated from entries in the laboratory notebook and time stamps from the recorded data. The number of hours of operation on each day of testing is listed along with an indication of the inspection times. After nine hours of operation following the initial startup, the compressor was disassembled and inspected. The wick material was found to be totally saturated with oil and no noticeable wear was found on any of the surfaces. The compressor was then reassembled and operated for a large number of hours before the next inspection. This procedure was repeated several times with the compressor in the horizontal configuration with no noticeable wear.

On February 13, the compressor was disassembled, inspected, and placed back into the system in a vertical orientation. The system was operated for a brief period of time before indications of lubrication problems were evident. Sight glasses in the oil return line showed no sign of oil flow and the measured power consumption increased gradually. Disassembly and inspection showed no signs of wear in the brief run time. Several changes in the lubrication system followed by brief run times and inspections ensued as indicated in Table 7. As the lubrication problems were solved and confidence in the system was gained, longer periods of operation were attained between inspections. In all, over four hundred hours of operation were placed on the prototype compressor assembly without any signs of significant wear.

Table 8. Prototype Compressor Run Time

Date	# Hours	Date	# Hours	Date	# Hours
09-26-90	4	01-14-91	7	03-29-91	3
09-28-90	5	01-15-91	8	04-01-91	2
10-03-90*	6	01-16-91	7	04-02-91	3
10-09-90	4	01-23-91	10	04-03-91*	2
10-10-90	5	01-25-91	8	04-05-91	3
10-11-91	5	01-28-91	9	04-08-91	4
10-22-90	6	01-30-91	9	04-09-91	2
10-24-90	5	01-31-91	8	04-10-91	4
10-30-90	5	02-01-91	9	04-11-91	5
11-05-90	4	02-05-91	8	04-12-91	4
11-07-90	9	02-06-91	5	05-16-91	6
11-09-90*	3	02-13-91*	3	05-20-91	4
11-12-90	3	02-14-91*	4	05-24-91	3
11-13-90	3	02-25-91*	4	05-29-91	6
12-18-90	4	03-07-91	5	05-30-91	4
12-19-90	6	03-08-91	4	05-31-91	8
12-20-90	5	03-12-91*	3	06-05-91	4
12-21-90	3	03-15-91	3	06-06-91	3
12-27-90	9	03-18-91	5	06-07-91	6
12-28-90	7	03-19-91*	4	06-13-91*	7
01-03-91	11	03-20-91	7	06-14-91	4
01-07-91	5	03-22-91	4	06-29-91	6
01-09-91*	11	03-26-91	3	06-30-91	12
01-10-91	12	03-27-91*	4	07-01-91	12
01-11-91	7	03-28-91	3	07-02-91	6
				Total	414
*Denotes Compressor teardown and inspection					

8. HEAT PUMP PACKAGING

This section describes how the prototype heat pump system was integrated into several packages for final testing and delivery to NASA for evaluation. The first package consists of the actual heat pump, i.e., compressor, evaporator, condenser, etc. The second consists of the water storage tank, circulation pump, and solenoid valves. The third is an electrical enclosure for the compressor motor controller while the fourth package contains the programmable controller and assorted electrical components. A fifth package, which is not actually part of the heat pump system, consists of test support equipment. The Space Station Integration section describes how all of these components could be integrated into a single compact enclosure for installation into SSF or other manned missions.

8.1 Prototype Integration

All of the heat pump components in the bench test configuration were integrated into a compact, semi-hermetic enclosure. This package is similar to the final component assembly for the SSF application. Figure 36 shows the package layout for the prototype heat pump. The compressor is mounted in the center of the package between two ring assemblies. Vibration isolators were used to tie the compressor to the bottom and to the center of the enclosure. This mounting method allows the operation of the heat pump in any orientation. The oil separator is mounted on the side of the compressor. A support frame extends up from a 1/2 in. aluminum base plate to hold the evaporator on the bottom, the compressor in the center, and the condenser on top. The support frame allows the entire package to be inverted.

Once the bench testing had determined the evaporator and condenser lengths required to obtain the desired performance, the heat exchangers were refabricated in tightly wound spiral coils of 18 in. diam. For the evaporator, a single 3/8 in., stainless steel tube 100 ft long was bent into a spiral coil consisting of 20 turns. After delivery to Foster-Miller, a 1/2 in. ID by 5/8 in. OD nylon tube was slid over the stainless steel tube to contain the water flow. For the condenser, two stainless steel tubes were fabricated into a coil of 11 turns. The inner tube was made of 3/8 in. OD stainless steel, while the coaxial second tube was made of 7/16 in. OD stainless steel. After delivery to Foster-Miller, a 5/8 in. ID by 3/4 in. OD nylon tube was slid over the coil. Figure 37 shows the evaporator and condenser as they were mounted into the prototype package. The heat

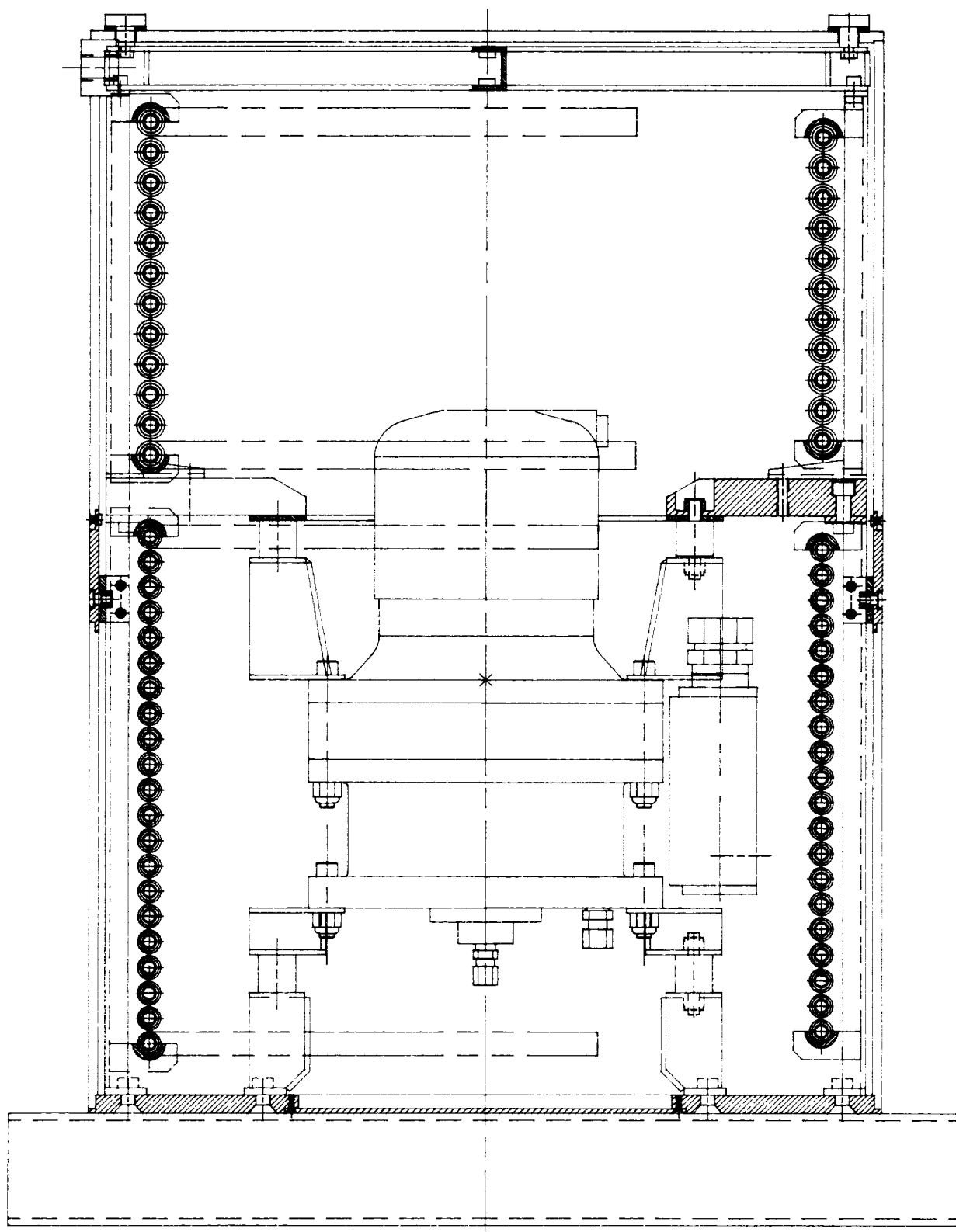


Figure 36. Heat Pump Package Layout

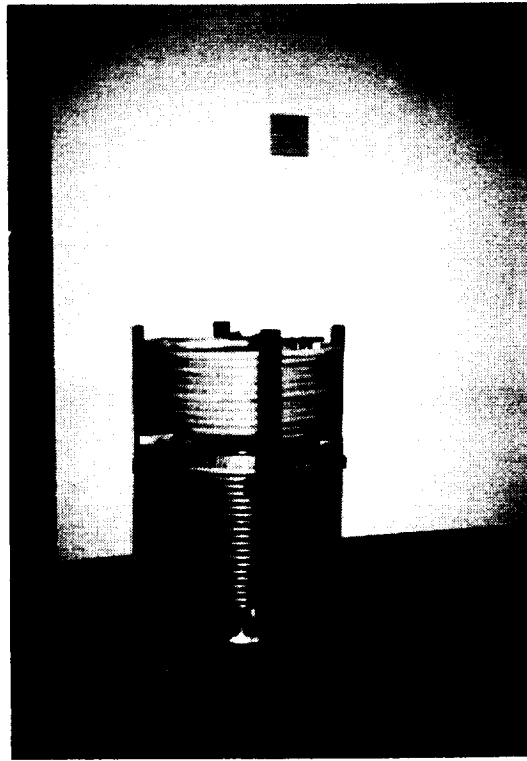


Figure 37. Evaporator and Condenser Coils - Uninsulated

exchangers were then insulated with three inches of a blown in place foam insulation as shown in Figure 38.

A semi-hermetic enclosure method was used for simple assembly and disassembly (if required). No attempt was made to make the prototype package leakproof as required for the final SSF hardware. The enclosure consists of: the aluminum base plate, a Lexan cylinder (1/4 in. thick), an aluminum center ring, another Lexan cylinder, and a Lexan top cover. Feedthroughs for condenser water in and out, and evaporator water in and out are provided near the top of the unit. Feedthroughs for electrical power for the compressor and instrumentation are also provided at this location. An access cover in the aluminum base plate directly under the compressor provides a means for refrigerant and oil charging. The entire package rest on a metal skid that has the necessary hardware to facilitate lifting. The prototype heat pump package as shown in the photograph of Figure 39 measures 21 in. in diam and 32 in. in height.

The water storage tank package is shown in Figure 40. The main component is a 14 gal Amtrol residential water storage tank. An RTD temperature transducer and pressure transducer

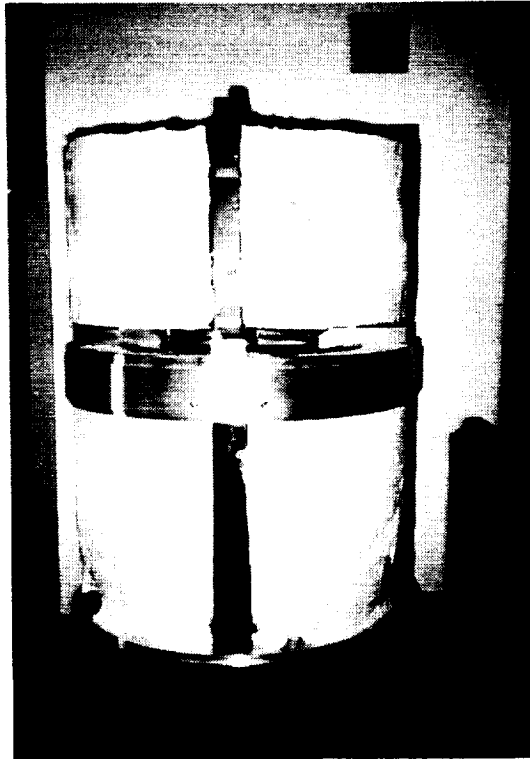


Figure 38. Evaporator and Condenser Coils - Insulated

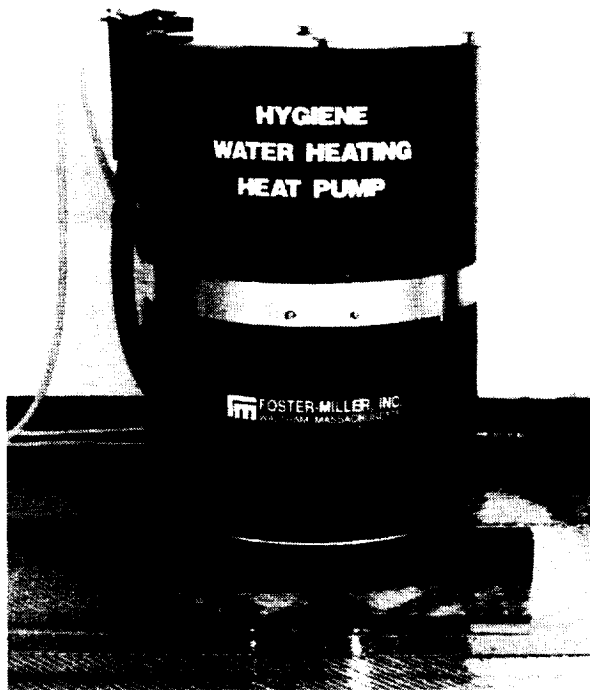


Figure 39. Prototype Heat Pump Package

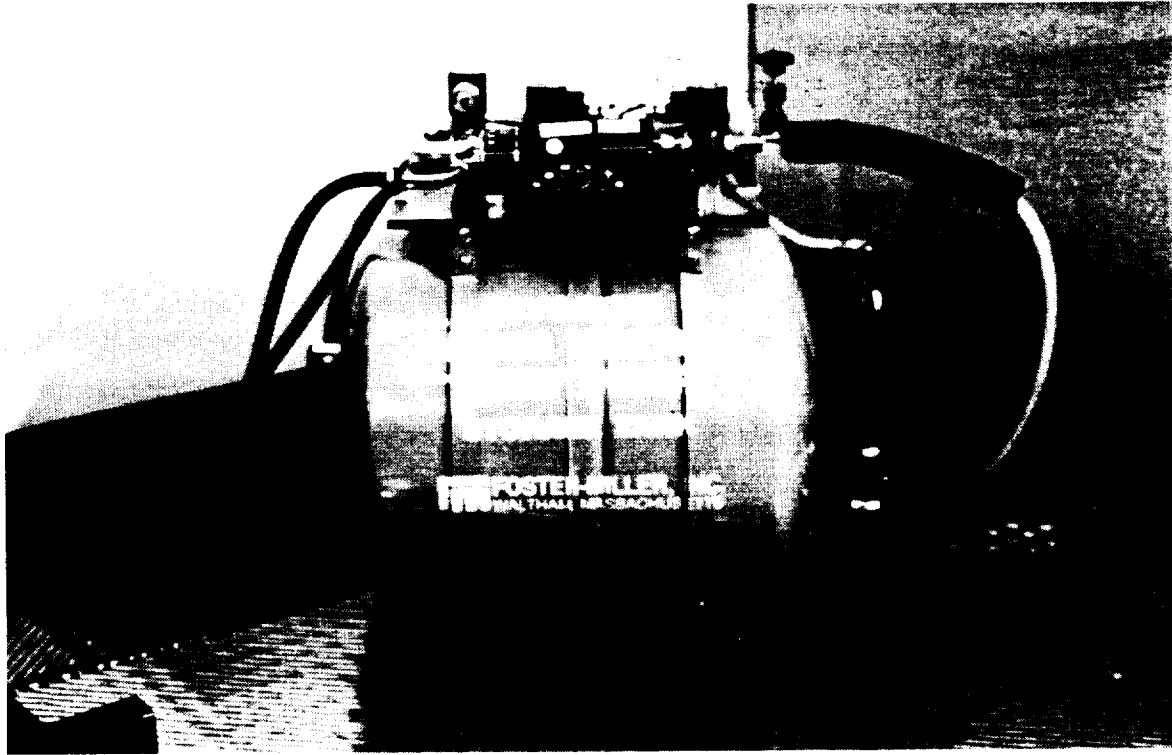


Figure 40. Heat Pump Storage Tank Package

located in the plumbing line at the tank outlet are used for system control. A platform on top of the tank is used for mounting the circulation pump, valves, connecting plumbing, and electrical enclosures. The circulation pump is a positive displacement gear pump manufactured by Micropump. A positive displacement pump is used here to establish a constant flow rate through the condenser under varying back pressure. (The water flowing through the condenser enters the water storage tank which changes pressure with volume.) The three solenoid valves shown in the control system schematic of Figure 24, are also mounted on the tank package and plumbed according to the schematic. The solenoid valves are normally closed, 120 vac, and are energized as required by the programmable controller. Solenoid S1 is opened when the tank is being refilled. Solenoid S2 is opened when the tank water needs reheating, and solenoid S3 is opened according to a time schedule to simulate appliance use. A fourth valve is a manually adjustable metering valve which is used to set the flow rate out of the tank to the appliance supply line. Two electrical enclosures provide the cabling interface for electrical power and instrumentation to the main control package.

Figure 41 shows the three other components of the prototype heat pump system. The electrical enclosure in the center of the photograph is the main control box for the heat pump. It contains the Allen-Bradley programmable controller which monitors temperatures and pressures and activates the compressor, circulation pump, and solenoid valves accordingly. A three-phase watt transducer which is used for monitoring compressor power is also located in this box as well as a power supply required for the instrumentation and a pair of relays. The electronics package is equipped with a main power switch for activating/deactivating the heat pump system. Power and instrument cables connect the main electronics package with each of the other heat pump component packages. Quick disconnect fittings are used on each end of the cables for easy assembly and disassembly. The electrical enclosure on the right of Figure 41 contains the compressor motor controller. This component was placed in a separate box due to its generation of RFI "noise" which could effect the operation of the programmable controller. A cooling fan provides air circulation for heat rejection. The last assembly shown in the photograph of Figure 41 is a water control panel. The water temperature and flow rate to the evaporator and condenser may be adjusted and controller with the equipment on this panel. Each flow path contains a mixing valve, metering valve, and flow meter. The mixing valves require a hot and cold supply of water. The valves are adjustable and include a thermometer so that the correct temperature water may be supplied to each heat exchanger. The metering valve is used to set the flow rate while the flow meters are connected to the data acquisition system for measuring the water flow rate.

Figure 42 shows the entire prototype heat pump as assembled in the Foster-Miller laboratory. Testing in this configuration confirmed system performance equivalent to that obtained in the bench test. Figure 43 is a system schematic with the measured state points indicated. A sample set of data is included.

8.2 Space Station Integration

For the SSF application, a single hermetic enclosure will contain all of the heat pump components (compressor, condenser, evaporator, expansion devise, and interconnecting piping) as well as the 14 gal water tank. The heat pump package fits neatly into a standard rack as shown in Figure 44, consuming approximately one eighth of the rack volume. The heat pump Orbital Replacement Unit (ORU), shown in Figure 45, consists of a 19 in. diam by 29 in. long cylinder surrounded by a rectangular frame with a display panel on the front (Figure 46). The only penetrations to the enclosure are disconnects in the rear of the ORU for waste heat water in and out, hygiene water in and out and wiring connections for compressor power and

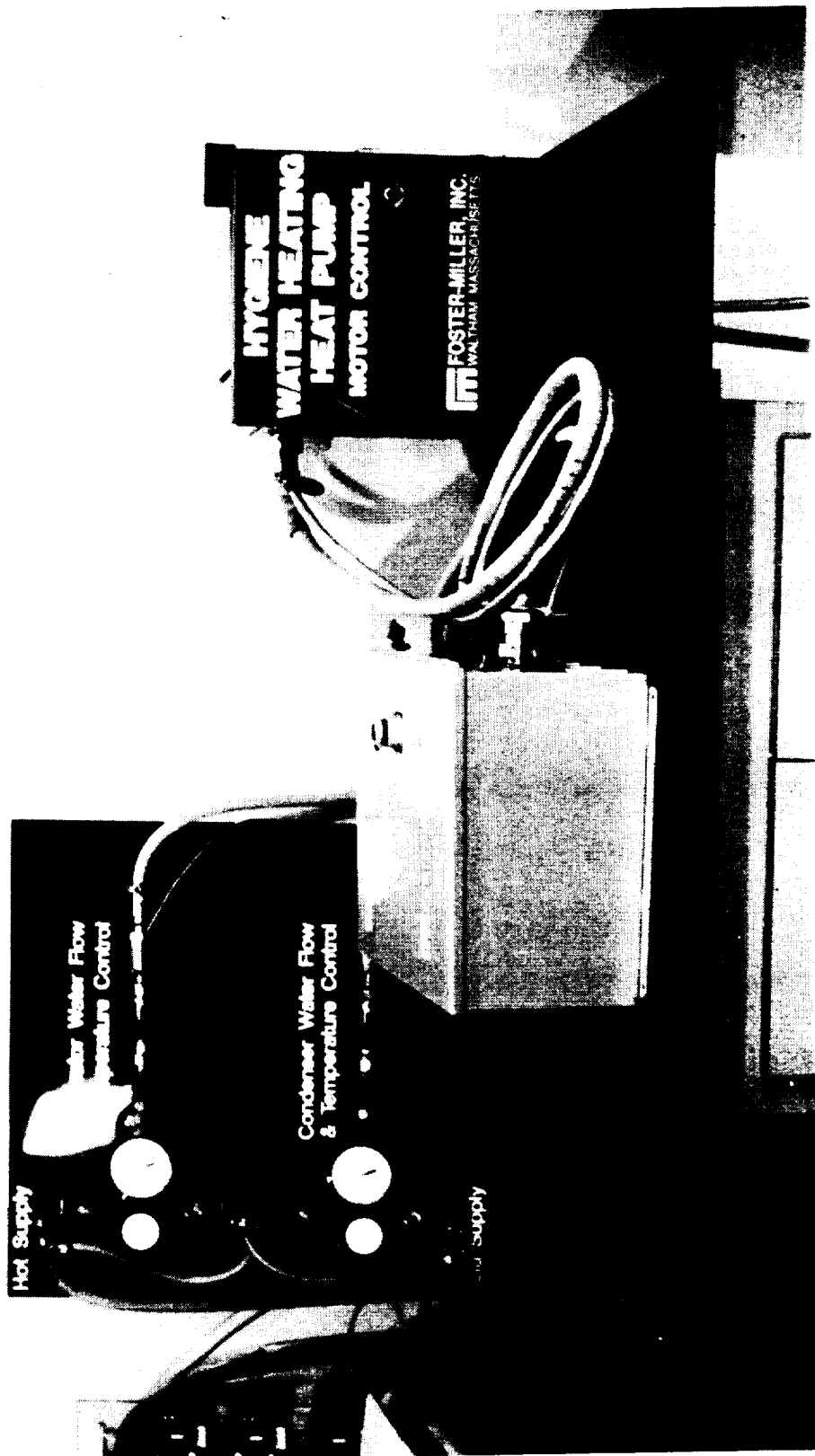


Figure 41. Heat Pump Controls and Test Equipment

ORIGINAL PAGE
BLACK AND WHITE PHOTOGRAPH



Figure 42. Assembled Prototype Heat Pump System

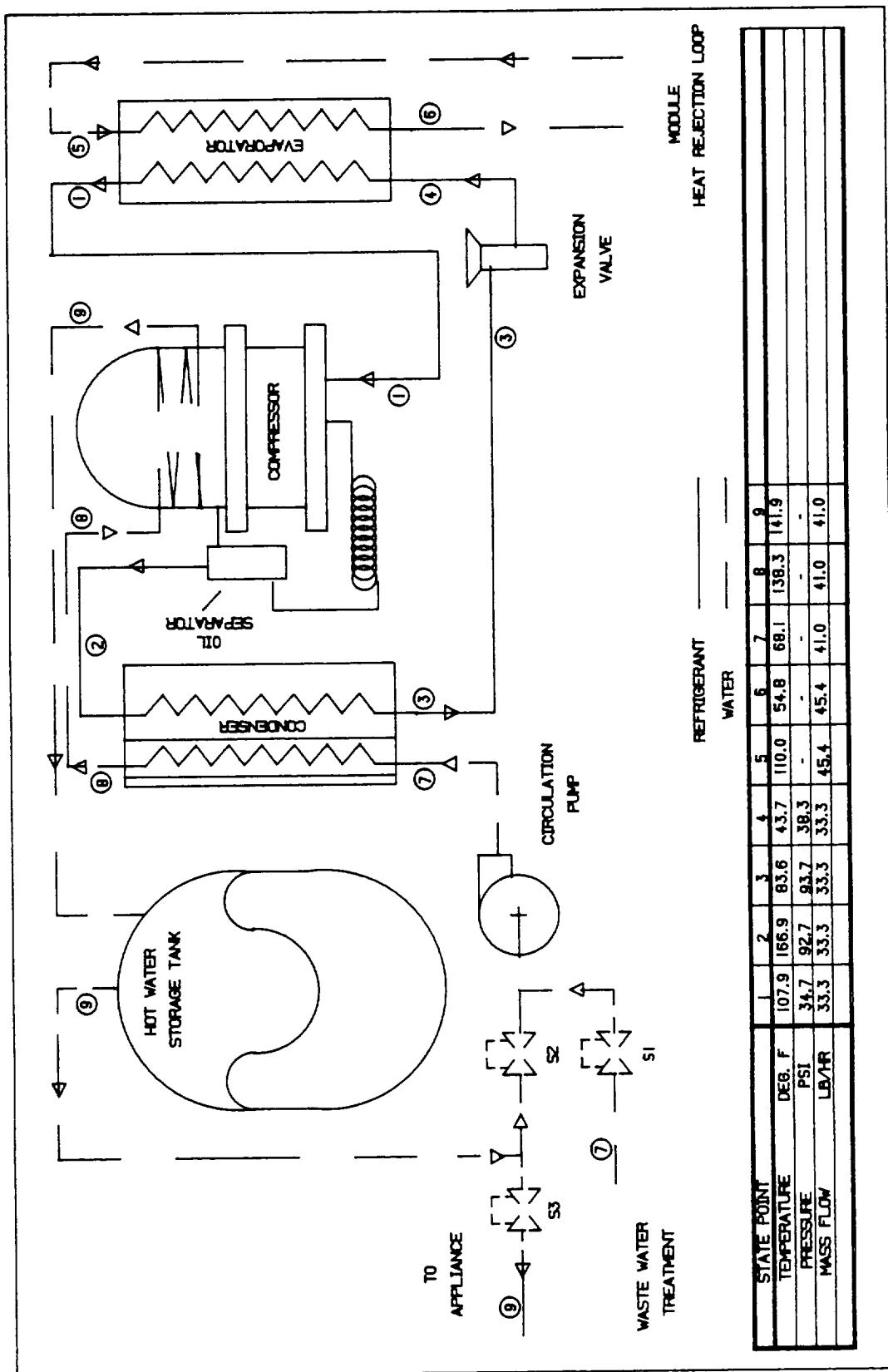


Figure 43. Heat Pump System Schematic

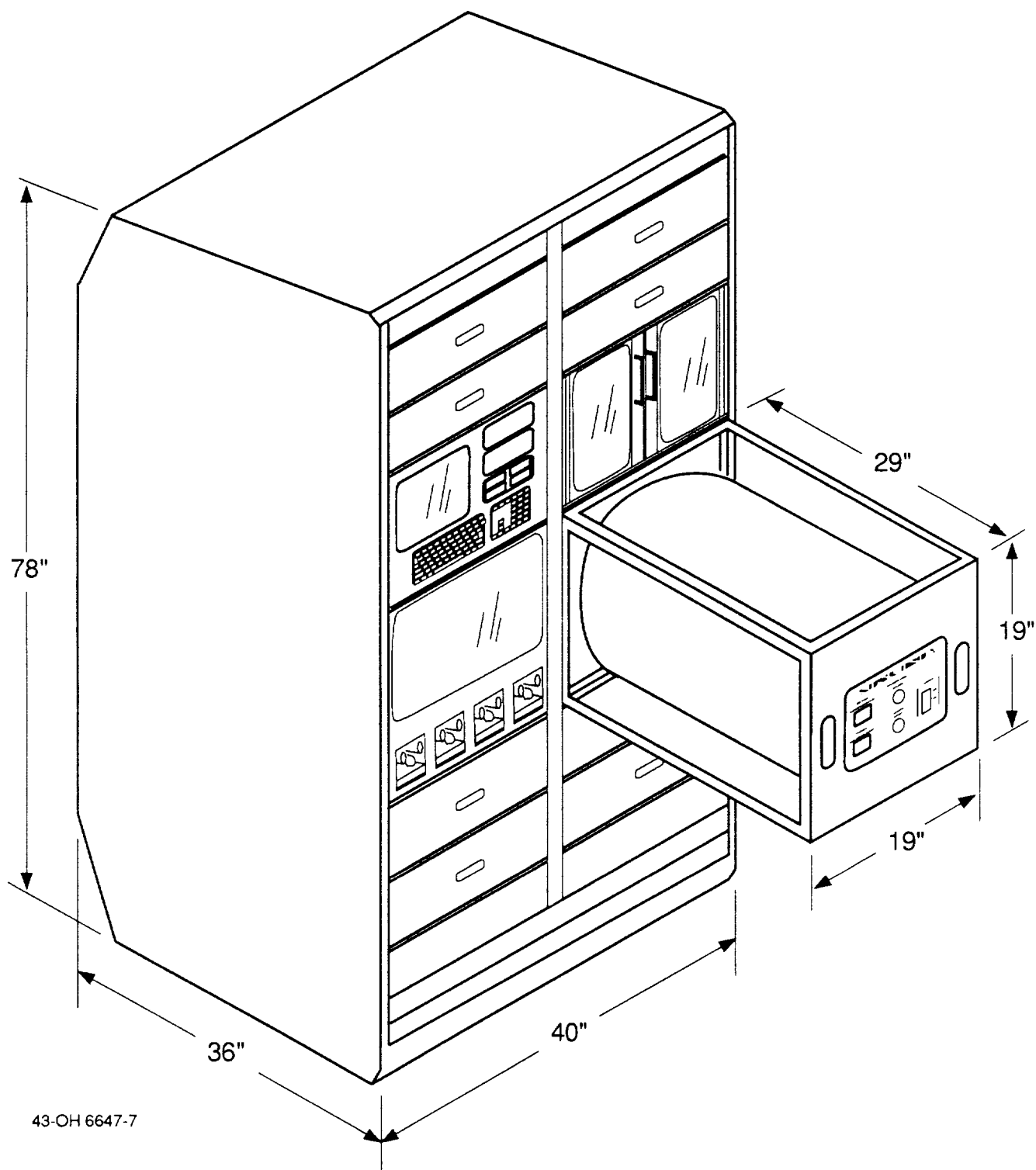


Figure 44. Nonazeotropic Heat Pump Rack Installation

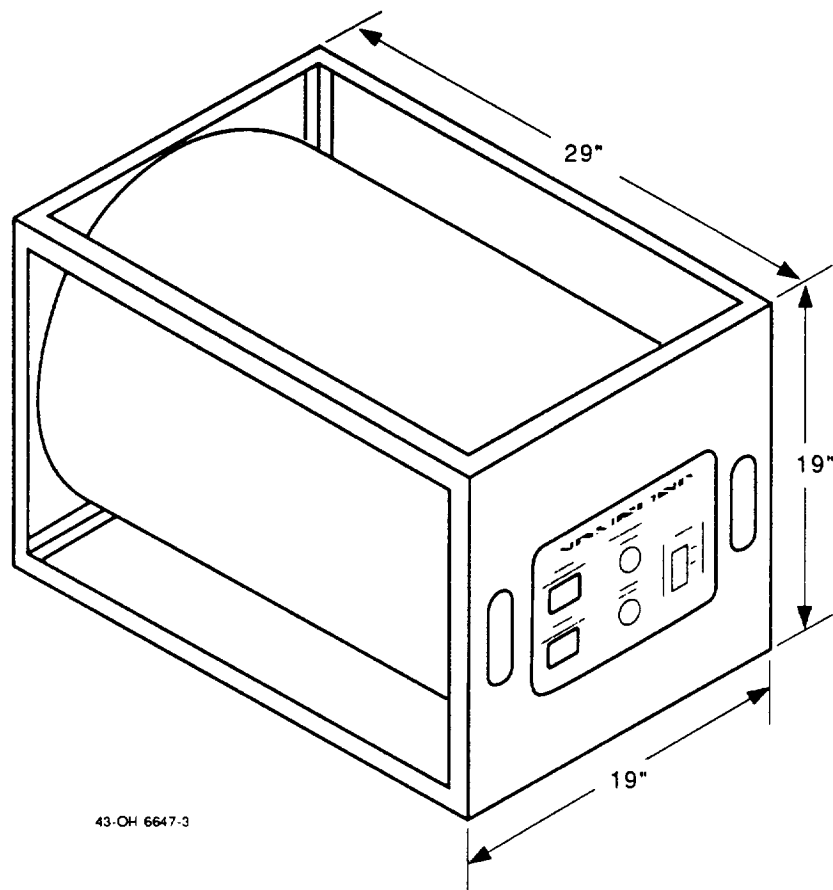


Figure 45. Nonazeotropic Heat Pump Orbital Replacement Unit

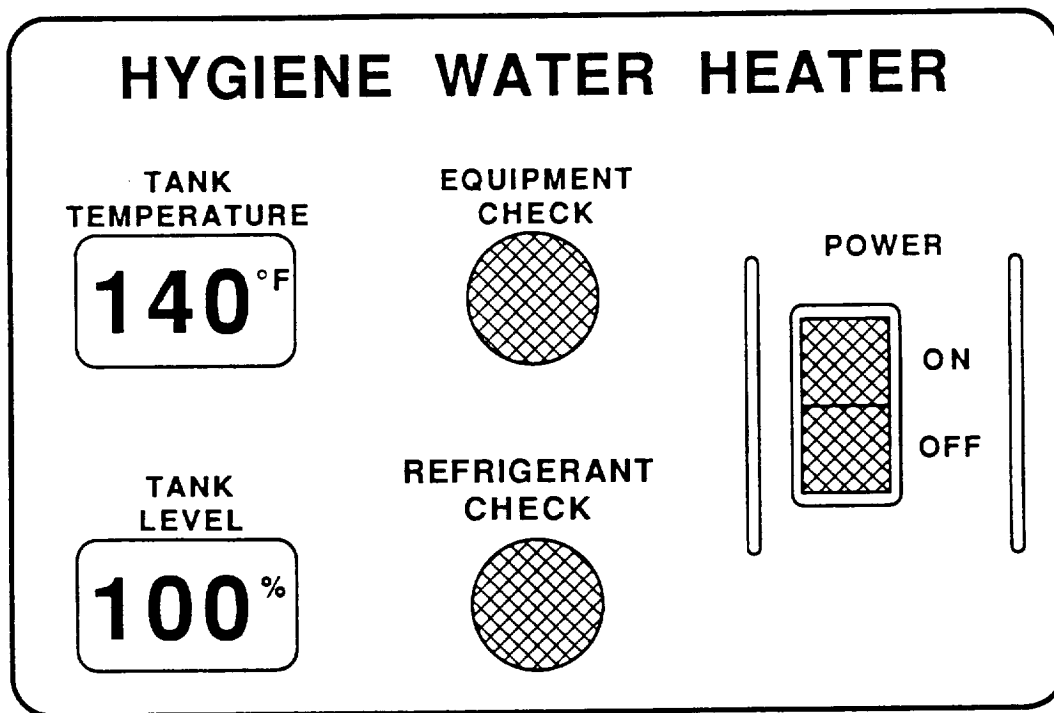
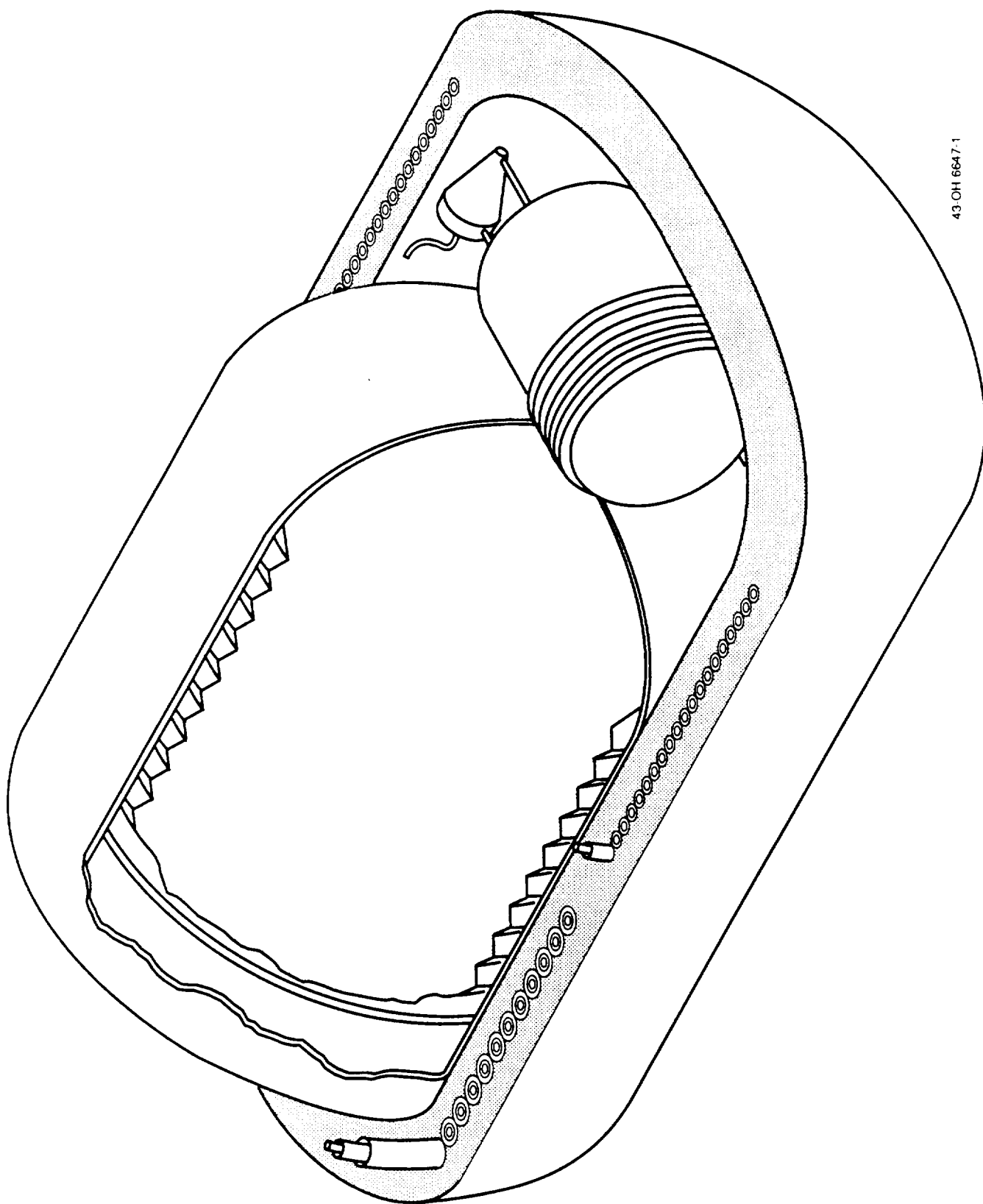


Figure 46. Nonazeotropic Heat Pump Display Panel

instrument/display panel interface. The sealed hermetic enclosure provides double containment in the event of a refrigerant leak.

A cutaway view of the ORU is shown in Figure 47. The water tank located in the center of the unit, contains a bellow type diaphragm. The evaporator and condenser tube-in-tube heat exchangers are coiled around the tank and imbedded in 2 in. of rigid foam insulation. The compressor, expansion device, connecting piping, and control module are located in the space at the end of the water tank. The semi-hermetic prototype scroll compressor developed under this program would be replaced with a completely sealed hermetic unit as shown in Figure 48. It is anticipated that the compressor required for this application could be made as small as 5 in. diam by 8 in. long through proper sizing at the scroll components, shaft, and motor. (The unit developed under this program was based on the smallest of-the-shelf compressor available but was still significantly oversized.) The control module monitors system temperatures and pressures and activates the heat pump compressor and circulation pump as required. The amount of water in the tank is determined through pressure measurements and location indicators for the diaphragm. Any time the tank level is below 100 percent full, the control system activates the compressor and water pump. A decrease in water temperature in the tank due to standby losses will also activate the compressor and recirculation pump. The control system also monitors the module heat rejection loop water temperature as it leaves the evaporator and will shut the system down should the water temperature approach freezing. The control system checks for refrigerant leaks in two ways. The static water loop surrounding the refrigerant tube in the condenser is monitored for an increase in pressure while the compressor compartment contains refrigerant leak detectors. The control system will shut the system down should a leak occur and a warning light on the display panel will flash.



43 OH 6647-1

Figure 47. Nonazeotropic Heat Pump Cutaway View

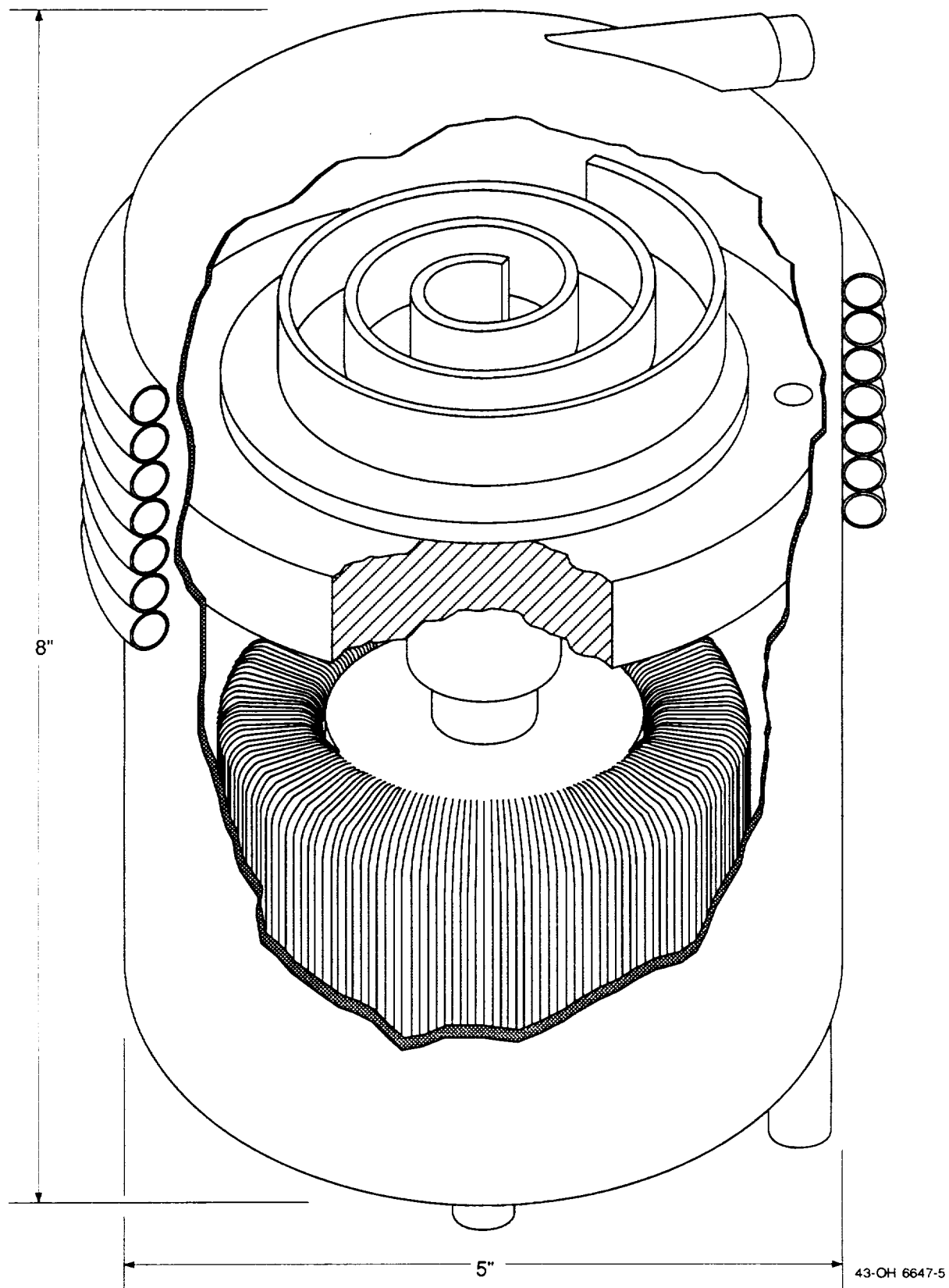


Figure 48. Cutaway View of Scroll Compressor

9. CONCLUSIONS AND RECOMMENDATIONS

The principal objective of the Phase II program effort was to design, fabricate, and test a nonazeotropic heat pump capable of producing hygiene water at the desired temperature and flow rate as required for the SSF application. The heat pump would be designed to limit peak power draw to an absolute minimum due to the modest power production capabilities. In pursuit of this goal, the following steps were taken.

The design specifications for the SSF hygiene water heating system were determined including the number and type of appliances to be serviced, the anticipated usage pattern, and the amount and temperature of the water required by each appliance. The operating parameters of the thermal bus utilized as the heat source for the nonazeotropic heat pump were also defined as well as material compatibility, packaging and safety requirements.

Various heat pump system configurations were then defined and investigated as potential candidates in meeting the design specifications. The system with the lowest power draw and energy consumption was selected for further development. The nonazeotropic working fluid constituents and composition were selected to match the temperature glide of the hygiene water and maximize COP. Several models were developed to assist in the design process including a heat pump cycle state point routine, heat exchanger heat transfer and pressure drop model, and a Life Cycle Cost (LCC) analysis. Trade studies were then performed to optimize component sizing followed by the detailed design of the heat pump components. Compact, lightweight heat exchangers were designed to provide efficient counterflow heat transfer as required by the refrigerant mixture. A compressor/motor package was also developed based on a compliant scroll which has the ability to operate at a very high overall efficiency. A special lubrication system was designed into the unit to maintain lubrication in both zero-g (SSF application) and one-g (for ground testing).

A bench test heat pump system was fabricated in the Foster-Miller laboratory. Extensive testing was then done to evaluate first the components, and then the system to determine the changes necessary in order to obtain the desired performance. The heat exchangers were then refabricated in coils for packaging of the entire heat pump into a compact prototype for final testing and delivery.

The Phase II program resulted in the successful demonstration of a nonazeotropic heat pump system for meeting the hygiene water heating requirements of SSF. The prototype heat pump system produced the desired amount of hygiene water at the temperatures required by the end use appliances. The measured COP ranged from 6.5 to 8.0, nearly double that expected from a single-constituent (i.e., R-12) heat pump. More importantly, the power consumption of the nonazeotropic heat pump was less than 200 W. For the SSF application, this represents a 90 to 95 percent reduction in power draw compared to the currently baselined electric cartridge system. In meeting the heating load at the efficiencies mentioned above, the prototype scroll compressor performed up to expectations. Gravity insensitive lubrication was demonstrated as the compressor was operated in both horizontal and vertical orientations.

In response to the successful Phase II program, the following recommendations are made for the further development of the Nonazeotropic Heat Pump for hygiene water heating:

- Performance mapping of heat pump system
- Further design refinement of the prototype compressor specifically for the selected refrigerant mixture and design load
- Inclusion of heat pump in terrestrial ECLSS testing
- Initial planning, development and integration of heat pump for space station use in later stages of operation (eight-man crew)
- Investigate heat pump uses in other manned missions such as a lunar base or a mission to Mars.

10. REFERENCES

1. Reuter, J., "Water Thermal Conditioning Study," Marshall Space Flight Center, Huntsville, AL, July 1989.
2. McLinden, M., and G. Morrison, NIST Standard Reference Database 23, Thermodynamic Properties of Refrigerants and Refrigerant Mixtures, U.S. Department of Commerce, National Institute of Standards and Technology, Gaithersburg, MD, December 1989.
3. DeGrush, D. and W.F. Stoecker, "Measurements of Heat Transfer Coefficients of Nonazeotropic Refrigerant Mixtures Condensing Inside Horizontal Tubes," ORNL/Sub/81-7762/6&1, November 1987.
4. Hill, W.S., "Hybrid Measurement of Two-Phase Flow," NAS9-17941, September 1988.
5. Eastman, R.E., "Spacecraft Straight-Tube Evaporator Design," WRDC-TR-85-3024, March 1985.

APPENDIX A
TEST DATA

RUN #: 0385

WEDNESDAY JANUARY 09, 1991 06:23:50 P.

MIXTURE: 997. GRAMS
.247 R-22
.753 R-11

CONDENSER :	1	2	3	4	5	6	7
WATER TEMP :	133.5	124.8	113.7	103.5	91.4	81.6	70.0
REFRIG TEMP:	160.4	133.1	122.1	110.8	98.3	88.4	79.4
PRESSURE :	94.2		89.8		87.2		85.5
ENTHALPY :	112.5		73.0		40.3		28.0
QUALITY :	.969		.484		.105		.000
DTLM :		15.9		7.6		8.1	
U :		55.1		129.5		117.2	
Q :		812.		914.		877.	
DTLM OVER :	16.6						
U OVERALL :	30.1						
Q OVERALL :	2780.						
WATER DP :	1.7						
REFRIG DP :	8.7						
WATER FLOW :	41.0						
REFRIG FLOW:	30.8						
DEGREE SUPH:	-2.5						
DEGREE SUBC:	12.3						

EVAPORATOR :	1	2	3	4	5	6	7
WATER TEMP :	50.1	53.7	56.9	60.5	68.2	80.9	109.9
REFRIG TEMP:	45.3	49.8	53.3	57.0	62.8	70.9	100.9
PRESSURE :	42.5		39.8		14.7		34.3
ENTHALPY :	21.1		42.7		103.5		108.0
QUALITY :	.011		.257		1.000		1.000
DTLM :		4.2		4.4		7.0	
U :		76.3		119.1		277.0	
Q :		309.		513.		1893.	
DTLM OVER :	6.7						
U OVERALL :	69.8						
Q OVERALL :	2715.						
WATER DP :	5.1						
REFRIG DP :	8.2						
WATER FLOW :	45.4						
REFRIG FLOW:	31.2						
DEGREE SUPH:	2.0						
DEGREE SUBC:	-1.5						

COMPRESSOR:

POWER: 134.5 WATTS	COOLONG WATER IN :	133.5 DEG F
SPEED: 1800. RPM	COOLING WATER OUT :	137.8 DEG F
TEMP : 128. DEG F	HEAT REJECTION :	176. BTU/H
COP1 : 6.06	UTILIZATION RATIO :	.88
COP2 : 6.91	CONTROLLER EFFICIENCY:	.44

RUN #	CHARGE	SPEED	QCOND	QEVAP	POWER	TWATER	COP1	COP2	UTIL
260	606	1800	2300	2497	135.1	126.3	4.99	6.42	0.78
261	606	1800	2247	2497	133.4	125.2	4.93	6.48	0.76
262	606	1800	2296	2492	131.5	125.4	5.12	6.55	0.78
263	606	1500	2128	2365	101.7	121.6	6.13	7.81	0.78
264	606	1500	2083	2361	99.2	120.4	6.15	7.97	0.77
265	606	1500	2066	2361	99.2	115.7	6.10	7.97	0.77
266	606	2100	2399	2597	156.7	128.1	4.48	5.86	0.77
267	606	2100	2407	2601	155.9	128.6	4.52	5.89	0.77
268	606	2100	2431	2606	156.7	129.6	4.55	5.87	0.77
269	709	2100	2685	2756	173.2	136.4	4.54	5.66	0.80
270	709	2100	2735	2765	173.5	137.5	4.62	5.67	0.81
271	709	2100	2757	2765	174.4	138.3	4.62	5.67	0.81
272	709	1800	2645	2724	140.4	135.6	5.52	6.68	0.83
273	709	1800	2636	2724	140.4	135.5	5.50	6.68	0.83
274	709	1800	2616	2719	142.4	135.2	5.38	6.60	0.82
275	709	1500	2452	2624	109.8	131.2	6.54	8.00	0.82
276	709	1500	2415	2620	109.8	130.5	5.44	7.99	0.81
277	709	1500	2407	2615	110.4	130.3	6.39	7.94	0.80
278	813	1500	2530	2660	129.5	133.2	5.72	7.02	0.82
279	813	1500	2526	2679	131.8	133.3	5.61	6.95	0.81
280	813	1800	2677	2765	145.0	137.1	5.41	6.59	0.82
281	813	1800	2706	2769	144.9	137.8	5.47	6.60	0.83
282	813	2100	2825	2842	180.2	140.7	4.59	5.62	0.82
283	813	2100	2882	2851	182.1	142.2	4.64	5.59	0.83
300	700	2100	2358	2611	130.5	127.4	5.29	6.86	0.77
301	700	1800	2206	2524	101.9	124.1	6.34	8.26	0.77
302	798	2100	2468	2701	136.9	130.4	5.28	6.78	0.78
303	798	1800	2312	2656	103.6	126.2	6.54	8.51	0.77
304	798	1800	2333	2660	104.7	126.2	6.53	8.45	0.77
305	798	1800	2358	2665	104.9	126.5	6.58	8.44	0.78
306	798	1500	2136	2515	76.8	122.2	8.15	10.60	0.77
308	798	1500	2144	2511	77.1	122.3	8.15	10.54	0.77
310	902	1800	2567	2751	111.8	132.7	6.73	8.21	0.82
311	902	1800	2563	2756	113.7	132.6	6.60	8.10	0.82
312	902	1800	2567	2756	113.2	132.6	6.64	8.13	0.82
315	902	1500	2370	2624	80.8	127.0	8.59	10.52	0.82
316	902	1500	2358	2624	80.4	126.9	8.59	10.56	0.81
317	902	1500	2353	2629	78.6	126.8	8.77	10.80	0.81

RUN #	CHARGE	SPEED	QCOND	QEVAP	POWER	TWATER	COP1	COP2	UTIL
318	1006	2100	2669	2824	168.6	134.8	4.64	5.91	0.79
319	1006	2100	2653	2824	165.5	134.5	4.70	6.00	0.78
320	1006	2100	2636	2824	163.1	134.1	4.74	6.07	0.78
321	1006	1800	2435	2801	115.7	129.5	6.17	8.09	0.76
322	1006	1800	2435	2797	115.8	129.6	6.16	8.08	0.76
324	1006	1800	2440	2797	115.8	129.8	6.17	8.08	0.76
325	1006	1500	2366	2729	85.8	127.7	8.08	10.32	0.78
326	1006	1500	2337	2729	85.3	127.0	8.03	10.37	0.77
327	1006	1500	2337	2724	85.0	127.0	8.06	10.39	0.78
331	896	2100	2657	2828	154.1	135.0	5.05	6.38	0.79
332	896	2100	2665	2810	154.0	135.3	5.07	6.35	0.80
333	896	2100	2661	2806	149.6	135.1	5.21	6.50	0.80
334	896	2100	2665	2815	149.4	135.2	5.23	6.52	0.80
335	896	1800	2431	2819	118.8	129.7	6.00	7.95	0.75
336	896	1800	2431	2819	122.5	129.6	5.82	7.74	0.75
337	896	1800	2448	2815	119.9	129.7	5.98	7.88	0.76
338	896	1500	2230	2765	81.6	124.3	8.01	10.93	0.73
339	896	1500	2226	2774	82.5	124.2	7.91	10.85	0.73
340	896	1500	2235	2783	81.5	124.3	8.03	11.01	0.73
341	1006	2100	2571	2865	167.8	133.1	4.49	6.00	0.75
342	1006	2100	2575	2865	167.3	133.3	4.51	6.02	0.75
343	1006	2100	2554	2878	163.6	132.9	4.57	6.15	0.74
344	1006	1800	2476	2869	130.9	130.2	5.54	7.42	0.75
345	1006	1800	2472	2865	130.9	130.1	5.53	7.41	0.75
346	1006	1800	2476	2860	129.5	130.1	5.60	7.47	0.75
347	1006	1500	2394	2801	104.0	127.1	6.75	8.89	0.76
348	1006	1500	2399	2801	104.4	127.2	6.73	8.86	0.76
349	1006	1500	2394	2801	104.3	127.2	6.73	8.87	0.76
350	1107	2100	2895	2910	194.7	140.9	4.36	5.38	0.81
351	1107	2100	2899	2919	194.0	141.0	4.38	5.41	0.81
352	1107	2100	2903	2919	196.0	141.0	4.34	5.36	0.81
353	1107	1800	2763	2874	153.0	137.6	5.29	6.50	0.81
354	1107	1800	2755	2878	152.9	137.4	5.28	6.52	0.81
355	1107	1800	2751	2878	154.4	137.4	5.22	6.46	0.81
356	1107	1500	2599	2828	116.2	133.5	6.55	8.13	0.81
357	1107	1500	2595	2838	116.8	133.4	6.51	8.12	0.80
358	1107	1500	2591	2833	116.0	133.3	6.54	8.16	0.80
359	1000	2100	2952	2774	183.9	142.3	4.70	5.42	0.87
360	1000	2100	2948	2769	182.0	142.4	4.75	5.46	0.87
361	1000	2100	2940	2774	183.2	142.4	4.70	5.44	0.86
362	1000	1800	2768	2733	147.2	137.5	5.51	6.44	0.86

RUN #	CHARGE	SPEED	QCOND	QEVAP	POWER	TWATER	COP1	COP2	UTIL
363	1000	1800	2768	2729	147.5	137.7	5.50	6.42	0.86
364	1000	1800	2768	2729	144.1	137.7	5.63	6.55	0.86
365	1000	1500	2542	2620	109.9	132.3	6.78	7.98	0.85
366	1000	1500	2538	2620	108.9	132.1	6.83	8.05	0.85
367	1000	1500	2534	2615	109.8	132.1	6.76	7.98	0.85
368	900	1500	2169	2488	100.3	123.1	6.34	8.27	0.77
369	900	1500	2173	2497	99.7	123.2	6.39	8.34	0.77
370	900	1500	2161	2511	99.9	123.4	6.34	8.36	0.76
371	900	1800	2468	2670	137.9	130.3	5.24	6.67	0.79
372	900	1800	2485	2670	137.8	130.7	5.28	6.68	0.79
373	900	1800	2489	2674	138.8	130.8	5.25	6.64	0.79
374	900	2100	2854	2751	172.0	139.4	4.86	5.69	0.85
376	900	2100	2849	2747	168.7	139.4	4.95	5.77	0.86
377	900	2100	2850	2747	172.2	139.5	4.85	5.67	0.85
378	900	2400	3079	2774	181.9	145.5	4.96	5.47	0.91
379	900	2400	3079	2774	182.0	145.6	4.96	5.47	0.91
380	900	2400	3100	2778	181.2	145.7	5.01	5.49	0.91
381	997	1500	2530	2615	103.6	131.8	7.15	8.40	0.85
382	997	1500	2538	2624	103.9	131.8	7.16	8.40	0.85
383	997	1500	2530	2615	102.7	131.7	7.22	8.46	0.85
384	997	1800	2772	2719	135.7	137.7	5.98	6.87	0.87
385	997	1800	2780	2715	134.5	137.8	6.06	6.91	0.88
386	997	1800	2780	2724	136.2	137.6	5.98	6.86	0.87
387	997	2100	2964	2756	169.9	142.5	5.11	5.75	0.89
388	997	2100	2964	2760	170.6	142.5	5.09	5.74	0.89
389	997	2100	2964	2760	171.0	142.7	5.08	5.73	0.89
390	997	2400	3186	2792	197.0	148.0	4.74	5.15	0.92
391	997	2400	3186	2778	199.0	148.0	4.69	5.09	0.92
392	997	2400	3190	2783	204.8	147.7	4.56	4.98	0.92
393	1096	1500	2628	2733	110.8	134.1	6.95	8.23	0.84
394	1096	1500	2628	2715	107.0	134.0	7.20	8.43	0.85
396	1096	1500	2616	2724	107.8	133.8	7.11	8.40	0.85
397	1096	1800	2792	2788	145.2	138.2	5.63	6.62	0.85
398	1096	1800	2796	2778	140.8	138.2	5.82	6.78	0.86
399	1096	1800	2796	2774	141.4	138.1	5.79	6.75	0.86
400	1096	2100	2956	2806	175.1	142.2	4.95	5.69	0.87
401	1096	2100	2964	2806	177.0	142.4	4.91	5.64	0.87
402	1096	2100	2968	2806	177.8	142.5	4.89	5.62	0.87
404	1096	2400	3132	2842	191.6	146.1	4.79	5.35	0.90
405	1096	2400	3128	2828	189.3	146.1	4.84	5.38	0.90
406	1096	2400	3137	2833	191.9	146.2	4.79	5.33	0.90

RUN #	CHARGE	SPEED	QCOND	QEVAP	POWER	TWATER	COP1	COP2	UTIL
407	1196	2400	3173	2847	198.8	147.1	4.68	5.20	0.90
408	1196	2400	3169	2851	200.5	147.1	4.63	5.17	0.90
409	1196	2400	3169	2851	201.4	147.2	4.61	5.15	0.90
410	1196	2100	3009	2815	184.5	143.5	4.78	5.47	0.87
411	1196	2100	3001	2819	185.9	143.4	4.73	5.44	0.87
412	1196	2100	2997	2824	184.2	143.3	4.77	5.49	0.87
419	1196	1800	2845	2769	145.4	138.9	5.73	6.58	0.87
420	1196	1800	2845	2774	147.0	138.9	5.67	6.53	0.87
421	1196	1800	2841	2774	146.0	138.9	5.70	6.57	0.87
422	1196	1500	2644	2719	116.6	133.9	6.65	7.83	0.85
423	1196	1500	2661	2724	117.2	134.3	6.65	7.81	0.85
424	1196	1500	2653	2729	116.3	134.1	6.68	7.87	0.85
425	898	1500	2464	2724	116.2	130.2	6.21	7.87	0.79
426	898	1500	2468	2729	114.2	130.3	6.33	8.00	0.79
427	898	1500	2481	2729	115.1	130.5	6.31	7.95	0.79
428	898	1800	2755	2765	149.3	137.3	5.41	6.43	0.84
429	898	1800	2768	2774	151.8	137.5	5.34	6.35	0.84
430	898	1800	2768	2769	153.5	137.6	5.28	6.29	0.84
431	898	2100	3071	2810	190.7	144.7	4.72	5.32	0.89
433	898	2100	3063	2806	189.8	144.6	4.73	5.33	0.89
434	898	2100	3063	2797	190.0	144.6	4.72	5.31	0.89
435	898	2400	3268	2824	242.1	149.8	3.95	4.42	0.90
436	898	2400	3243	2819	242.5	149.6	3.92	4.41	0.89
437	898	2400	3276	2828	211.0	149.7	4.55	4.93	0.92
438	1002	1500	2608	2765	119.1	133.8	6.41	7.80	0.82
440	1002	1500	2599	2765	121.1	133.7	6.29	7.69	0.82
441	1002	1500	2604	2765	119.9	133.7	6.36	7.76	0.82
442	1002	1800	2927	2833	160.6	141.4	5.34	6.17	0.87
443	1002	1800	2932	2833	160.9	141.5	5.34	6.16	0.87
444	1002	1800	2927	2828	161.8	141.5	5.30	6.12	0.87
449	1002	2100	3100	2847	199.2	145.3	4.56	5.19	0.88
450	1002	2100	3091	2847	200.8	145.5	4.51	5.15	0.88
451	1002	2100	3091	2838	198.3	145.6	4.57	5.19	0.88
452	1002	2400	3251	2847	266.6	149.4	3.57	4.13	0.87
453	1002	2400	3255	2851	271.2	149.4	3.52	4.08	0.86
454	1002	2400	3251	2847	267.1	149.4	3.57	4.12	0.87
455	1104	1500	2661	2792	129.1	135.2	6.04	7.34	0.82
456	1104	1500	2659	2797	127.8	135.4	6.12	7.41	0.83
457	1104	1500	2669	2788	127.4	135.4	6.14	7.41	0.83
458	1104	1850	2968	2838	172.9	142.2	5.03	5.81	0.87
459	1104	1850	2973	2842	174.0	142.3	5.01	5.79	0.87
460	1104	1850	2968	2838	172.7	142.2	5.04	5.81	0.87

RUN #	CHARGE	SPEED	QCOND	QEVAP	POWER	TWATER	COP1	COP2	UTIL
462	1104	2100	3128	2838	214.1	146.5	4.28	4.88	0.88
465	1104	2100	3145	2847	212.9	146.6	4.33	4.92	0.88
466	1104	2100	3157	2851	213.6	146.6	4.33	4.91	0.88
467	1104	2400	3370	2856	274.8	152.2	3.59	4.04	0.89
468	1104	2400	3383	2856	258.7	152.0	3.83	4.23	0.90
469	1104	2400	3370	2860	249.2	152.1	3.96	4.36	0.91
470	1232	1500	2776	2819	135.5	137.8	6.00	7.10	0.85
471	1232	1500	2772	2815	135.2	137.7	6.01	7.10	0.85
472	1232	1500	2780	2824	135.7	137.8	6.00	7.10	0.85
473	1232	2100	3251	2874	225.6	149.4	4.22	4.73	0.89
474	1232	2100	3243	2874	224.0	149.2	4.24	4.76	0.89
476	1232	2100	3259	2869	226.5	149.4	4.22	4.71	0.89
477	1232	1850	3059	2856	188.4	144.3	4.76	5.44	0.87
478	1232	1850	3055	2851	190.0	144.3	4.71	5.40	0.87
479	1232	1850	3055	2847	191.6	144.5	4.67	5.35	0.87
480	1232	2400	3407	2865	294.0	153.1	3.40	3.85	0.88
481	1232	2400	3395	2860	294.6	152.9	3.38	3.84	0.88
482	1232	2400	3395	2865	293.1	152.9	3.39	3.86	0.88
500	704	1800	2464	2620	160.6	129.9	4.50	5.78	0.78
501	704	1800	2456	2615	160.3	129.8	4.49	5.78	0.78
502	704	1800	2448	2624	160.3	129.8	4.47	5.80	0.77
503	704	1500	2198	2479	113.4	123.8	5.68	7.40	0.77
504	704	1500	2194	2483	105.7	123.6	6.08	7.88	0.77
505	704	1500	2202	2479	100.9	123.6	6.39	8.20	0.78
506	800	1800	2636	2679	129.7	134.7	5.96	7.05	0.84
507	800	1800	2628	2679	128.1	134.5	6.01	7.13	0.84
508	800	1800	2616	2679	128.3	134.3	5.97	7.12	0.84
509	800	1500	2329	2561	95.4	127.0	7.15	8.86	0.81
510	800	1500	2325	2561	95.9	126.9	7.10	8.82	0.80
511	800	1500	2321	2556	95.2	126.8	7.14	8.87	0.81
512	901	1800	2768	2756	129.6	137.5	6.26	7.23	0.87
513	901	1800	2755	2756	130.6	137.3	6.18	7.18	0.86
514	901	1800	2755	2760	130.2	137.3	6.20	7.21	0.86
515	901	1500	2513	2629	100.5	131.6	7.35	8.56	0.85
516	901	1500	2509	2624	99.2	131.6	7.41	8.75	0.85
517	901	1500	2513	2624	99.1	131.6	7.43	8.76	0.85
518	598	1800	2464	2515	145.7	129.8	4.96	6.06	0.82
519	598	1800	2489	2520	143.3	130.2	5.05	6.15	0.83
520	598	1800	2481	2515	144.1	130.2	5.04	6.11	0.82

RUN #	CHARGE	SPEED	QCOND	QEVAP	POWER	TWATER	COP1	COP2	UTIL
521	697	1800	2731	2647	149.4	136.4	5.36	6.19	0.87
522	697	1800	2735	2647	148.7	136.6	5.39	6.22	0.87
523	697	1800	2722	2651	149.6	136.5	5.33	6.19	0.86
524	697	1500	2464	2533	117.7	130.1	6.13	7.31	0.84
525	697	1500	2464	2533	117.9	130.3	6.12	7.30	0.84
526	697	1500	2472	2533	117.3	130.5	6.18	7.33	0.84
529	801	1800	3034	2742	165.4	144.0	5.37	5.86	0.92
530	801	1800	3030	2747	165.3	143.9	5.37	5.87	0.92
531	801	1800	3026	2747	164.8	143.9	5.38	5.88	0.91
532	801	1500	2747	2629	127.7	137.1	6.30	7.03	0.90
533	801	1500	2747	2638	128.4	136.9	6.27	7.02	0.89
534	801	1500	2763	2638	126.4	137.0	6.41	7.11	0.90
540	602	1800	2341	2506	120.7	127.4	5.68	7.08	0.80
541	602	1800	2349	2511	119.7	127.6	5.75	7.15	0.80
542	602	1800	2358	2506	119.4	127.8	5.79	7.15	0.81
543	702	1800	2624	2642	124.7	134.3	6.17	7.21	0.86
544	702	1800	2640	2647	125.9	134.6	6.14	7.16	0.86
545	702	1800	2636	2651	128.3	134.6	6.02	7.05	0.85
546	702	1500	2423	2556	94.3	128.8	7.53	8.94	0.84
547	702	1500	2419	2551	92.2	128.7	7.69	9.11	0.84
548	702	1500	2444	2547	93.2	129.2	7.68	9.01	0.85
549	801	1800	2845	2701	129.3	139.4	6.45	7.12	0.91
550	801	1800	2837	2706	131.2	139.3	6.34	7.04	0.90
551	801	1800	2833	2706	130.3	139.2	6.37	7.08	0.90
552	801	1500	2554	2615	93.6	132.4	8.00	9.19	0.87
553	801	1500	2558	2620	94.5	132.5	7.93	9.12	0.87
554	801	1500	2571	2620	92.4	132.6	8.15	9.31	0.88
555	904	1800	3001	2724	136.7	143.2	6.43	6.84	0.94
556	904	1800	2993	2724	139.5	143.2	6.29	6.72	0.94
557	904	1800	2997	2729	137.0	143.3	6.41	6.84	0.94
558	904	1500	2739	2665	101.6	136.8	7.90	8.69	0.91
559	904	1500	2747	2670	101.5	137.0	7.95	8.72	0.91
560	904	1500	2751	2674	101.8	137.0	7.92	8.70	0.91
570	701	2000	2735	2729	154.4	136.9	5.19	6.18	0.84
571	701	2000	2743	2724	156.7	137.2	5.13	6.09	0.84
572	701	2000	2747	2710	157.1	137.4	5.12	6.05	0.85
573	701	1900	2686	2701	127.8	135.8	6.16	7.19	0.86
574	701	1900	2694	2697	130.7	136.0	6.04	7.05	0.86
575	701	1900	2706	2701	130.4	136.3	6.08	7.07	0.86

RUN #	CHARGE	SPEED	QCOND	QEVAP	POWER	TWATER	COP1	COP2	UTIL
576	701	1800	2698	2674	128.1	135.4	6.17	7.12	0.87
577	701	1800	2694	2674	126.7	130.2	6.23	7.18	0.87
578	701	1800	2686	2679	127.1	130.0	6.19	7.17	0.86
580	701	1700	2624	2656	118.1	133.9	6.51	7.59	0.86
581	701	1700	2628	2660	116.0	134.0	6.64	7.72	0.86
582	701	1700	2620	2651	118.7	134.0	6.47	7.54	0.87
583	701	1600	2530	2620	103.2	131.8	7.18	8.44	0.85
584	701	1600	2538	2611	103.2	131.9	7.21	8.41	0.86
585	701	1600	2538	2620	103.7	131.9	7.17	8.40	0.85
586	701	1500	2452	2570	92.4	129.8	7.77	9.15	0.85
587	701	1500	2452	2570	92.2	129.9	7.79	9.17	0.85
588	701	1500	2448	2565	92.5	129.8	7.75	9.13	0.85
589	798	2000	2858	2760	148.5	140.1	5.64	6.45	0.87
590	798	2000	2866	2756	151.8	140.2	5.53	6.32	0.88
591	798	2000	2882	2760	153.5	140.5	5.50	6.27	0.88
592	798	1900	2792	2756	134.8	138.2	6.07	6.99	0.87
593	798	1900	2800	2760	134.8	138.5	6.09	7.00	0.87
595	798	1900	2784	2756	135.6	138.1	6.02	6.95	0.86
599	798	1800	2780	2742	136.6	137.8	5.96	6.88	0.87
600	798	1800	2788	2738	139.7	138.0	5.85	6.74	0.87
602	798	1800	2788	2742	143.2	136.0	5.70	6.61	0.86
603	798	1700	2694	2719	113.3	136.0	6.97	8.03	0.87
604	798	1700	2698	2724	114.2	136.1	6.92	7.99	0.87
605	798	1700	2702	2724	114.3	136.2	6.93	7.98	0.87
606	798	1600	2591	2679	103.9	133.2	7.31	8.55	0.85
607	798	1600	2591	2688	104.6	133.3	7.28	8.53	0.85
608	798	1600	2591	2683	105.4	133.3	7.20	8.46	0.85
609	798	1500	2530	2651	94.6	131.7	7.84	9.21	0.85
610	798	1500	2534	2647	96.8	131.8	7.67	9.01	0.85
611	798	1500	2530	2656	94.6	131.7	7.84	9.23	0.85
613	900	2000	3034	2801	192.6	144.5	4.82	5.26	0.88
615	900	2000	3079	2792	193.4	145.3	4.66	5.23	0.89
616	900	1900	3026	2806	150.7	143.6	5.88	6.48	0.91
618	900	1900	3022	2801	150.1	143.5	5.90	6.47	0.91
619	900	1800	2977	2778	139.7	142.9	6.24	6.83	0.91
620	900	1800	2973	2783	139.5	142.8	6.24	6.85	0.91
621	900	1800	2973	2783	139.2	142.6	6.26	6.86	0.91
622	900	1700	2891	2747	127.5	140.7	6.64	7.31	0.91
623	900	1700	2903	2747	129.7	141.1	6.58	7.26	0.91
624	900	1700	2899	2742	129.6	141.0	6.55	7.20	0.91
625	900	1600	2829	2715	114.8	139.1	7.22	7.93	0.91
626	900	1600	2845	2719	114.7	139.5	7.27	7.95	0.91
627	900	1600	2841	2719	116.9	139.4	7.12	7.81	0.91

RUN #	CHARGE	SPEED	QCOND	QEVAP	POWER	TWATER	COP1	COP2	UTIL
628	900	1500	2727	2710	103.5	136.6	7.72	8.67	0.89
629	900	1500	2722	2710	103.3	136.4	7.72	8.69	0.89
630	900	1500	2718	2701	103.6	136.3	7.69	8.64	0.89
631	700	2000	2702	2719	139.6	136.2	5.67	6.71	0.85
632	700	2000	2698	2729	138.0	136.1	5.73	6.79	0.84
633	700	2000	2702	2729	138.5	136.2	5.72	6.77	0.84
634	700	2000	2698	2729	138.7	136.1	5.70	6.76	0.84
635	700	1900	2710	2665	132.7	135.7	5.98	6.88	0.87
636	700	1900	2706	2665	130.8	135.6	6.06	6.97	0.87
637	700	1900	2710	2665	131.6	135.8	6.03	6.93	0.87
638	700	1900	2714	2665	130.8	135.9	6.08	6.97	0.87
639	700	1900	2718	2665	131.3	136.1	6.07	6.95	0.87
640	700	1800	2677	2651	123.5	135.4	6.35	7.29	0.87
641	700	1800	2698	2651	123.4	135.9	6.41	7.30	0.88
642	700	1800	2677	2651	123.7	135.4	6.34	7.28	0.87
643	806	2000	3067	2738	156.4	145.1	5.75	6.13	0.94
644	806	2000	3087	2747	156.9	145.4	5.77	6.13	0.94
645	806	2000	3083	2747	156.9	145.3	5.76	6.13	0.94
646	806	1900	3005	2742	145.3	143.1	6.06	6.53	0.93
647	806	1900	3013	2747	146.5	143.4	6.03	6.49	0.93
648	806	1900	2993	2738	146.1	142.9	6.00	6.49	0.92
649	806	1800	2956	2729	134.0	142.1	6.46	6.97	0.93
650	806	1800	2956	2729	134.6	142.1	6.43	6.94	0.93
651	806	1800	2956	2729	134.6	142.2	6.43	6.94	0.93
652	799	2000	2956	2751	147.7	142.3	5.86	6.46	0.91
653	799	2000	2956	2747	148.5	142.1	5.83	6.42	0.91
654	799	2000	2948	2742	147.1	142.1	5.87	6.46	0.91
655	799	1900	2899	2733	140.1	141.1	6.06	6.72	0.90
656	799	1900	2903	2733	140.9	141.1	6.04	6.68	0.90
657	799	1900	2919	2742	140.6	141.3	6.08	6.71	0.91
658	799	1900	2911	2738	139.6	141.1	6.11	6.75	0.91
659	799	1800	2829	2719	128.8	138.7	6.44	7.19	0.90
660	799	1800	2841	2724	129.1	138.9	6.45	7.18	0.90
661	799	1800	2829	2719	128.1	138.6	6.47	7.22	0.90

NASA
National Aeronautics
Space Administration

Report Documentation Page

1. Report No. NAS-8407-FM-9017-482		2. Government Accession No. N/A		3. Recipient's Catalog No. N/A	
4. Title and Subtitle Development of a Nonazeotropic Heat Pump for Crew Hygiene Water Heating				5. Report Date 8/21/91	
				6. Performing Organization Code 30233	
7. Author(s) David H. Walker, Glenn I. Deming				8. Performing Organization Report No. NAS-8407-FM-9017-482	
				10. Work Unit No. N/A	
9. Performing Organization Name and Address Foster-Miller, Inc. 350 Secon Avenue Waltham, MA 02154-1196				11. Contract or Grant No. NAS8-38407	
				13. Type of Report and Period Covered Draft Final From: 6/89 To: 8/91	
12. Sponsoring Agency Name and Address George C. Marshall Space Flight Center National Aeronautics & space Administration Marshall Space Flight Center, AL 35812				14. Sponsoring Agency Code N/A	
15. Supplementary Notes Contracting Officer Technical Representative: Douglas G. Westra/205-544-3120					
16. Abstract This report describes a Phase II SBIR Program funded by the NASA Marshall Space Flight Center to develop a Nonazeotropic Heat Pump. The heat pump system which was designed, fabricated and tested in the Foster-Miller laboratory, is capable of providing crew hygiene water heating for future manned missions. The heat pump utilizes a nonazeotropic refrigerant mixture which, in this application, provides a significant Coefficient of Performance improvement over a single-constituent working fluid. In order to take full advantage of the refrigerant mixture, compact tube-in-tube heat exchangers were designed. A high efficiency scroll compressor with a proprietary lubrication system was developed to meet the requirements of operation in zero-gravity. The prototype heat pump system consumes less than 200W of power compared to the alternative of electric cartridge heaters which would require 2 to 5 kW.					
17. Key Words (Suggested by Author(s)) Nonazeotropic, refrigerant mixtures, heat pump, hygiene water heating, Space Station, scroll compressor, heat transfer, coefficient of perofrmance			18. Distribution Statement In accordance with FAR 52.227-7025, SBIR Data Rights Clause		
19. Security Classif. (of this report) Unclassified		20. Security Classif. (of this page) Unclassified		21. No. of pages 99	
				22. Price \$497,087	

